SYNTHESIS AND CHARACTERIZATION OF FILMS AND MEMBRANES OF METAL-ORGANIC FRAMEWORK (MOF) FOR GAS SEPARATION APPLICATIONS

A Thesis

by

MIRAL NARESH SHAH

Submitted to the Office of Graduate Studies of
Texas A&M University
in partial fulfillment of the requirements for the degree of

MASTER OF SCIENCE

Approved by:

Chair of Committee,	Hae-Kwon Jeong
Committee Members,	Mustafa Akbulut
	Hong-Cai (Joe) Zhou
Head of Department,	M. Nazmul Karim

December 2012

Major Subject: Chemical Engineering

ABSTRACT

Metal-Organic Frameworks (MOFs) are nanoporous framework materials with tunable pore size and functionality, and hence attractive for gas separation membrane applications. Zeolitic Imidazolate Frameworks (ZIFs), a subclass of MOFs, are known for their high thermal and chemical stability. ZIF-8 has demonstrated potential to kinetically separate propane/propene in powder and membrane form. ZIF-8 membranes propane-propene separation performance is superior in comparison to polymer, mixed matrix and carbon membranes.

The overarching theme of my research is to address challenges that hinder fabrication of MOF membranes on a commercial scale and in a reproducible and scalable manner. 1. Current approaches, are specific to a given ZIF, a general synthesis route is not available. Use of multiple steps for surface modification or seeding causes reproducibility and scalability issues. 2. Conventional fabrication techniques are batch processes, thereby limiting their commercialization. Here we demonstrate two new approaches that can potentially address these challenges.

First, we report one step *in situ* synthesis of ZIF-8 membranes on more commonly used porous α-alumina supports. By incorporating sodium formate in the *in* situ growth solution, well intergrown ZIF-8 membranes were synthesized on unmodified supports. The mechanism by which sodium formate promotes heterogeneous nucleation was investigated. Sodium formate reacts with zinc source to form zinc oxide layer, which in

turn promotes heterogeneous nucleation. Sodium formate promotes heterogeneous nucleation in other ZIF systems as well, leading to ZIF-7, $Zn(Im)_2$ (ZIF-61 analogue), ZIF-90, and SIM-1 films. Thus one step *in situ* growth using sodium formate provides a simplified, reproducible and potentially general route for ZIF film fabrication.

One step *in situ* route, although advantageous; is still conventional in nature and batch process with long synthesis time. This limits commercialization, due to scalability and manufacturing cost issues. Taking advantage of coordination chemistry of MOFs and using temperature as driving force, continuous well-intergrown membranes of HKUST-1 and ZIF-8 in relatively short time (15 min) using Rapid Thermal Deposition (RTD). With minimum precursor consumption and simplified synthesis protocol, RTD provides potential for a continuous, scalable, reproducible and commercializable route for MOF membrane fabrication. RTD-prepared MOF membranes show improved separation performances, indicating improved microstructure.

DEDICATION

To my loving and caring family and friends

ACKNOWLEDGEMENTS

I would like to thank my committee chair, Dr. Jeong, and my committee members, Dr. Akbulut and Dr. Zhou for their guidance and support throughout the course of this research.

Thanks also to my friends and colleagues and the department faculty and staff for making my time at Texas A&M University a great experience.

Finally, thanks to family for their encouragement, patience and love.

TABLE OF CONTENTS

LIST OF FIGURES

Page

Page

Page

Page

Page

LIST OF TABLES

CHAPTER I

INTRODUCTION

1.1 Motivation and objectives

In spite of the maturity of the petrochemical and commodity chemical industries there are still tremendous needs for improving a variety of technologically relevant separations.[8] Traditional separation methods, such as distillation and condensation, are highly energy intensive. Membrane-based separations offer great potential in terms of their lower energy consumption and smaller carbon footprint.

The current membrane market for gas separation is dominated by polymeric membranes partially due to the fact that polymer membranes have low production costs, exhibit high gas fluxes and mechanical flexibility.[9] However, polymer membranes in general have short membrane lifetimes, low thermal and chemical stabilities and low selectivities. Robeson[10] defined an upper bound for polymer membranes delineating a limit on their selectivity/permeability performance (see Figure 1). Although this limit has been adjusted since its inception,[11] it still indicates there is a limiting tradeoff between a polymer membrane's selectivity and permeability. Besides, some of these challenges make polymer membranes generally limited to separation of non-condensable gases (H_2/N_2, CO_2/CH_4, N_2/air, etc.).[9] Condensable gas separations such as olefin/paraffin or butane isomer separations are an important area for membrane technology to expand into.[9] Unfortunately few polymer membranes are capable of olein/paraffin separation in an economically viable way and none can do so without

difficulty with issues such as durability and longevity.[9, 12] This is particularly troublesome for polymer membranes as the operating conditions these membranes are exposed to often result in membrane plasticization.[9]

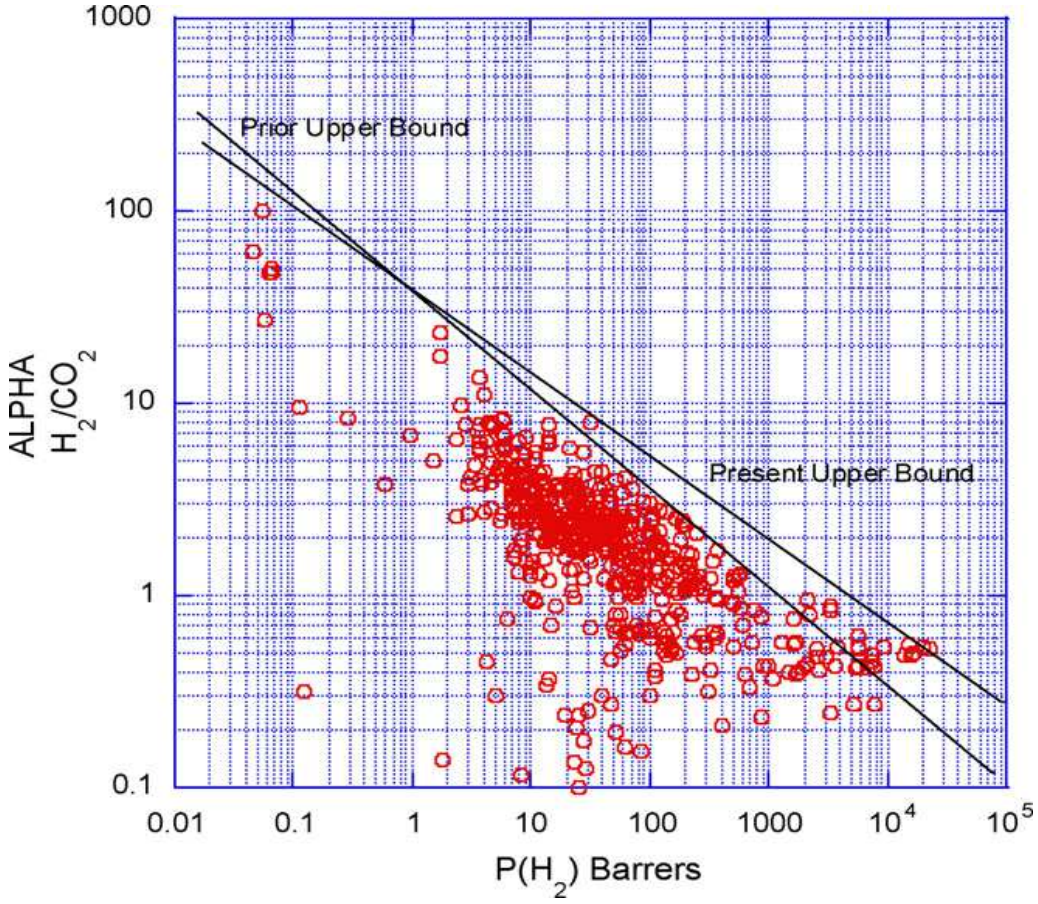

Figure 1: Upper bound correlation for H_2/CO_2 separation. (Ref.4)

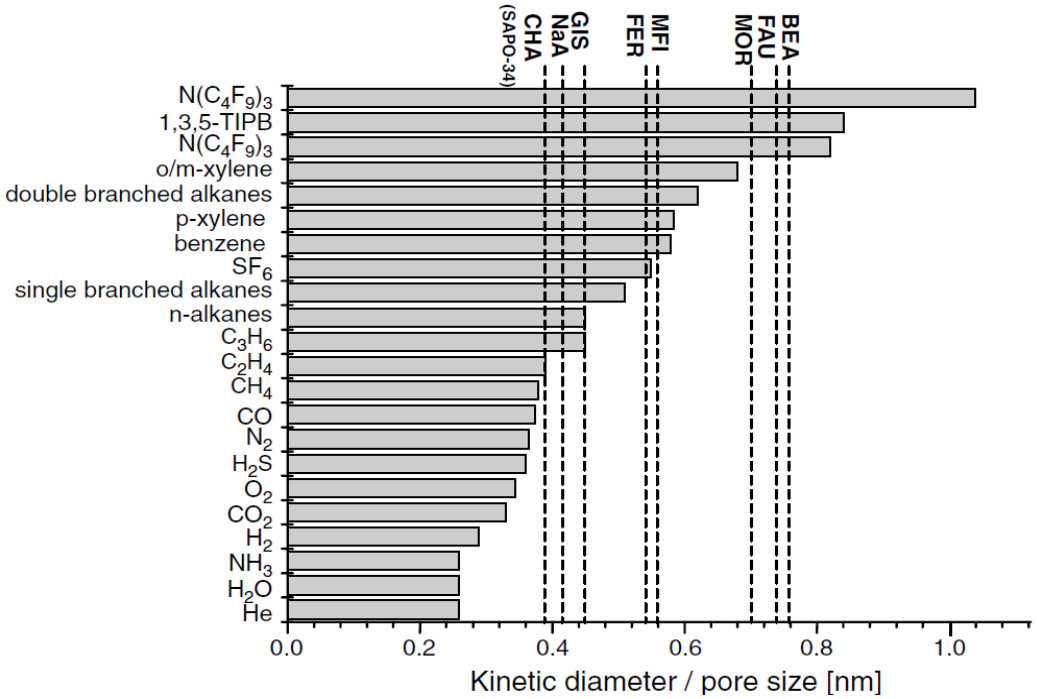

Figure 2: Comparison of effective zeolite pore sizes with kinetic diameters of common gases. Reproduced with permission. (Ref. 98)

Zeolite molecular sieves have been investigated for application in membrane separations because of their well-defined, regular pore structure and thermal and chemical stability.[13] Their well-defined pores allow zeolite membranes to achieve gas separation with high selectivity due to the molecular sieving effect.[13d, 14] The high thermal and chemical stability of these materials also makes them attractive for separation applications under high temperature and harsh chemical environments. However, zeolites also have a discontinuous and limited range of available pore sizes

(i.e., zeolites of proper pore sizes may not be available for gas mixtures of certain sizes). Figure 2 shows the kinetic diameters of various gases and the effective pore sizes of a few well-known zeolites. Apart from the high cost of production,[15] limited chemical tailorability of zeolites is another issue for wider applications of zeolite membranes in gas separations.

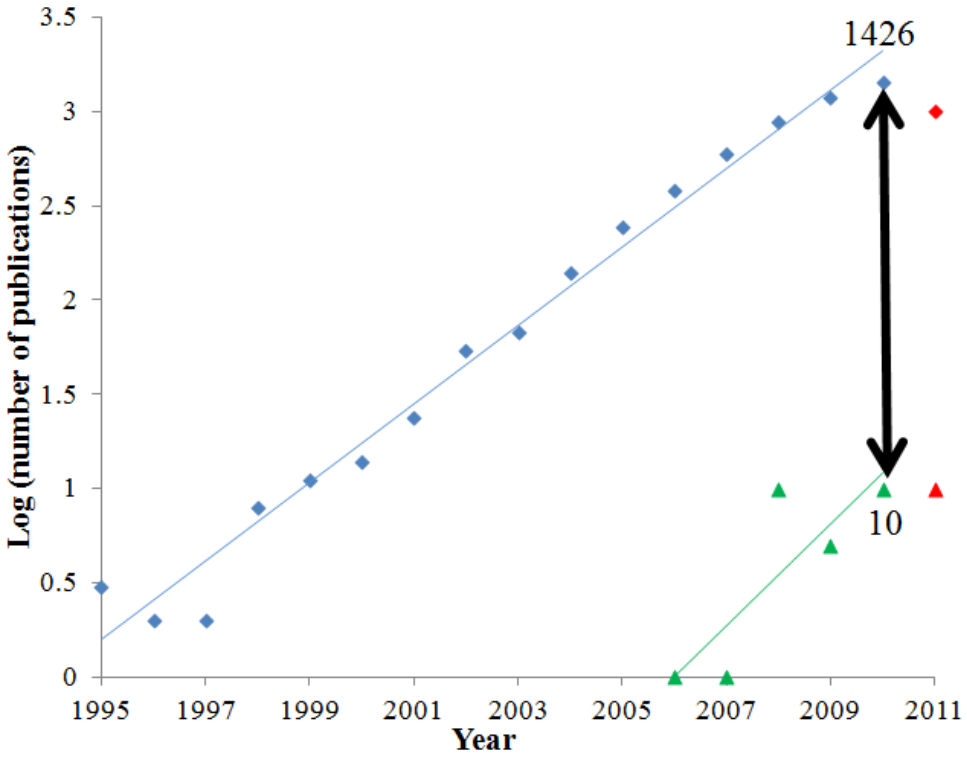

Figure 3: Publications per year containing the phrase: (■) "metal organic framework" and (▲) "metal organic framework" and "thin film". Data obtained from Sci-Finder. Data points in red indicate values up until 25th July, 2011

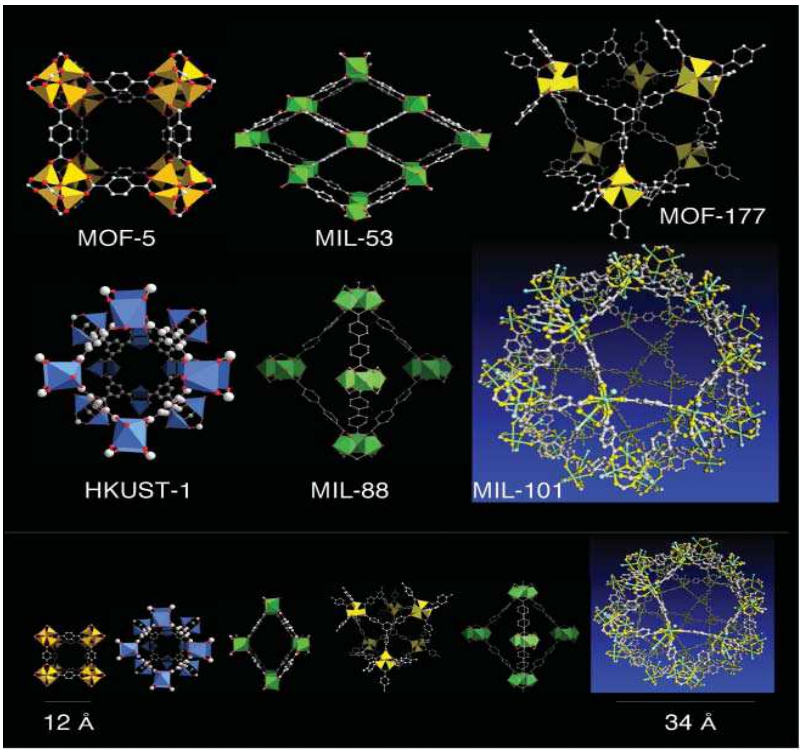

Figure 4: Various reported MOF structures. Structures are arranged according to effective pore size along the bottom. Reproduced with permission. (Ref. 11c)

Another avenue of membrane research is focused on mixed matrix membranes.[16] These membranes are generally polymer/inorganic composites consisting of a primary polymer phase and a secondary phase of dispersed inorganic particles. The intention for these types of membranes is to combine the advantages of the materials of both phases such as the high flux of polymer membranes and the high selectivity of the inorganic phase (e.g. zeolite phase). In general, it is however difficult to achieve a close interface between the two phases.[17] If there is a repulsive interaction between the phases, then the

interstitial space acts as a non-selective diffusion path. This creates difficulties in achieving permeability/selectivity performance greater than that of the polymer phase. Another issue is to incorporate inorganic particles in the submicrometer-thick selective skin layers.

Metal-organic frameworks (MOFs),[18] a relatively new class of hybrid materials (Figure 3 and 4) consisting of organic and inorganic moieties in crystalline lattices, have the potential to answer some of the challenges facing materials for gas-separating membranes.[19] Pore size tailorability combined with tunable sorption behavior provides promising avenues for applications of MOFs as membranes for gas separation applications. Synthesis conditions are less energy intensive as compared to zeolites. For instance, most MOFs do not require high temperature pressure conditions for their fabrication and can be synthesized using click chemistry. Also, unlike zeolites, structure-directing agents are not required, therefore subsequent calcination step is not necessary. Zeolitic imidazolate frameworks (ZIFs), a sub-class of MOFs, are of particular interest for gas separation applications mainly due to their ultra-micropores in the scale of small gas molecules as well as their remarkable thermal and chemical stability. [1, 20]

The focus of current MOF research for the most part has been the discovery and characterization of new MOF structures. As illustrated in Figure 3, the number of publications discussing metal-organic frameworks has increased significantly recently. Despite this rising interest, the number of reports of MOF thin films is quite small, orders of magnitude fewer (see Figure 3).[13f, 21] Still fewer in number are the reports of

MOF membranes for gas separation,[6, 22] the first MOF membranes having been published in 2009.[22b, c]

This scarcity of reports can perhaps be attributed to the challenges involved in fabricating thin films of MOF materials such as poor stability and/or poor binding to substrates among others.[23] In particular, various MOFs have been noted for their poor interaction with native substrates such as Au,[21b] silica[21c] and α-alumina,[21k, 22i, 22l] necessitating a linking agent to attach these MOFs to supports for film fabrication. This scarcity of reports can perhaps be attributed to the challenges involved in fabricating thin films of MOF materials such as poor stability and/or poor binding to substrates among others.[23] In particular, various MOFs have been noted for their poor interaction with native substrates such as Au,[21b] silica[21c] and α-alumina,[21k, 22i, 22l] necessitating a linking agent to attach these MOFs to supports for film fabrication. Thus MOF membrane fabrication provides interesting alternate avenues for enhanced gas separations. However there have not been many reports on MOF membranes due to several difficulties involved in their fabrication. Also some of the membranes reported do not show the expected gas permeation behavior.

The first MOF membranes were reported in 2009 by the Lai and Jeong groups.[22b, c] These were polycrystalline IRMOF-1 membranes and exhibited Knudsen diffusion. Although Knudsen selectivity is unsurprising considering the large pore size of IRMOF-1 (14.5 Å) [22b] these reports demonstrated the feasibility of fabricating MOF membranes for gas separation. The absence of macroscopic cracks in both of these reports was demonstrated by pressure dependent gas permeation measurements. Polycrystalline

membranes of few MOFs have been reported: such as IRMOF-1[22b, c], IRMOF-3[24], HKUST-1[22d, 22g, 22i], MMOF[22l], ZIF-7[22e, f], ZIF-8[6, 22m], ZIF-22[22j], ZIF-69[22h], ZIF-90[22n] and MIL-53[25], SIM-1[26],MIL-47[27] (on polymer surface).

In general, fabrication of thin films of crystalline framework materials follows one of two approaches: *in situ* growth and secondary or seeded growth.[13e] *In situ* growth here refers to a film fabrication method in which the substrate is immersed in the growth solution without any crystals previously attached to the surface; nucleation, growth and intergrowth of crystals on the substrate all happen during the same fabrication step. Secondary or seeded growth refers to film growth from pre-attached seed crystals. Although not as simple as *in situ* growth, secondary growth has been noted to allow better control over microstructure as well as reduced dependence on the nature of supports in polycrystalline films.[28]

There have been reported many different MOF film synthesis techniques[13f, 29] including chemical modification of the support surfaces with self assembled monolayers (SAMs).[21b-d, 21f] Though not discussed here, those who are interested in MOF film synthesis should direct their attention to recent review articles.[13f, 29] It is worthy of noting here that the requirements of MOF membranes are much more demanding than those of MOF films. Therefore, it is much more challenging to prepare MOF membranes than MOF films. MOF membranes require crystals to be well-intergrown so as to minimize non-selective gas transport through grain boundary defects. Also presence of pinhole defects, intracrystalline and intercrystalline cracks (even submicron-scale cracks) can significantly mar the gas separation performance of the membrane. Stability in harsh

environments as well as the consistency of performance for long periods of operation would be some of the other requirements that become critical from the point of view of the commercial application of MOF membranes. MOF films (generally for sensor applications) do not need to fulfill these requirements.

1.1.1 One step *in situ* method for ZIF membrane fabrication

Zeolitic imidazolate frameworks (ZIFs) are a sub-class of metal-organic frameworks (MOFs), comprising hybrid organic-inorganic moieties and exhibiting regular crystalline lattices with well-defined pore structures.[1, 18c, 29-30] ZIFs consist of metal nodes coordinated to imidazolate-based ligands. The metal-linker-metal bond angle (~145°) in ZIFs is comparable to the T-O-T bond angle in zeolites, thereby resulting in zeolite topologies. Their exceptional thermal and chemical stabilities coupled with microporous cavities [1] make them desirable candidates for gas sensors [21r], catalytic membrane reactors [31], and gas separation membranes [6, 22f-h, 22j, 22m, n]. As a result, synthesis of ZIF films and membranes has attracted a great deal of interest in recent years [5, 21j].

Among other ZIF systems, ZIF-8 is of particular interest due to their robust synthesis protocol as well as their potentials in small-gas separations. ZIF-8 consists of Zn atoms interconnected with 2-methylimidazolate ligands, forming the sodalite (SOD) zeolite-like structure with large cavities (11.6 Å) and small pore apertures (3.4 Å).[1] Diverse synthesis protocols for ZIF films and membranes have been reported [5] and can be classified into two categories: *in situ* growth[6] and secondary (seeded) growth[4, 7]. Recently Pan et al. [4] synthesized ZIF-8 membranes using secondary growth method and

showed excellent propylene/propane gas separation performance. However, secondary growth method requires a seeding step in addition to solvothermal growth step. Increased number of steps adds to the complexity of the process, thereby potentially causing reproducibility issues.[5] ZIF-8 membranes have been synthesized using *in situ* method as well. To promote heterogeneous nucleation of ZIF-8 crystals, the supports were often times modified[22m] or more expensive supports such porous titania as compared to more commonly-used α-alumina were used.[6]

Here we report one step *in situ* synthesis of ZIF-8 membranes on unmodified porous α-alumina supports in the presence of sodium formate. This approach is different from our previously reported technique[22m] in which ligand-modified supports were used to promote heterogeneous nucleation. In this work, ZIF-8 membranes were prepared on as-prepared supports, thereby eliminating the need for support modification and simplifying the process. The role of sodium formate in this one step *in situ* method was investigated. Besides the previously reported role of sodium formate as a deprotonator promoting the intergrowth of ZIF crystals[22m], we identified the unknown role of sodium formate of promoting heterogeneous nucleation on α-alumina supports. One step *in situ* method was used to prepare continuous films of several other ZIFs including ZIF-7[1], $Zn(Im)_2$ (ZIF-61 analogue)[18d, 32], ZIF-90[33] and SIM-1[31a], suggesting the general applicability of the method.

1.1.2 MOF membrane fabrication by rapid thermal deposition (RTD)

Polycrystalline MOF membranes reported in the literature are made by mainly two broad approaches: *in situ* growth and secondary growth. *In situ* growth can be carried out

on modified or unmodified supports. Typically, inorder to promote heterogeneous nucleation of MOFs on traditional supports like α-alumina, they are modified with silanes,[22j, 22n] organic linkers,[22m] followed by nucleation and growth of during solvothermal synthesis. Supports can also be modified to act as a secondary metal source for *in situ* growth.[22d] Secondary growth involves seeding the support by manual deposition (rubbing), seed attachment using polymer binder,[7a] slip coating,[7b] dipping, ultrasonication,[34] microwave[21i, 22b] etc., followed by secondary growth of these seed crystals. Thus nucleation and growth steps are decoupled. Thus for most cases, alongwith solvothermal growth, additional steps are required for support modification (*in situ* growth) or seeding (secondary growth). This adds to the complexity of the process and limits its scalability and reproducibility.

Although properties of MOFs (co-ordination chemistry) are fairly different from those of zeolites (covalent chemistry), the above mentioned synthesis strategies are inherited primarily from the zeolite membrane community. As a result commercialization of MOF membranes, would also be limited by factors similar to those for zeolites: slow batch processes, reproducibility and scalability issues due to multiple complex steps and expensive supports, thereby making them extremely cost intensive ($4000/m^2).[35] MOF membranes reported in the literature require long time (ranging from few hours to days) for synthesis. A typical solvothermal growth step is carried out in batch reactors (autoclaves) in which pressures often exceed atmospheric pressure. Furthermore, MOF synthesis typically uses exotic ligands that are generally expensive (most of them are synthesized in the lab and not available commercially). For membrane

fabrication, a substantial amount of ligand is consumed during *in situ* or secondary growth. Also large amount of usually non-environment friendly solvents are used. These factors further increase the cost of MOF membranes.

Thus there is a strong need for novel out of the box approach for making MOF membranes. The new technique should have advantages of being rapid, continuous, scalable, reproducible, economical and at the same time generate high quality of MOF membranes. Keeping in mind the limitations of current techniques and taking advantage of the fundamentally different MOF chemistry (co-ordination chemistry) as compared to zeolite chemistry (covalent chemistry), we developed a novel out of the box approach for making polycrystalline MOF membranes, henceforth referred to as Rapid Thermal Deposition (RTD) technique. Using temperature as the driving force, membranes were synthesized rapidly (within few minutes) without sacrificing the membrane performance. This relatively simple, robust and potentially general RTD technique can be easily commercialized as a continuous method. Superior attachment of films to substrates at higher temperatures, minimum consumption of precursors, enhanced mechanical properties, improved microstructure and microstructure control are other noteworthy features of the RTD technique. Here we used two prototypical MOFs, HKUST-1 and ZIF-8, to demonstrate the applicability of the RTD technique.

1.2 Proposal

To overcome limitations of conventional approaches, two new approaches were developed for synthesis of MOF membranes. The membranes thus obtained were

characterized using X-Ray Diffraction (XRD), Scanning Electron Microscopy (SEM), Energy Dispersive X-Ray Spectroscopy (EDS), single and binary gas permeation testing using time-lag and Wicke-Kallenbach techniques.

1.2.1 One step *in situ* method for ZIF membrane fabrication

A simple one step *in* situ method is demonstrated to make continuous well-intergrown ZIF-8 membranes in a reproducible manner. The essence of this method is the addition of sodium formate to the *in situ* growth solution (containing metal and ligand precursors).

1.2.1.1 What is the role played by sodium formate in one step *in situ* method?

The presence of sodium formate promotes formation of zinc oxide layer on the support surface. This zinc oxide layer acts as a secondary metal source and a nucleation site to promote heterogeneous nucleation of ZIF-8 crystals. Once these crystals are nucleated on the support surface, the previously reported role of sodium formate as deprotonator[22m] allows the crystals to grow uniformly in all directions and leads to continuous well-intergrown films of membrane quality.

1.2.1.2 Can one step *in situ* method be applied to other ZIFs in general?

Since the formation of zinc oxide is not dependent on the type of ligand used for growth and because most ZIFs have zinc as metal center, this technique or role of sodium formate can be extended to the synthesis of other ZIF membranes. ZIF-7,[1]

$Zn(Im)_2$ (ZIF-61 analogue)[18d, 32], ZIF-90[33] and SIM-1[31a] films were synthesized to demonstrate the general applicability of the technique. The synthesis conditions can be optimized to yield membrane quality films.

1.2.2 MOF membrane fabrication by Rapid thermal deposition (RTD)

Rapid Thermal Deposition (RTD) technique is an unorthodox approach for the synthesis of MOF membranes. Schematic illustration of the RTD technique is shown in Section 5.2. An unmodified α-alumina disc support was slip coated with the RTD precursor solution (for details refer to the experimental section). Temperature was used as the driving force to promote solvent evaporation, supersaturation, heterogeneous nucleation and growth of MOF crystals, leading to rapid synthesis of MOF membranes. The potential of this technique was first demonstrated for prototypical and relatively stable MOF, HKUST-1.[14a] The technique was then extended to more promising candidates like ZIF-8. Following are the questions that we tried to answer to demonstrate our new method.

1.2.2.1 What physical processes occur during RTD and how are they controlled?

During RTD, processes such as flow of liquid inside the support, evaporation of solvent, formation of crystals and drying and activation of crystals occur almost simultaneously. The time scales of crystal formation and solvent evaporation were found critical. Rapid formation of crystals relative to solvent evaporation time scale causes excessive homogeneous nucleation to occur whereas the other extreme of rapid solvent

evaporation greatly hinders crystal formation and its growth. In either case, the film quality is poor. As a result both the time scales need to be optimized so that continuous, well intergrown membrane quality films are realized before the solvent is evaporated. The parameters used to control crystallization and evaporation rates include molar composition and concentration of precursors in the RTD solution, the RTD temperature, deprotonators or catalysts to speed up reaction rate, the type of solvent and its vapor pressure.

1.2.2.2 What are the potential advantages of RTD over conventional synthesis approaches?

Membranes with improved microstructure were synthesized in tens of minutes. Microstructure is different from conventionally synthesized membranes. Crystal facets are difficult to distinguish and grow from inside of the support leading to enhanced mechanical properties and gas separation performance.

1.3 Outline

Chapter I explains the motivation, proposal and the main objectives of this research. Chapter II provides background information on chemistry of MOFs in general, their limitations and criteria for choosing MOFs for membrane applications. Currently pursued approaches for MOF membrane synthesis, challenges associated with it and strategies reported to address these problems are also discussed in this chapter. In Chapter III, detailed experiment procedures are provided for the preparation of

MOF/ZIF membranes by one step *in situ* method and RTD and their characterization thereafter.

Chapter IV presents the one step *in situ* method using sodium formate, the investigation of role of role sodium formate and the general applicability of the technique. Chapters V, VI and VII deal with RTD technique for MOF membranes fabrication. Chapter V reviews the RTD technique for MOF membrane synthesis in general. Specific details related synthesis and characterization of HKUST-1 and ZIF-8 membranes by RTD are discussed in Chapter VI and VII respectively. oriented MFI zeolite membranes with controlled thickness, orientation and grain boundary. Finally, Chapter VIII summarizes the results obtained in this dissertation, and suggestions are given for the future work.

CHAPTER II

CURRENT STATUS OF METAL-ORGANIC FRAMEWORK (MOF) MEMBRANES FOR GAS SEPARATIONS: PROMISES AND CHALLENGES*

2.1 MOFs structure, chemistry and stability

Metal-organic frameworks have attracted research interest as noteworthy porous materials for over a decade.[18] MOFs are comprised of metal nodes and organic linkers connected by coordination covalent bonds with typical pore size ranging from ultra-microscale to mesoscale. Chemical functionalization of the organic linkers in the structures of MOFs affords facile control over pore size and chemical/physical properties, making MOFs attractive materials to overcoming the limitations of not only current membrane materials but also conventional membrane system design/integration and operation.[36]

.

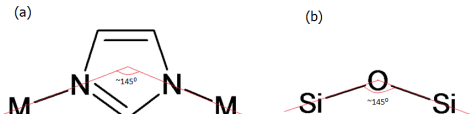

Figure 5: The bridging angles in metal imidazolates (a) and in zeolites (b)

*Reprinted with permission from "Current Status of Metal–Organic Framework Membranes for Gas Separations: Promises and Challenges." by M. Shah, M.C. McCarthy, S. Sachdeva, A.K. Lee, H.-K. Jeong, Industrial & Engineering Chemistry Research 2012, 51 (5), 2179-2199. Copyright 2012 American Chemical Society.

In this section, we discuss the structures, chemistry, and stability of metal-organic frameworks. This discussion is relevant to the later discussions on the synthesis of MOF membranes.

2.1.1 MOF structures

Thousands of metal-organic framework structures have been reported to date, exhibiting properties useful for gas separation[30c], gas storage[37], chemical sensors[21g], and optical devices.[21q] Figure 4 illustrates some of the MOF structures that are most extensively studied including two prototypical MOFs used in pioneering MOF membrane reports (MOF-5[22c] and HKUST-1[22d]). There are several excellent review articles[8c, 12c, 14] on the MOF structures (and chemistry) for those who are interested more about the chemistry and structure of MOFs.

An important subclass of metal-organic frameworks, especially when considering gas separation applications, is zeolitic imidazolate frameworks (ZIFs).[20] These materials, first reported in 2006 by Park et al.[1] and expanded upon significantly in later reports,[18d, 38] are remarkable for their exceptional thermal and chemical stability. The thermal/chemical stability of ZIFs in combination of their small pores (generally less than 5 Å) make ZIFs particularly promising candidates for membrane-based gas separation applications. ZIFs consist of metal nodes (usually zinc or cobalt) connected to imidazolate linkers and exhibit zeolite-like structures, perhaps due to the metal-linker-metal bond angle of ~145° (close to the Si-O-Si angle found in many zeolites)[1] as shown in Figure 5. However, unlike zeolites which possess rather well-defined pores, ZIFs (like

many other MOFs) exhibit framework flexibility on gas adsorption. This framework flexibility has been demonstrated by experimentation and simulations for ZIF-8.[39] It is noteworthy that to date, more ZIFs have been investigated for gas separation membranes than any other kind of MOF.[6, 22a, 22e, 22g, h, 22j, 22m]

2.1.2 Mechanisms of MOF formation and chemistry

One attractive attribute of MOFs is the ease with which they can be synthesized, the so called "click-chemistry." Approaches to design and synthesis of these materials have been discussed in detail elsewhere.[40] Although the chemical steps leading to MOF formation are still debatable, there are two generally understood explanations (mechanisms). One explanation involves the formation of building blocks of molecules called secondary building units (SBUs) that in turn come together to form coherent structures.[21c, 40c, d] Not much evidence of this synthesis route is available, though there is one report that gives X-ray absorption Extended X-ray absorption fine structure (EXAFS) evidence of intact trimeric iron oxide SBUs during the crystallization of MIL-89.[41]

The second explanation does not include SBUs, but rather hydrolysis or condensation reactions between dissolved metal salts and organic ligands in solution (see Figure 6).[42] This explanation states that metal salts dissolve in solution and form point of zero charge (pzc) molecules. These metal complexes at their isoelectric points organize into supramolecular assemblies which then undergo condensation/hydrolysis to form crystalline structures.

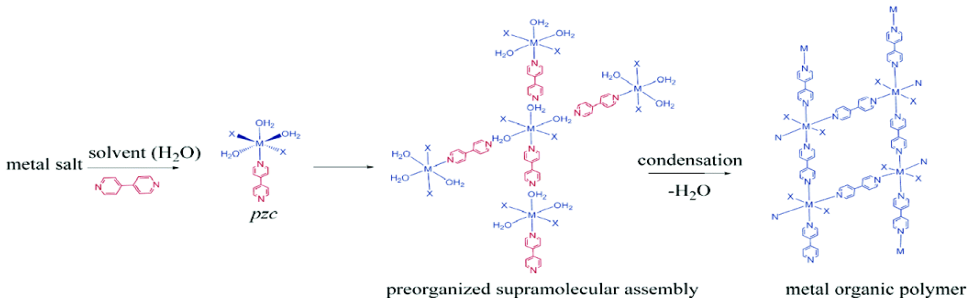

Figure 6: Proposed scheme of MOF crystal formation in solution through formation of point of zero charge (pzc) molecules and hydrolysis/condensation reactions with dissolved metal salts. Reproduced with permission. (Ref. 42)

Irrespective of the mechanisms, however, the bonding between metal and organic linker in the final MOF structure (irrespective of the mechanism) is coordination bonding, which is kinetically weaker (i.e., more labile) than covalent or covalent/ionic bonding seen in zeolites. This coordination bonding is likely the major factor contributing to many of the challenges associated with fabrication of MOF membranes.

2.1.3 Stability of coordination bonds in MOFs

As mentioned above, coordination bonds between metal nodes and organic ligands are one of the major features of MOF structures. Coordinate covalent bonds involve the sharing of a pair of electrons, both donated from a Lewis base (organic linkers in MOFs) to a Lewis acid (metal nodes in MOFs). These special covalent bonds are thermodynamically as stable as other covalent bonds, but are not kinetically as stable (i.e. they can be replaced or substituted with other ligands or species such as water).

Complexes featuring coordination bonds between a metal and an organic ligand have been widely studied.[43] Although we will not attempt to give a complete overview of the nature of metal-organic coordination bonds, it is instructive to consider a few points that will help us to understand the stability or instability of MOF structures.

The well-known Irving-Williams series (listed below) describes the relative stability of metal-organic octahedral complexes in terms of metal ions regardless (generally) of ligands.[44]

$Ba^{2+} < Sr^{2+} < Ca^{2+} < Mg^{2+} < Mn^{2+} < Fe^{2+} < Co^{2+} < Ni^{2+} < Cu^{2+} > Zn^{2+}$

There are a few explanations for this trend such as the decreasing ionic radius from Ba^{2+} to Zn^{2+} and the increasing crystal field stabilization energy (CSFE) from Mn(II) to Ni(II). Although copper does not fit the CFSE trend, it is generally accepted that distorted octahedral Cu(II) complexes are stabilized by the Jahn-Teller effect. [43] The Jahn–Teller theorem states that any non-linear molecular system in a degenerate electronic state will be unstable and will undergo distortion to form a system of lower symmetry and lower energy, thereby removing the degeneracy.[45] The Irving-Williams series may give some insight into the stability trends of MOFs in general based on the stability of their octahedral complexes, but it is helpful for our purposes to discuss in particular those MOFs that have been developed as membranes. Collectively, these MOFs feature only a few particular coordinate covalent bonds: Zn-O (IRMOF-1), Cu-O (HKUST-1), Al-O (MIL-53) and Zn-N (ZIF series). Of these, IRMOF-1 is the least stable since it will readily change phase to a nonporous structure in ambient humidity via water substitution of the carboxylic groups.[46] Apart from Al-O based MIL-53, the ZIF

series are likely the most stable of these MOFs. In fact many ZIFs (ZIF-8,[1] ZIF-11,[1] and ZIF-69[22h]) have been observed to maintain their crystal structure even in boiling solvents such as benzene and water.

To gain insight into the relative stabilities of these compounds it is instructive to consider the hard or soft character of the cations and anions as first classified by Pearson in 1963.[47] Hard or soft character is determined by polarizabilities of species which in turn depends on their charge density.[45] Zn^{2+} and Cu^{2+} are both classified as intermediate acids (borderline between hard and soft). Ligands with carboxylate groups (such as acetate) are considered hard bases whereas imidazole is an intermediate base (see Table 1).[48] Pearson's rule states that hard acids prefer bonding to hard bases and soft acids prefer bonding to soft bases. Consequently, it makes sense that ZIFs are more stable MOFs than the aforementioned MOFs (except MIL-53) used for membranes since the cation and anion have the same character (intermediate).

Table 1: Examples of hard and soft acids and bases. Reproduced with permission. (Ref. 47)

	Hard	Soft	Borderline
Acids	H^+, Li^+, Na^+, K^+, Be^{2+}, Mg^{2+}, Ca^{2+}, Sr^{2+}, Mn^{2+}, Al^{3+}, Cr^{3+}, Co^{3+}, Fe^{3+}	Cu^+, Ag^+, Au^+, Hg^+, Pd^{2+}, Cd^{2+}, Pt^{2+}, Hg^{2+}, Pt^{4+}, Te^{4+}	Fe^{2+}, Co^{2+}, Cu^{2+}, Zn^{2+}, Pb^{2+}, Sn^{2+}, Sb^{2+}, Bi^{3+}, NO^+, SO_2, R_3C^+, $C_6H_5^+$
	Si^{4+}, Ti^{4+}, Zr^{4+}, Sn^{4+}, Hf^{4+}, BF_3, AlH_3, $Al(Me)_3$, SO_3, RSO_2^+, RPO_2^+, HF, HCl	RS^+, I^+, Br^+, I_2, Br_2, O, Cl, Br, I	
Bases	H_2O, OH^-, F^-, Cl^-, RO^-, PO_4^{3-}, ClO_4^-, SO_2^{2-}, CO_3^{2-}, ROH, RO, ROR, RCOR, $RCOO^-$, NH_3, RNH_2, NH_2NH_2	R_2S, RSH, RS^-, I^-, SCN^-, CN^-, I^-, R^-, H^-, $S_2O_3^{2-}$	Br^-, NO_3^-, SO_2^{2-}, N_2, $PhNH_2$, pyridine
		$CH_2=CH_2$, C_6H_6	
		CO, NO	Imidazole

2.2 Criteria for MOFs for membrane-based gas separations

For membrane-based gas separations, both the solubility and the diffusivity of the mixture components contribute to the separation factor. While the solubility of a gas molecule is governed by thermodynamic affinity of the molecule on membrane surface, its diffusivity is governed by the relative size of molecules with respect to the size of the framework pores. In principle, strongly adsorbing and faster diffusing species lead to higher separation factors. The solubility and/or diffusivity can be varied by the presence of side groups on the organic linkers. These side groups are responsible for not only altering the pore size but can also the change the thermodynamic interaction or sorption behavior to achieve the desired separation.

For solubility-based separations, separations of molecules are based on the difference in the solubilities of gases. In this case, the framework pores are larger than the size of molecules of interest. The solubility of one component can be selectively enhanced by controlling surface properties. For example, it has been shown that by replacing carbon with nitrogen in imidazolates, one can tune the hydrophilicity of ZIFs and also affinity for CO_2, thereby increasing CO_2 solubility.[49] Not only the ligands but also the functional groups (e.g., the CHO side groups for ZIF-90 and SIM-1 were post-synthetically modified with ethanolamine and dodecylamine respectively)[31b, 50] provide variable pore volume and interaction based on their radii and hydrophilic and hydrophobic character. Thus the thermodynamic (and kinetic behaviors) can be varied for improved membrane performance.[50]

In the case of molecular size-based separations the kinetic diameters of the molecules to be separated determine the pore size of MOFs suitable for separation of the molecules.[19b] MOFs whose pore sizes lie in the desired range can be chosen accordingly. Framework interpenetration can also lead to the reduced pores for kinetic separations.[51] It is important to note here that molecules with kinetic diameter greater than the pore size can pass through the membrane due to framework flexibility. Duren and co-workers[39] have shown by molecular simulation and experimental results that the structure of ZIF-8 can be modified by gas adsorption, thereby increasing the porosity. This phenomenon is akin to the swing effect seen in case of imidazolate linkers at very high pressures (14700 bar).[52] At lower partial pressure of N_2, gas adsorption is in agreement with ZIF-8 structure under ambient conditions, however, at higher partial pressures the high uptake is due to the swing effect of imidazolate linkers.[39] As a result, some of these membranes may not exhibit a sharp drop in permeance for molecules with kinetic diameter greater than the pore size. Nijem and co-workers[53] have demonstrated that for a flexible MOF, Zn2(bpdc)2(bpee) (bpdc = 4,40-biphenyl dicarboxylate and bpee = 1,2-bis(4-pyridyl)ethylene), the CO_2-framework (guest-host) interaction leads to the twisting of one of its ligands made possible by bpee pillars. This is responsible for gate opening phenomenon and enhanced uptake of CO_2 over N_2.

Other important factors to be considered are as follows:

1. Ease of fabrication: While zeolites typically require high temperature-pressure conditions for synthesis, most MOFs require lower activation energy for their synthesis. Room temperature fabrication of HKUST-1, ZIF-8, MOF-5, MOF-74, MOF-177, MOF-

199, IRMOF-0 has been reported.[18e, 54] This enhances the robustness of membrane fabrication in shorter time with milder conditions.

2. Ease of activation: A large variety of MOFs can be synthesized using water and alcohol as solvent.[54b, 55] As a result, activation of such MOF membranes does not require time and energy consuming steps such as calcination and solvent exchange.

3. Active metal centers: Unsaturated metal sites facilitate electrostatic interaction with the guest molecules, Li and co-workers[56] demonstrated 100% oxidation of CO oxidation to CO_2 using Cu(mip) (mip = 5-methylisophthalate). The remarkable catalytic activity was attributed to high density of active Cu sites.[56]

4. Gate opening or breathing effect: Several MOFs show gate opening effect due to adsorbent-adsorbate interactions.[57] The breathing effect is determined by threshold pressures which are different for different gas molecules, thereby make them exciting for gas separation applications, especially olefin/paraffin separation.[3] Controlling the partial pressure of species to desired threshold value might be challenging.

2.3 Challenges specific to polycrystalline MOF membranes

Successful fabrication of polycrystalline metal-organic framework membranes of sufficient quality for gas separation is a challenging task mainly due to the unfavorable heterogeneous nucleation and the relative weakness of the coordination bonds. For instance, various MOFs have been noted for their poor interaction with native substrates such as Au,[21b] silica,[21c] and α-alumina.[21k, 22i, 22l]

The relative weakness of the coordination bond (as discussed in the previous section) is of particular challenge. The labile nature of the coordination bond in the MOF lattice leads to numerous complexities for MOF membranes fabrication (discussed in the following sections). Other nanoporous inorganic materials that have been studied for gas-separating membranes (e.g. zeolites) do not have to contend with these same challenges.[58]

It is perhaps self-evident that not all MOFs will present the same issues when incorporated into polycrystalline membranes for gas separation. However, a general understanding of the challenges encountered for some prototypical MOFs that have already been reported as polycrystalline membranes will help to mitigate and overcome similar challenges in the future. The common challenges facing polycrystalline MOF membranes can be broken down into the following categories: 1) poor membrane-substrate bonding, 2) poor membrane stability, and 3) macroscopic crack formation during membrane fabrication or activation.

2.3.1 Poor substrate bonding

Various MOFs have been noted for their lack of sufficient interfacial interaction with native supports for membrane fabrication.[22b, 22e, 22i, j, 22l] IRMOF-1, for example, was found to easily detach when synthesized on anodized aluminum oxide (AAO) supports.[21i] As illustrated in Figure 7, films of IRMOF-1 grown on AAO easily break off under sonication. However, IRMOF-1 films on graphite coated AAO were much more strongly bound (~80% coverage remained after an hour of sonication). Although investigations of MOF film attachment are not abundant, this study illustrates the utility of linking agents for MOF film fabrication on porous supports. Some reported techniques used to improve MOF crystal adhesion to porous supports for membrane fabrication include the use of polymer binders,[22e, 22l] and graphite coatings,[22b] which enhance secondary bonding like H-bonding or van der Waals interactions whereas silane tethers (Figure 8),[21b, 22j, 22n] and support modification with the precursor chemicals of the MOF of interest[22i, 22m] enhance the covalent attachment. The covalent attachment of the ligand to the substrate can also occur during *in situ* growth.[31a, 59] This last technique is notable as it requires no more chemicals than are already necessary for MOF growth.

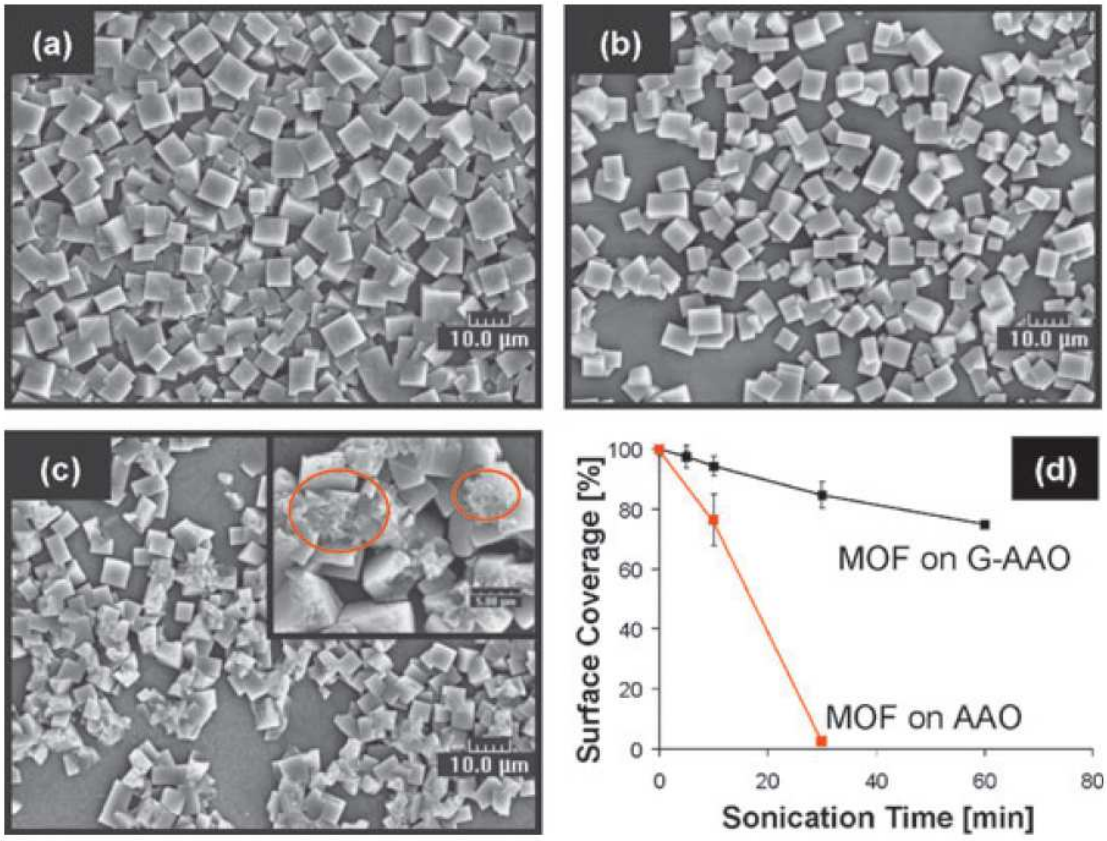

Figure 7: SEM images of IRMOF-1 films on graphite coated AAO treated under sonication for (a) 0 min, (b) 10 min, and (c) 60 min. Section (d) shows the results of a sonication time-dependent surface coverage study comparing IRMOF-1 on bare AAO to IRMOF-1 on graphite coated AAO. Reproduced with permission. (Ref. 21i)

2.3.2 Poor stability (in ambient conditions)

Many MOFs (in particular MOFs based on Zn-O coordination bonds) exhibit poor stability. For instance, IRMOF-1 has been noted for its instability in contact with ambient humidity due to the exchange reaction of carboxylates with water.[21m, 46, 60] Although initial MOF membrane reports have not investigated this matter, it is nonetheless a crucial issue to be addressed before MOF membranes for gas separation can be industrially applied.

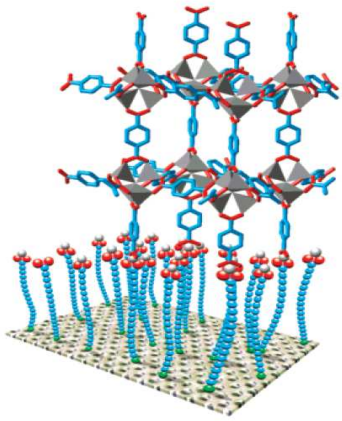

Figure 8: The concept of anchoring a typical MOF-5 building unit to a carboxylic acid-terminated SAM. Reproduced with permission. (Ref. 21b)

Post-synthetic modification of metal-organic frameworks has been studied to improve their stability. Nguyen and Cohen [60] showed that modification of the IRMOF-3 structure with long alkyl chains showed hydrophobic behavior, thereby improving stability against moisture. We have recently investigated IRMOF-3 membranes for application to CO_2 separation.[24] IRMOF-3 is a natural choice for this application as the amine functionalized benzenedicarboxylate linkers increase the pore affinity for CO_2.[61] Pore functionalization of this MOF has also been demonstrated,[62] implying that membranes of this material would be useful as chemically tunable membranes. To stabilize these membranes, we have found it necessary to first coat the membranes, immediately after activation, with an amphiphilic surfactant (Span-80 in this case). It was found that this coating dramatically increased the material longevity, preventing ambient moisture from attacking the MOF structure.[24](Figure 9)

The ligand used for membrane fabrication itself can be modified to improve stability. Li and co-workers[63] have demonstrated for carboxylate-based bridging MOF with bipyridine pillar linker, that the presence of hydrophobic groups adjacent to coordinating nitrogen atom of the bipyridine protects the metal ions and leads to enhanced moisture resistance.

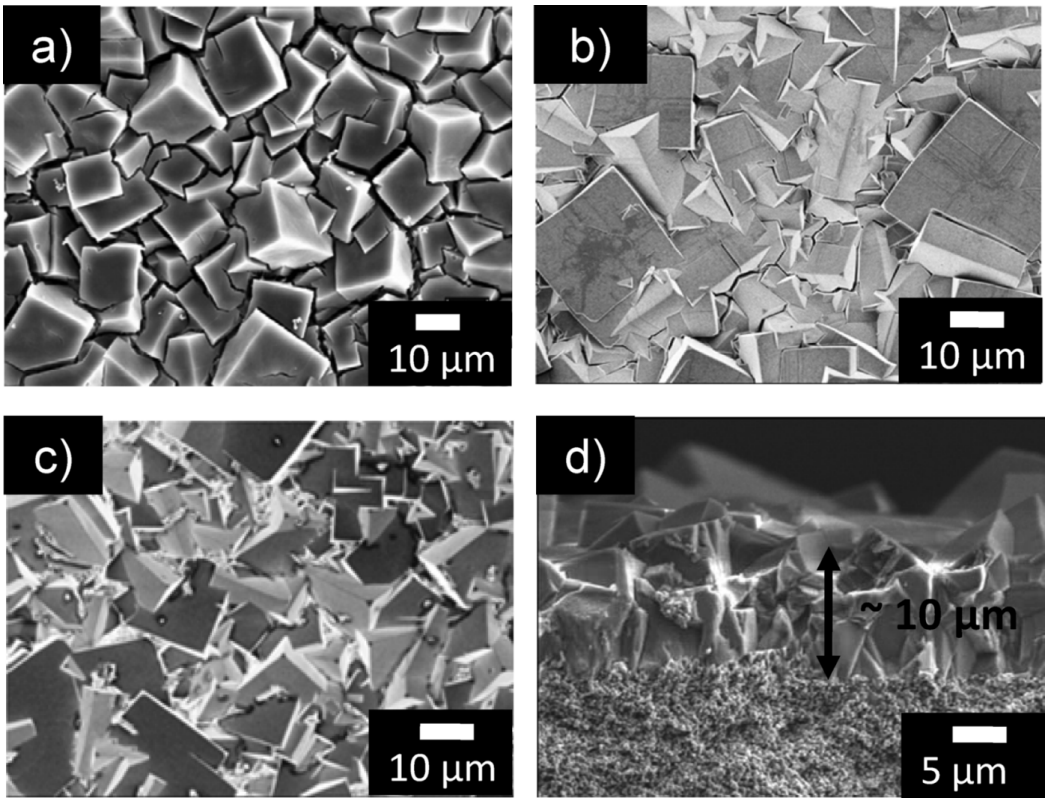

Figure 9: SEM images of IRMOF-3 membranes after drying (a) without surfactant (b) with a triblock copolymer, P-123, and (c) Span 80. The cross-sectional view (d) is from the membrane dried in the presence of Span 80. Reproduced with permission. (Ref. 24)

2.3.3 Crack formation during fabrication

Macroscopic or microscopic cracks in polycrystalline films can form for a number of reasons and will likely ruin a membrane's performance for gas separation.[14a] Crystalline materials such as zeolites are hard, but tend to crack rather than deform under stress.

MOFs, also being crystalline, are mechanically brittle. Consequently when using MOFs for polycrystalline gas-separating membranes, methods used for the prevention of cracks is a subject of importance.

Cracks in MOF membranes have been observed to form due to thermal stresses induced while cooling membranes after synthesis at elevated temperature.[22i] HKUST-1,[22i] ZIF-69,[22h] and IRMOF-1[22b, c] membranes were all reported to require slow (natural) cooling after synthesis rather than quenching (as is common after synthesis of zeolite membranes). The effect of cooling rate on HKUST-1 membranes is quite dramatic as seen in Figure 10. The reasons for crack formation in films that were rapidly cooled can perhaps be explained by the mismatch in thermal expansion between MOF film and porous supports. Although no MOF membrane report to date has given specific evidence of this (by measuring and comparing thermal expansion coefficients of film and support), several reports have mentioned natural cooling for long times as part of the membrane synthesis (sometimes for as long as 30 hours).[22b, c, 22h, i]

Drying of MOF membranes after synthesis can also result in crack formation. Capillary stresses in drying films are caused by surface tension at the solid/liquid interface in film pores during drying and by vapor-pressure differences at the liquid-gas interface in different film pores.[64] The vapor pressure at the liquid/gas interface is inversely proportional to the radius of curvature of the surface. Thus, as the film dries and the drying front of liquid moves into the film pores, any non-uniformity in the pore structure (such as grain boundaries or film defects) will lead to asymmetric stress in the film due to the differences in vapor pressure in adjacent pores. One method we have

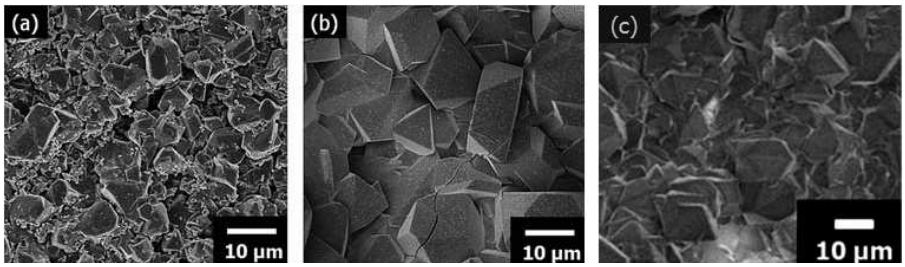

Figure 10: SEM images of HKUST-1 membranes we reported which illustrate the difference in rapid cooling (a) and slower cooling (b) slow cooling and slow drying in nearly saturated conditions (c) of films after synthesis. Reproduced with permission.(Ref. 22i)

found for reducing capillary stresses in MOF membranes is by decreasing the drying rate (drying in nearly saturated conditions) as shown in Figure 10c.[22i] Another method we have found for decreasing capillary stress is by introducing a surfactant to the film surface during the drying stage.[24] A surfactant serves to decrease solid/liquid surface tension and thereby decrease capillary stress.[64]

2.4 MOF membrane fabrication techniques

The first MOF membranes were reported in 2009 by the Lai and Jeong groups.[22b, c] These were polycrystalline IRMOF-1 membranes and exhibited Knudsen diffusion. Although Knudsen selectivity is unsurprising considering the large pore size of IRMOF-1 (14.5 Å) [22b] these reports demonstrated the feasibility of fabricating MOF membranes for gas separation. The absence of macroscopic cracks in both of these reports was demonstrated by pressure dependent gas permeation measurements. Polycrystalline

membranes of few MOFs have been reported: such as IRMOF-1[22b, c], IRMOF-3[24], HKUST-1[22d, 22g, 22i], MMOF[22l], ZIF-7[22e, f], ZIF-8[6, 22m], ZIF-22[22j], ZIF-69[22h], ZIF-90[22n] and MIL-53[25], SIM-1[26],MIL-47[27] (on polymer surface).

In general, fabrication of thin films of crystalline framework materials follows one of two approaches: *in situ* growth and secondary or seeded growth.[13e] *In situ* growth here refers to a film fabrication method in which the substrate is immersed in the growth solution without any crystals previously attached to the surface; nucleation, growth and intergrowth of crystals on the substrate all happen during the same fabrication step. Secondary or seeded growth refers to film growth from pre-attached seed crystals. Although not as simple as *in situ* growth, secondary growth has been noted to allow better control over microstructure as well as reduced dependence on the nature of supports in polycrystalline films.[28]

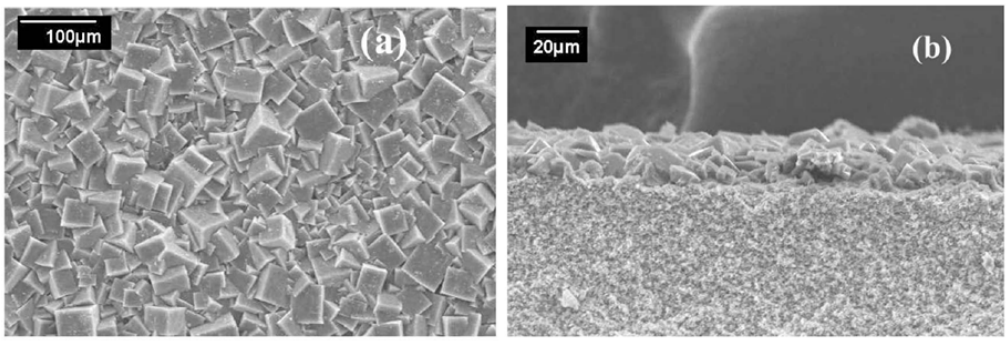

Figure 11: SEM images of MOF-5 membrane: (a) top view, (b) cross section. Reproduced with permission.(Ref. 22c)

There have been reported many different MOF film synthesis techniques[13f, 29] including chemical modification of the support surfaces with self assembled monolayers (SAMs).[21b-d, 21f] Though not discussed here, those who are interested in MOF film synthesis should direct their attention to recent review articles.[13f, 29] It is worthy of noting here that the requirements of MOF membranes are much more demanding than those of MOF films. Therefore, it is much more challenging to prepare MOF membranes than MOF films. MOF membranes require crystals to be well-intergrown so as to minimize non-selective gas transport through grain boundary defects. Also presence of pinhole defects, intracrystalline and intercrystalline cracks (even submicron-scale cracks) can significantly mar the gas separation performance of the membrane. Stability in harsh environments as well as the consistency of performance for long periods of operation would be some of the other requirements that become critical from the point of view of the commercial application of MOF membranes. MOF films (generally for sensor applications) do not need to fulfill these requirements.

2.4.1 *In situ* growth

2.4.1.1 *In situ* growth on unmodified supports

As mentioned above, fabrication of membranes of metal-organic frameworks is complicated by the fact that there is usually no strong interfacial bonding between MOFs and the native substrates of interest (which for MOF membranes are typically α-Al_2O_3 or TiO_2). Consequently, not many MOF membranes have been reported that were synthesized without some kind of pretreatment to the porous support. Liu and

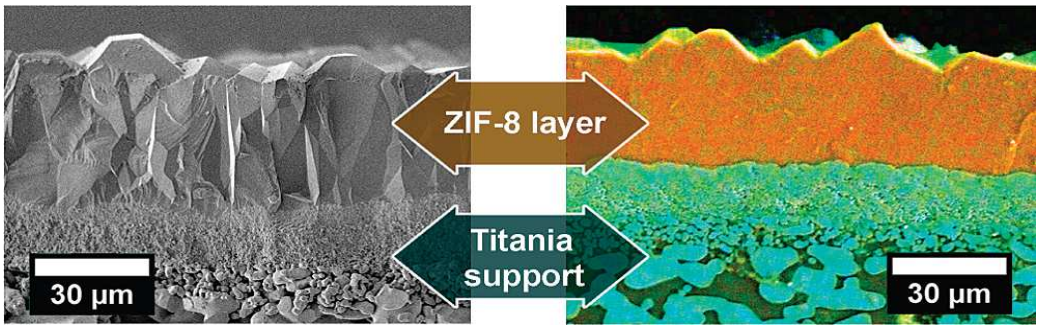

Figure 12: (left) SEM image of the cross section of a simply broken ZIF-8 membrane. (right) EDXS mapping of the sawn and polished ZIF-8 membrane (color code: orange, Zn; cyan, Ti). Reproduced with permission.(Ref 6)

coworkers were able to grow membranes of IRMOF-1[22c] (Figure 11) and ZIF-69[22h] on α-alumina without substrate modification. Bux et al.[6] grew membranes of ZIF-8 on bare titania using microwave irradiation (Figure 12). The nature of the bonding of their membranes with the substrate is not discussed. For MOFs based on ligands with carboxylic acid groups, however, it is very likely to form covalent bonds between the carboxyl groups of ligands and the surface hydroxyl groups of alumina supports.[59]

2.4.1.2 *In situ* growth on modified supports

Support modification, as mentioned previously, is an effective strategy for improving heterogeneous nucleation of MOFs for membrane fabrication. Caro and co-workers have reported ZIF-22[22j], ZIF-8[22j], ZIF-7[22j] and ZIF-90[22n] membranes on alumina supports modified with 3-aminopropyltriethoxysilane (APTES) as a covalent linker between ZIF crystals and alumina supports, thereby promoting heterogeneous nucleation and growth.

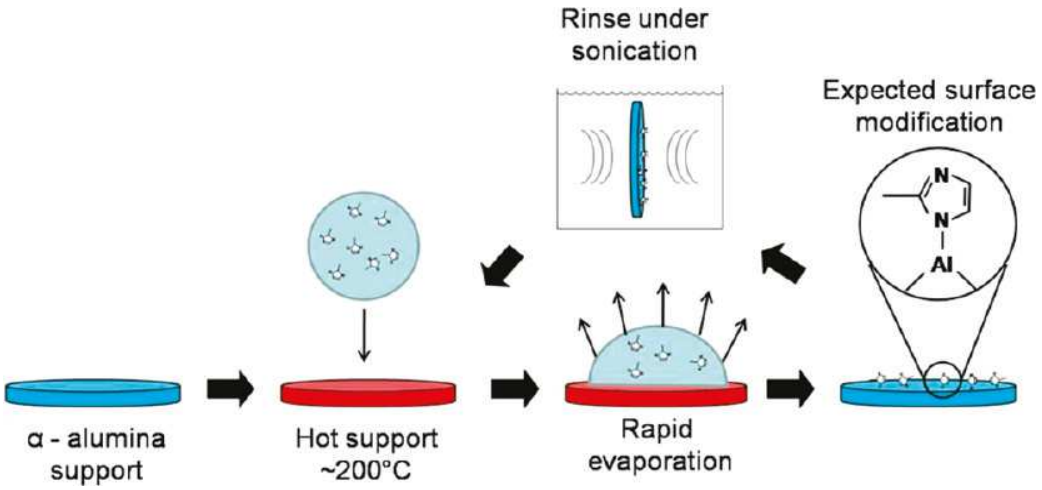

Figure 13: Illustration of the substrate modification process. Reproduced with permission. (Ref. 22m)

Thus, this technique provides a fairly general route to fabricate ZIF membranes on porous ceramic supports.

We have recently reported a silane-free route for substrate modification that yields well-attached polycrystalline MOF membranes.[22m] This method, demonstrated for ZIF-8/-7 membranes, is based on covalent linkage of imidazole ligands to supports via an Al-N bond.[22m] As illustrated in Figure 13, supports were thermally modified by rapid evaporation of a solution of the organic linker (2-methylimidazole in methanol for ZIF-8 or benzimidazole in methanol for ZIF-7) on the surface of hot α-alumina (~ 200°C). The solvent evaporates quickly, leaving organic linkers covalently attached to the α-alumina surface, as evidenced by N 1s XPS data as can be seen Figure 14. The XPS data also confirms that high temperature (~ 200ºC) is necessary for covalent bonding between the

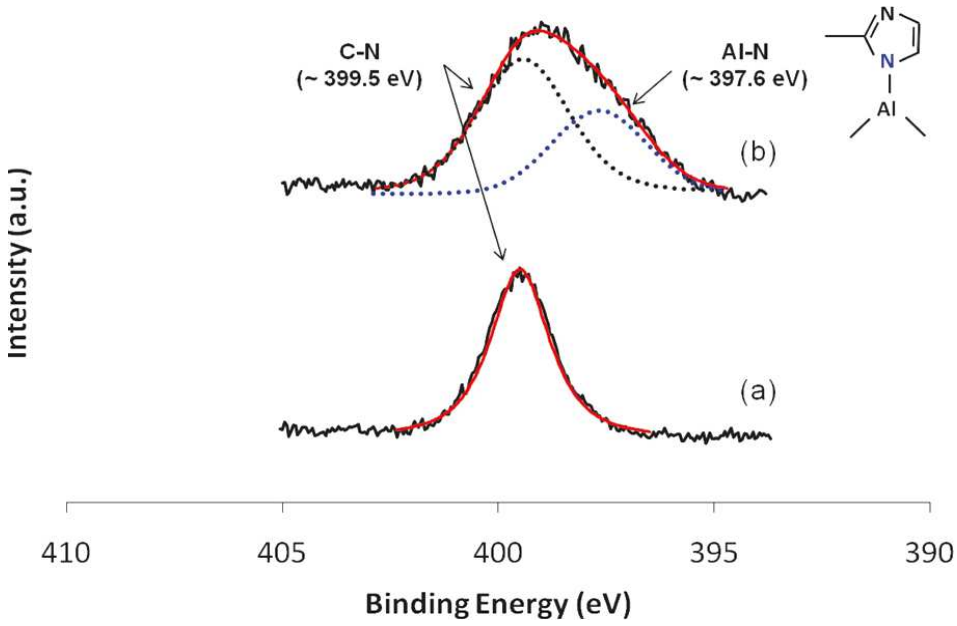

Figure 14: N 1s XPS spectra of α-alumina supports modified with 2-methylimidazole (a) at 25°C (a) and (b) at 200 °C (bottom). Reproduced with permission. (Ref. 22m)

organic linker and the surface as supports modified at room temperature did not have any XPS peaks characteristic of Al-N bonding. Solvothermal growth of supports modified in this way was found to yield ZIF-8 membranes half as thick (see Figure 15) as those reported previously.[6] These membranes exhibit preferential permeation of small gas molecules with selectivities far in excess of Knudsen selectivity. It is interesting to note though, that unlike molecular sieving observed in zeolite membranes, ZIF membranes have not been observed to exhibit sharp permeance cutoffs. This is understood as a result of the flexible nature of organic ligands in the ZIF structure.[39]

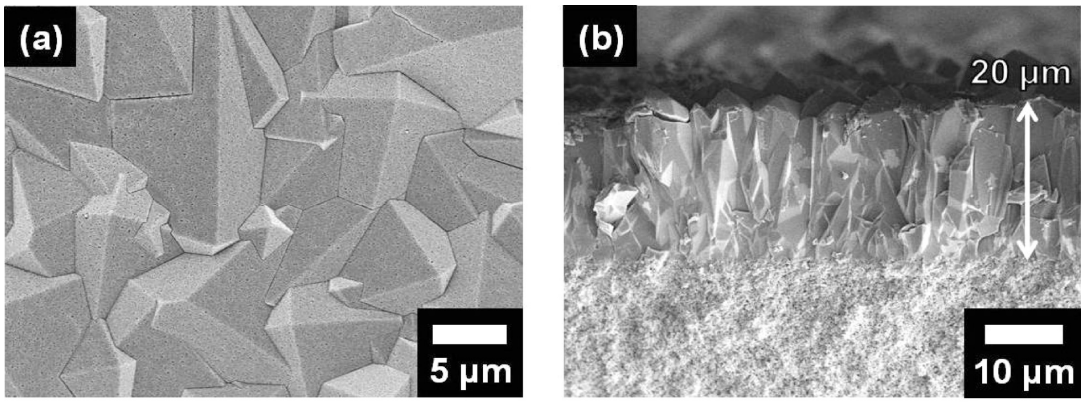

Figure 15: (a) Top-down and (b) side-view SEM images of ZIF-8 membranes fabricated using thermal deposition of imidazolate linkers on porous supports. Reproduced with permission. (Ref. 22m)

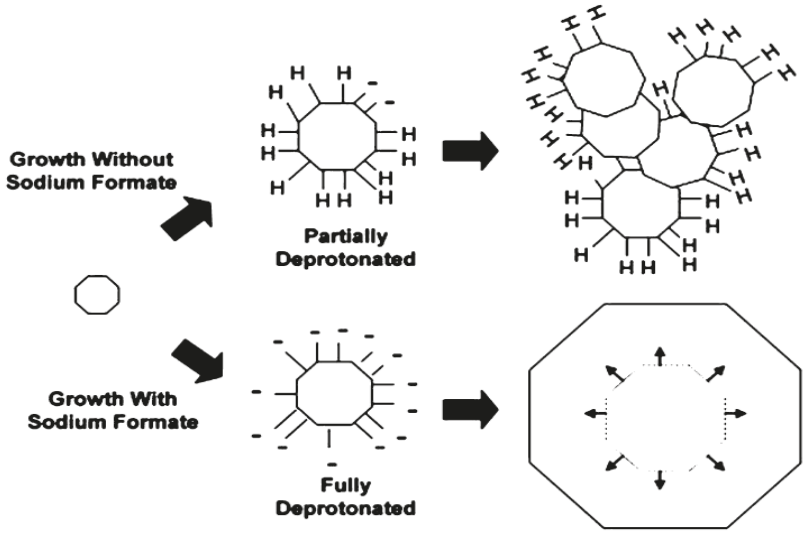

Figure 16: Illustration of possible role of HCOONa in ZIF-8 growth. Reproduced with permission. (Ref. 22m)

The role of sodium formate (HCOONa) as deprotonator has been found to be critical for the growth of well-intergrown films on supports modified by thermal deposition (Figure 16).[22m] We have shown that in the absence of HCOONa the ligand is partially protonated and this results in a microstructure that is poorly intergrown.[22m] As shown by Wiebcke and co-workers[65], neutral m-Im acts as a capping agent for ZIF-8 crystal growth. The deprotonation was confirmed by the increase in pH of the solution on addition of sodium formate. When poorly intergrown films were regrown using sodium formate, well intergrown films were obtained (Figure 17).[22m]

Farrusseng and co-workers[31a] postulated the presence of direct attachment of imidazolate to alumina in case of SIM-1 and ZIF-7 as shown in Figure 18.

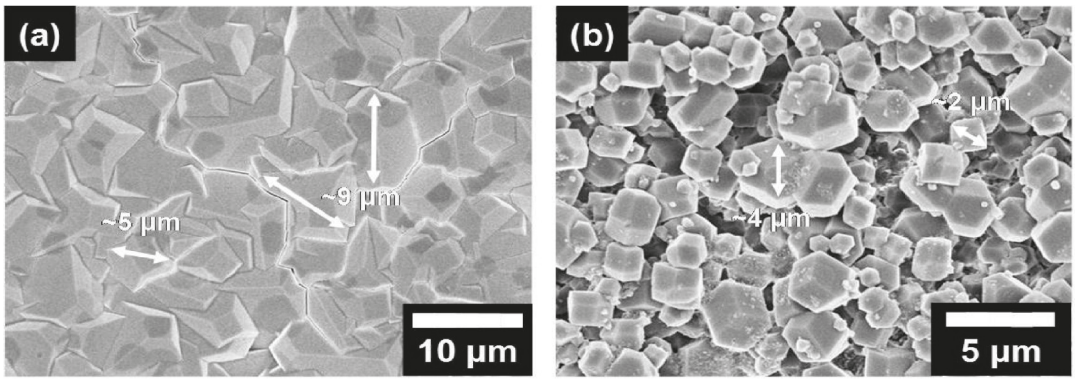

Figure 17: ZIF-8 films after secondary growth (a) with sodium formate (b) without sodium formate. Note that these films were regrown from poorly intergrown films. Reproduced with permission. (Ref. 22m)

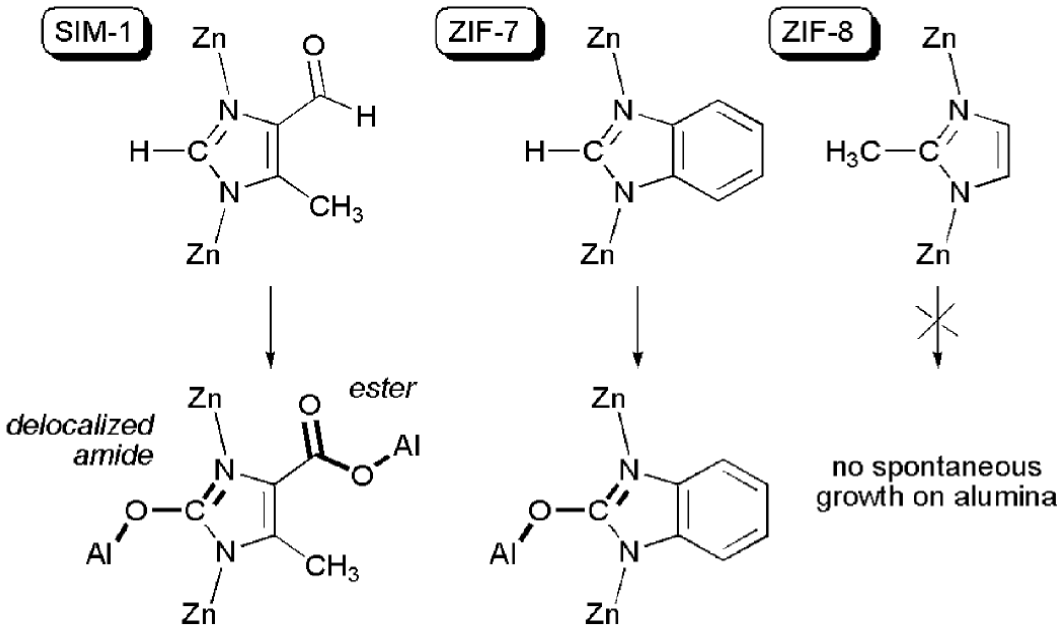

Figure 18: Postulated anchoring method of imidazolate based MOFs on alumina support. Reproduced with permission. (Ref. 31a)

2.4.1.3 *In situ* growth – secondary metal source

Some groups have used alternate metal sources to anchor MOF films.[21e, 22d] As mentioned above, MOF synthesis involves coordination bonding between organic and inorganic moieties in solution creating the hybrid organic-inorganic framework. In this approach, the support structure for the membrane itself is the same metal in the framework of the MOF of interest. Guo et al.[22d] reported an HKUST-1 membrane grown on an oxidized copper mesh (Figure 19). It should be noted that this membrane is essentially free-standing and is likely to have problems with mechanical stability for practical applications.

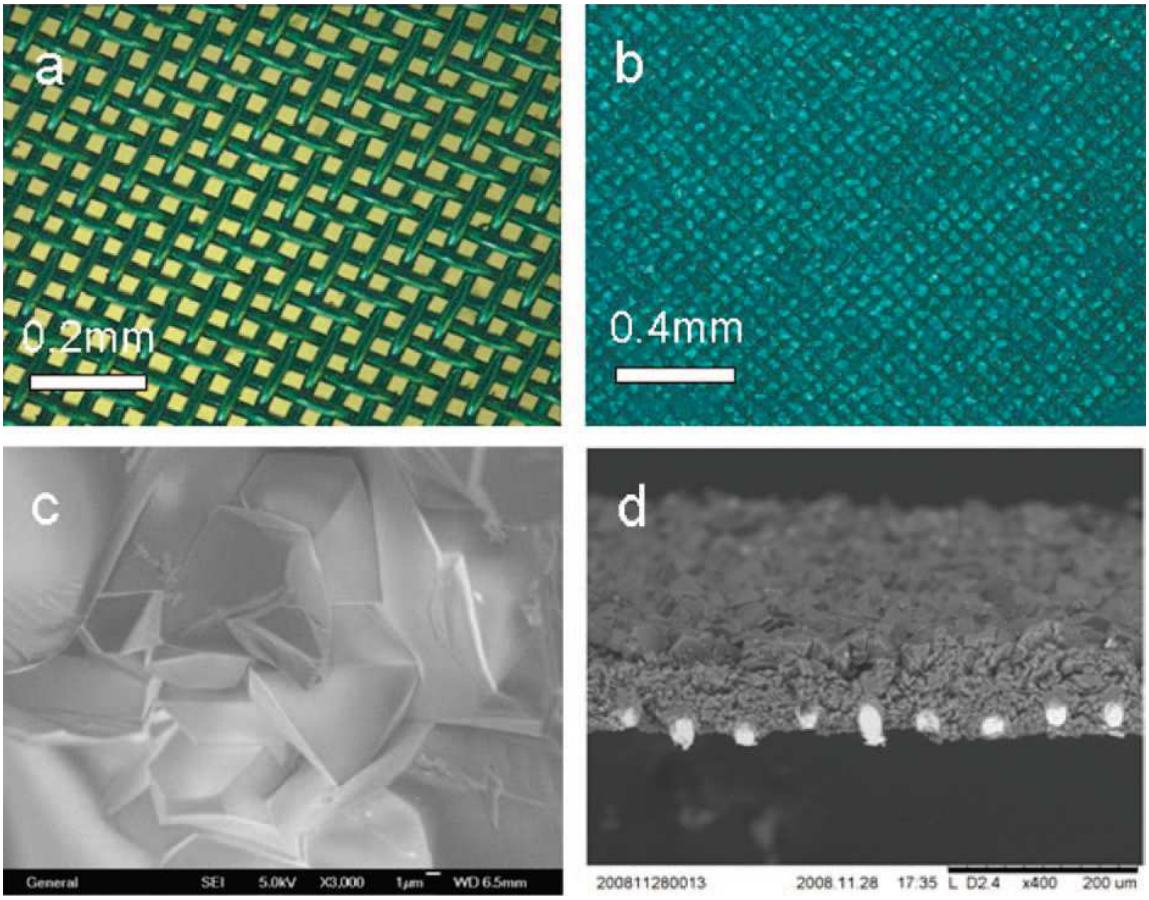

Figure 19: Optic micrographs of the (a) copper net and (b) net-supported Cu3(BTC)2 membrane; SEM image of (c) the surface and (d) cross section of the membrane. Reproduced with permission. (Ref. 22d)

2.4.2 Secondary (seeded) growth

Secondary growth is a film growth approach commonly used for zeolite membranes.[28b, c, 66] This method involves first seeding the support with seed crystals of the material of interest followed by hydrothermal or solvothermal growth. Secondary growth decouples the nucleation and growth steps for polycrystalline membrane fabrication.[13e] This allows for better control over film microstructure (density of grain boundaries, film thickness, orientation, etc.) by controlling the relevant properties of the seed crystal layer such as seed crystal size, thickness and orientation.[67] By having pre-attached seed crystals to the support, secondary growth also allows film growth to be somewhat substrate independent. For zeolite membranes, seed attachment is not an issue. Simple calcination of seed crystals on the surface of porous supports leads to a condensation reaction between surface hydroxyl groups and the zeolite seeds become covalently bound. For MOF membranes, this approach is not viable as MOFs cannot withstand high temperatures. Manual deposition (i.e., rubbing seed crystals on a support) and subsequent heat treatment for zeolite seed crystals is a simple method for attaching crystal seeds to a substrate,[68] but the reports of MOF membranes seeded in this way generally required the use of a polymer binder to attach seed crystals to the support.

2.4.2.1 Synthesis of MOF nanocrystals

It has been shown in zeolite membranes that when using the secondary growth, nano-sized seed crystals are much preferred to prepare zeolite membranes with controlled microstructures (such as thickness).[67] Therefore, the synthesis of submicron

sized MOF seed crystals with a narrow size distribution is desirable to form MOF membranes with controllable thickness. There have been reports on the synthesis of nano-sized MOFs using various methods ranging from conventional solvothermal methods[22a] to microwave assisted solvothermal synthesis,[69] sonochemical methods,[70] and nonsolvent induced crystallization.[71] MOFs whose nanocrystals have been synthesized include ZIFs,[22a, 54b, 65, 71-72] HKUST-1,[73] IRMOFs,[21b, 69, 74] MOCP-L and MOCP-H,[75] Cu–4,4-bipyridine–hexafluorosilicate(Cu-BPY-HFS),[76] and Cu(4,40-hexafluoroisopropyl-idenebis-benzoate)$_{1.5}$ (Cu_hfipbb).[70] These nanoparticles can also be used for the fabrication of mixed matrix membranes to provide higher interfacial area and thinner selective skin layers. Further morphology control of these nanocrystals (e.g., plates vs cubes) can allow for the fabrication of preferentially oriented polycrystalline MOF membranes, which might exhibit enhanced separation performance if MOFs of interest are anisotropic in gas transport.

2.4.2.2 Secondary growth - supports with physically attached seeds

Ranjan and Tsapatsis[22l] reported a membrane of a microporous MOF using secondary growth in 2009 (see Figure 20). The seeds were deposited by manually rubbing the crystals onto PEI coated α-alumina. According to the report, *in situ* growth did not yield membrane quality films. Their results showed *b*-out-of-plane orientation in their membrane, demonstrated using the crystallographic preferential orientation (CPO) indexing method and pole figure analysis. Although the seeds used for secondary growth were randomly oriented, the investigators attributed the membrane orientation to

faster crystal growth in the *b*-direction. The effective pore size of this MOF is 3.2 – 3.5 Å.[77]

Li et al.[22e] also used this approach to synthesize membranes of ZIF-7. Poor interaction between seed crystals and the substrate surface necessitated the use of polymer binder. Although use of a polymer binder attached seed crystals to the support surface, the seed crystals are not directly attached to the substrate. This means that seed attachment strength is only as good as the polymer attachment strength and one would expect that membranes fabricated in this way are only physically attached to the support surface. Venna et al. [22g] reported ZIF-8 tubular membrane obtained by secondary growth of ZIF-8 crystals seeded by rubbing. No polymer binder was used. The membranes thus obtained were fairly thin 5 - 9µm.

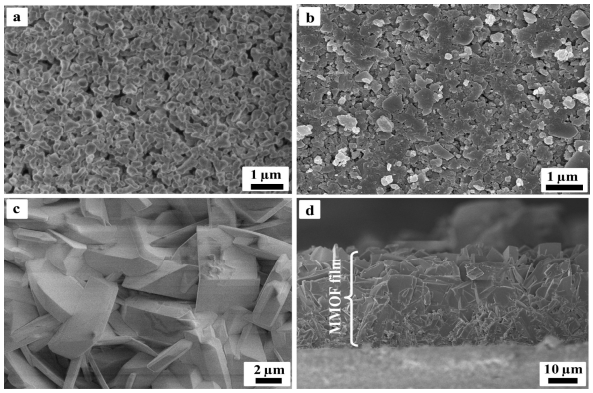

Figure 20: (a) Bare α-alumina support, (b) seeded support, (c) top-down image of MMOF membrane, (d) side view of MMOF membrane. Reproduced with permission. (Ref. 22l)

2.4.2.3 Secondary growth - supports with chemically attached seeds

We recently reported a novel secondary growth technique for MOF membranes which circumvents the problem of MOF crystal thermal instability and does not require foreign binders. This technique, termed thermal seeding, was demonstrated for HKUST-1 membranes.[22i] Thermal seeding consists of dropping HKUST-1 crystal seed solution onto hot (200 °C) porous α-alumina supports followed by rinsing under gentle sonication (see Figure 21). This process is repeated to insure sufficient coating of seed crystals. Solvothermal growth of supports seeded in this way result in continuous, crack-free, well intergrown membranes of HKUST-1. Separation performance of these membranes is comparable to those previously reported by Guo et al.[22d, 22i] It was observed that HKUST-1 seed crystals alone in solution during thermal seeding do not remain attached after sonication. Only when seeded in the presence of HKUST-1 precursor chemicals do the seed crystals adhere to the support. This indicates that crystals of HKUST-1 do not interact attractively with porous α-alumina and there is the need for linking chemicals. This method for MOF crystal seeding has the potential to be applied to other MOFs.

Lee and co-workers[25] showed that this seeding can be carried during *in situ* growth as well (Figure 22) . They first carried out *in situ* growth to generate seed crystals attached to the substrate. This seeded support was further used for secondary growth to generate well intergrown films of MIL-53. This technique is called reactive seeding.

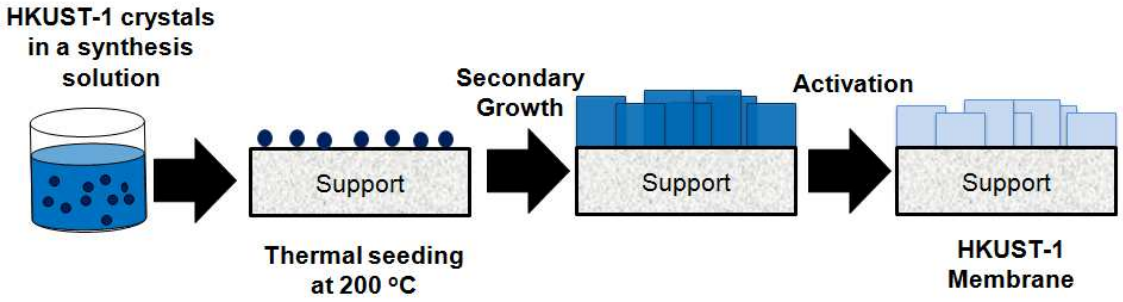

Figure 21: Illustration of HKUST-1 membrane fabrication using thermal seeding and secondary growth. Reproduced with permission. (Ref. 22i)

In one of the earliest MOF membrane reports,[21i, 22b] our group reported a membrane of IRMOF-1 produced by secondary growth using a seed layer that was deposited using microwave induced thermal deposition (MITD). Fast microwave seeding resulted in a dense, randomly oriented seed layer on α-alumina thinly coated with graphite. This was immersed in MOF-5 growth solution and produced well intergrown MOF-5 membranes. A thicker graphite layer was also used for MITD and resulted in oriented MOF-5 crystals attached to the surface (see Figure 23). When this oriented seed layer was grown solvothermally, it produced dense, highly oriented MOF-5 films. Unfortunately, the mechanical instability of these films (readily peeling off) made gas permeation measurement impossible.

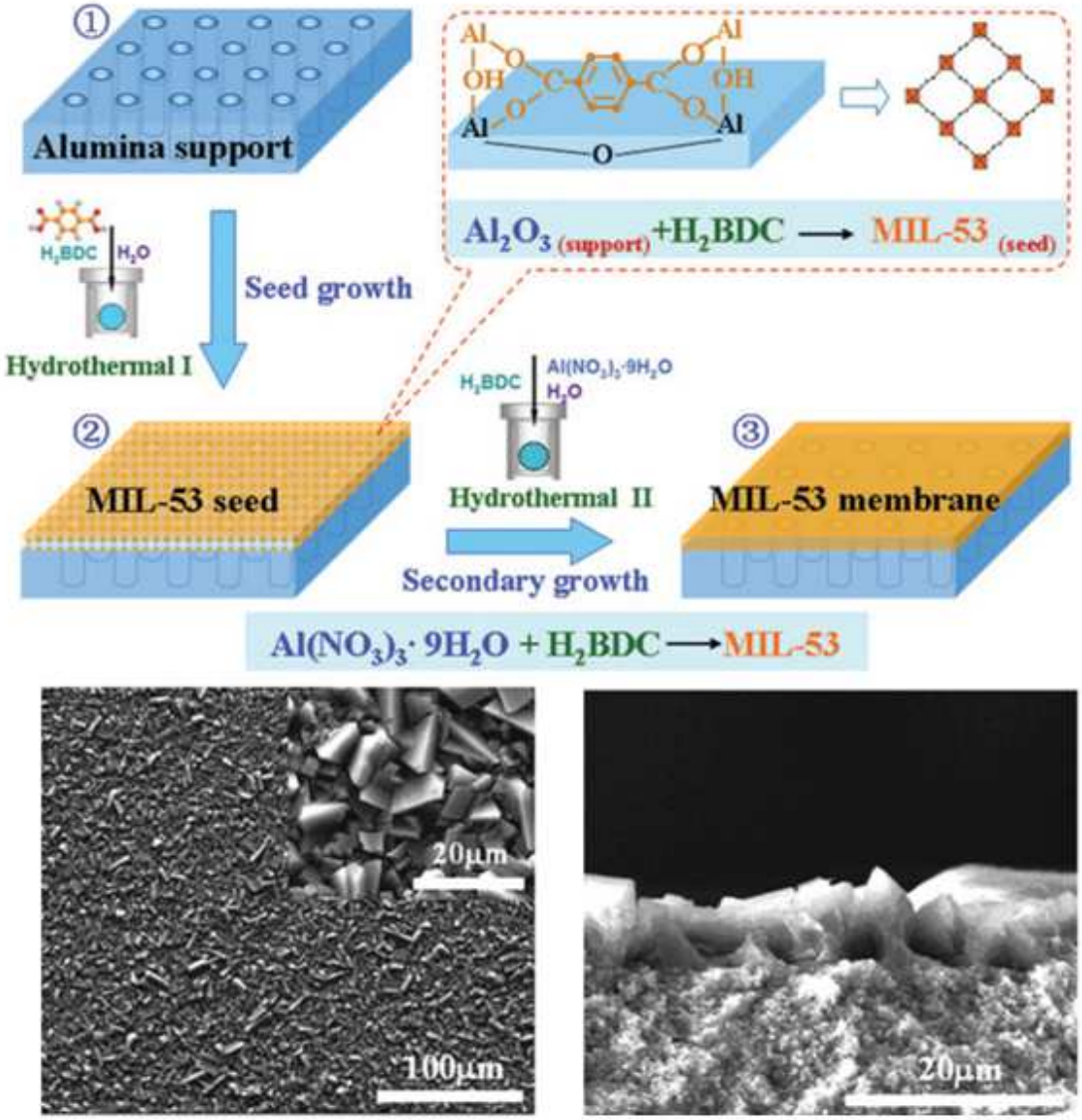

Figure 22: Schematic diagram of preparation of the MIL-53 membrane on alumina support via the RS method (above). SEM images of MIL-53 membrane surface and cross-section(below). Reproduced with permission. (Ref. 25)

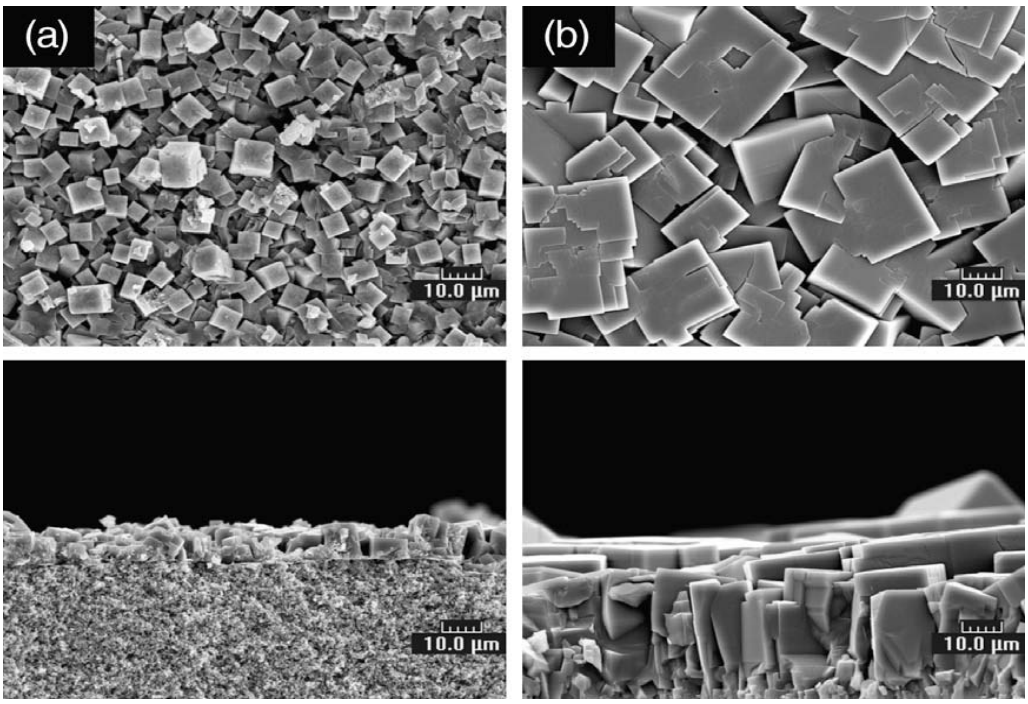

Figure 23: SEM images of the oriented IRMOF-1 seed layer (a) and the oriented membrane after secondary growth (b). Reproduced with permission. (Ref. 22b)

Li et al.[22a] recently reported oriented ZIF-7 membranes fabricated on porous α-alumina. Supports were seeded with ZIF-7 nanocrystals followed by secondary growth The orientation sharpening observed in this report is explained according to the Van der Drift growth model (also referred to as *evolutionary selection*).[78] This model states that crystals with fast-growing facets oriented vertically with respect to the support eventually overgrow crystals of other orientations during synthesis, yielding a preferentially oriented film.

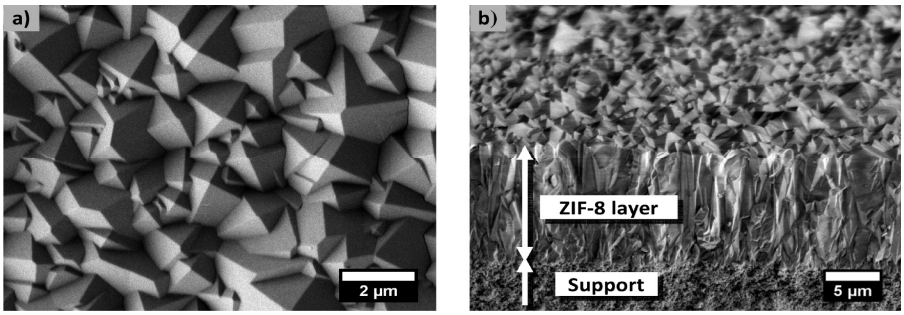

Figure 24: (a) SEM top view of the well-intergrown ZIF-8 layer after 2 h of secondary growth. (b) SEM top down view on the corresponding crosssection of the broken membrane. Reproduced with permission. (Ref. 7a)

Oriented ZIF-7 and ZIF-8 membranes have been reported.[7a, 22a](Figure 24) Oriented ZIF-8 membranes have relatively higher H_2/CH_4 separation factor.

2.4.3 Other techniques for membrane fabrication and modification

2.4.3.1 Liquid phase epitaxy (LPE)

Liquid phase epitaxy or stepwise layer by layer involves alternatingly immersing the substrate into metal and ligand solutions respectively.[79] This technique is typically used to synthesize MOF thin films, however, it has a potential to be applied for fabrication of thin membranes. Typically, the films are a few nanometers thick. Shekhah et al.[79] have demonstrated heteroepitaxial growth of $[Zn_2(ndc)_2(dabco)]_n$ on $[Cu_2(ndc)_2(dabco)]_n$ (ndc = 1,4-naphthalene dicarboxylate and dabco = 1,4-diazabicyclo(2.2.2)octane) using LPE to give rise to perfectly oriented hybrid MOF thin films. These oriented thin films are exciting for chemical sensor and gas separation applications. Nan et al.[80] showed a

similar approach (step by step procedure) can be used to prepare seeded supports of HKUST-1. These seeded supports under optimum hydrothermal secondary growth conditions yielded continuous and well-intergrown HKUST-1 membranes.

Recently, Betard et al.[81] reported Cu_2(BME-bdc)$_2$(dabco) and Cu_2(ndc)$_2$(dabco) (dabco = 1,4-diazabicyclo(2.2.2)octane, ndc = 1,4-naphtalenedicarboxylate, 2,5-bis(2-methoxyethoxy)-1,4-benzene-dicarboxylate = BME-bdc) MOF membranes using step by step liquid phase deposition. Here separation was carried out by MOF layer formed inside the macroporous support. Although the pumps were computer controlled, the synthesis time was fairly long (~ 2 days). Scale up of such a technique for commercial applications could be difficult. Using a spray based method[82] for LPE (demonstrated for HKUST-1 SURMOF), deposition time was significantly reduced but compromising the film quality. It should be noted here that LPE provides for fabrication of thin films (submicron regime) with controllable thickness. Thickness is governed by the number of cycles which can be easily tuned.

2.4.3.2. Post-synthetic modification

Side groups having functionality can be further subjected to post-synthetic modification after fabrication of membranes. This has been shown for IRMOF-3,[24] ZIF-90[50] (Figure 25), and SIM-1[31b]membranes. Amine functionalization of SIM-1 gives SIM-2 which shows catalytic activity and enhanced CO_2/N_2 separation.[31b]

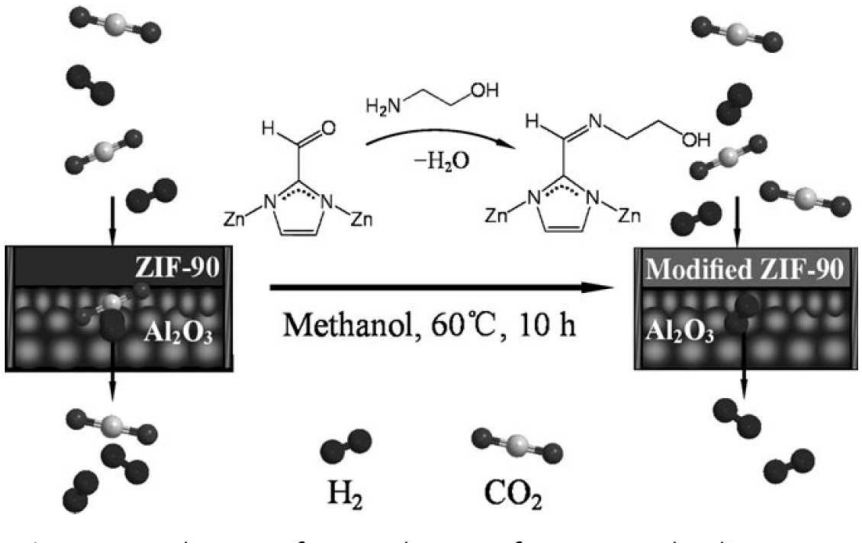

Figure 25: Covalent post-functionalization of a ZIF-90 molecular sieve membrane by imine condensation with ethanolamine to enhance H2/ CO2 selectivity. Reproduced with permission.(Ref. 50)

2.4.4 MOF films on polymer supports

Inorganic supports such as alumina and titania are generally expensive as compared to organic supports. So far most of MOF films and membranes have been grown on these rather expensive oxide supports. Due to their inorganic/organic hybrid nature, MOFs have potential to be fabricated on polymer substrates.[27, 83]

Centrone et al.[27] reported for the first time the fabrication of MOF material on polymer substrate using fast microwave irradiation (Figure 26). *In situ* functionalization of nitrile from PAN substrate to carboxylic acid groups leads to the MIL-47 growth on polymer surface. Yao et al.[83] demonstrated the growth of continuous and compact ZIF-8

membrane on nylon membrane using contra-diffusion method (Figure 27). These membranes use polymers as supports. In this regard, they are different from mixed matrix membranes, in which the MOF particles are dispersed in polymer matrix.

In either case the adhesion of MOF to polymer surface is necessary. The control of

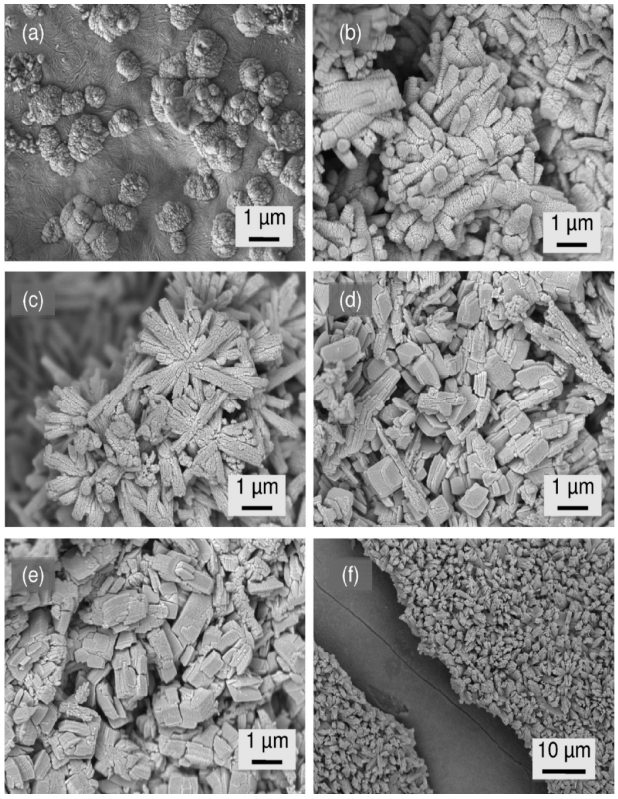

Figure 26: SEM images of polyacrylonitrile substrate prepared initially as an electrospun nanofiber mat, coated with MIL-47 material as a function of time: (a) 5 s, (b) 30 s, (c) 3 min, (d) 6 min, and (e) 10 min. Note that the initial fibers fused together and lost their identity very shortly after irradiation. (f) MIL-47-coated grooved PAN. Reproduced with permission. (Ref. 27)

MOF/polymer interface is relatively easier in general due to increased affinity of organic linkers to polymer surface. Further, post-synthetic modification of MOFs can allow modulation of surface properties of MOFs.[84] In case of MMM with ZIF-90[71] no interface modification was required. For MMMs of ZIF-7 in PBI[85] sub-nano interphase structure was formed between ZIF-7 and PBI which acted as an extension of ZIF-7 frameworks, thereby providing strong interfacial interactions.

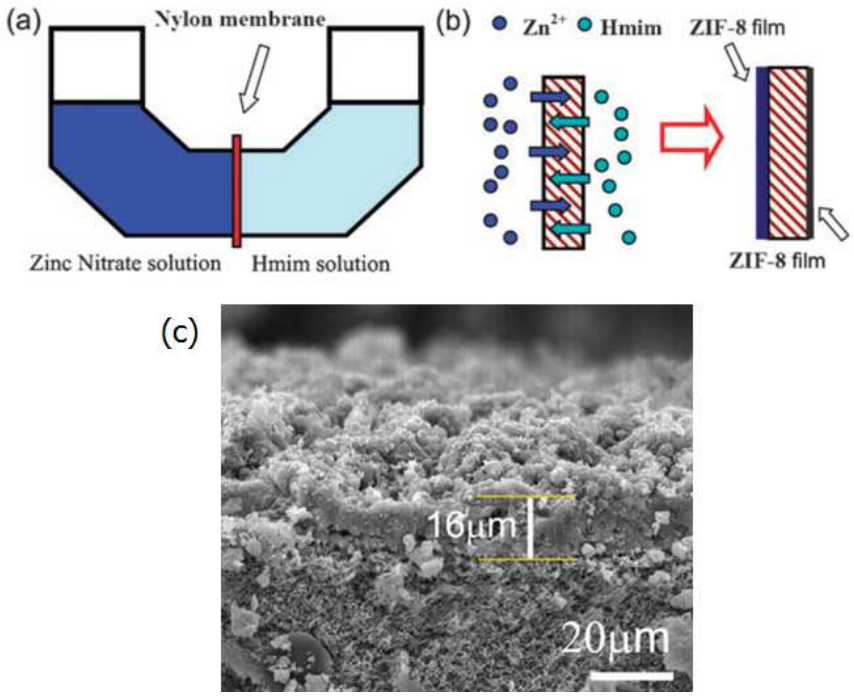

Figure 27: (a) Diffusion cell for ZIF-8 film preparation and (b) the schematic formation of ZIF-8 films on both sides of the nylon support via contra-diffusion of Zn2+ and Hmim through the pores of the nylon support (c) SEM image of the cross-section of the ZIF-8 film. Reproduced with permission. (Ref. 83)

2.4.5 Mixed matrix membranes with MOFs

Mixed matrix membranes (MMMs) with MOFs are a newly class of membranes which combine the advantages of polymers and MOFs. In general, MMMs with zeolites face difficulties which include expensive synthesis defect free crystal with long preparation times and limited range of zeolite structures with discontinuous pore size and little chemical tailorability and poor polymer zeolite interface. Synthesis of MOFs with various physical/chemical properties is relatively easier than that of zeolites and MOF/polymer interface can be controlled by varying the affinity of organic linkers to the polymer matrix. Also surface of MOFs can be modified by functionalization for favorable interaction with the polymer.[84] MOFs, in general, offer greater pore volumes and weigh lesser than zeolites. Thus for a given mass loading, a MMM with MOF will affect the membrane behavior significantly greater than MMM with zeolite. MMMs with MOFs that have been reported include Cu-BPY-HFS (Cu-4,40-bipyridine hexafluorosilicate) in Matrimid,[76] HKUST-1 in poly(sulfone),[86] MOF-5 in Matrimid,[74b] Cu-TPA (terephthalic acid) in poly(vinyl acetate),[83] ZIF-90 in 6FDA-DAM,[71] (6FDA: 2,2-bis (3,4-carboxyphenyl) hexafluoropropane dianhydride and DAM: diaminomesitylene), ZIF-7 in polybenzimidazole (PBI),[85] $Cu_3(BTC)_2$, ZIF-8 and MIL-53 (Al) in Matrimid,[87] ZIF-8 in Matrimid,[88] HKUST-1 in polyimide hollow fiber mixed matrix membrane,[89] HKUST-1 in Matrimid,[90] HKUST-1, MIL-53, MIL-47, ZIF-8 in PDMS.[91] In particular, ZIF-7/PBI nanocomposite[85] showed remarkably higher ideal H_2/CO_2 permselectivity, as compared to pure PBI membranes and pure polycrystalline ZIF-7 membranes. The enhanced selectivity was attributed to the strong interfacial

interactions between ZIF-7 and polymer which reduced non-selective pathways for gas transport. Thus mixed matrix membranes (MMMs) with MOFs provide potential alternatives as enhanced gas separation membranes. Some of these membranes might still face challenges of plasticization, poor thermal and chemical stability that limit polymeric membranes.

2.5 Gas separation performance of MOF membranes

Single gas permeation properties of reported MOF membranes are summarized in Table 2. Two reported MOFs exhibit ideal selectivity values that are consistent with Knudsen diffusion (MOF-5 (Figure 28) and ZIF-69).[22b, c, 22h] HKUST-1 membranes exhibit lower H_2/CH_4 separation than expected.[22d] The authors speculated that this was due to the slowly-diffusing and strongly-sorbing methane blocking the fastly-diffusing and slowly-sorbing hydrogen. Gas permeation results for the microporous MOF (MMOF) investigated by Ranjan et al.[22l] showed an ideal selectivity of 23 for H_2/N_2. Low fluxes were also reported for this membrane and ascribed to the randomly oriented seed layer impeding gas diffusion. Membranes of ZIF-7, ZIF-8 (Figure 29), and ZIF-22 exhibit molecular sieving, preferentially allowing higher permeation of small gases over larger molecules.[6, 22e, 22j]

Table 2: Summary of single gas permeances of MOF membranes. (Ref. 5) (* = equimolar binary gas measurement with 50% hydrogen, ** = ZIF-90 membrane single gas permeation measurement after post-synthetic modification with ethanolamine).

MOF	Ref.	T(°C)	da (nm)	dm (μm)	Reported permeances at ~ 1atm [10^{-8} (mol m^{-2} s^{-1} Pa^{-1})]								
					H_2	CH_4	N_2	CO	O_2	CO_2	SF_6	C_2H_4	C_2H_6
MOF-5	15b	25	1.4	40	80	39	30	-	-	25	-	-	-
MOF-5	15c	25	1.4	25	285	103.3	80	-	-	66.7	41.7	-	-
MOF-5	15c	25	1.4	85	131.7	56.7	40	-	-	33.3	21.7	-	-
ZIF-7	15g	220	0.29	1.5	4.55	0.31	0.22	-	-	0.35	-	-	-
*ZIF-7	15g	220	0.29	1.5	-	0.33	0.25	-	-	0.31	-	-	-
ZIF-7	15f	200	0.29	1.5	7.40	1.18	1.10	-	-	1.10	-	-	-
*ZIF-7	15f	200	0.29	1.5	-	1.35	1.03	-	-	1.19	-	-	-
ZIF-8	15h	20	0.34	5	-	472	-	-	-	2430	-	-	-
ZIF-8	15h	20	0.34	9	-	242	-	-	-	1690	-	-	-
*ZIF-8	84	25	0.34	25	-	-	-	-	-	-	-	1.8	0.65
ZIF-8	15n	25	0.34	20	17.3	1.33	1.49	-	5.22	4.45	-	-	-
ZIF-8	81	25	0.34	2.5	36.0	7.8	9.0	-	-	14.0	-	14.0	6.90
ZIF-8	15e	25	0.34	40	6.04	0.48	0.52	-	1.04	1.33	-	-	-
ZIF-22	15k	50	0.29	40	20.2	3.02	2.84	-	2.8	2.38	-	-	-
ZIF-69	15i	25	0.44	50	6.5	1.85	-	1.1	-	2.45	0.5	-	-
MMOF	15m	25	0.32	20	1.6	-	0.35	-	-	0.35	-	-	-
MMOF	15m	190	0.32	20	0.2	-	0.01	-	-	0.04	-	-	-
HKUST-1	15d	25	0.9	60	125.3	16.1	27.2	-	-	27.7	-	-	-
HKUST-1	69	25	0.9	25	74.8	25.7	20.0	-	-	14.8	-	-	-
HKUST-1	15j	25	0.9	25	200	80	50	-	-	50	-	-	-
HKUST-1	15j	190	0.9	25	110	20	15	-	-	22	-	-	-
SIM-1	50	25	0.34	25	8.2	3.3	3.3	-	-	3.5	-	-	-
ZIF-90**	32a	200	-	20	21.0	1.08	1.28	-	-	1.34	-	-	-
ZIF-90	15o	200	0.35	20	25.0	1.57	1.98	-	-	3.48	-	-	-

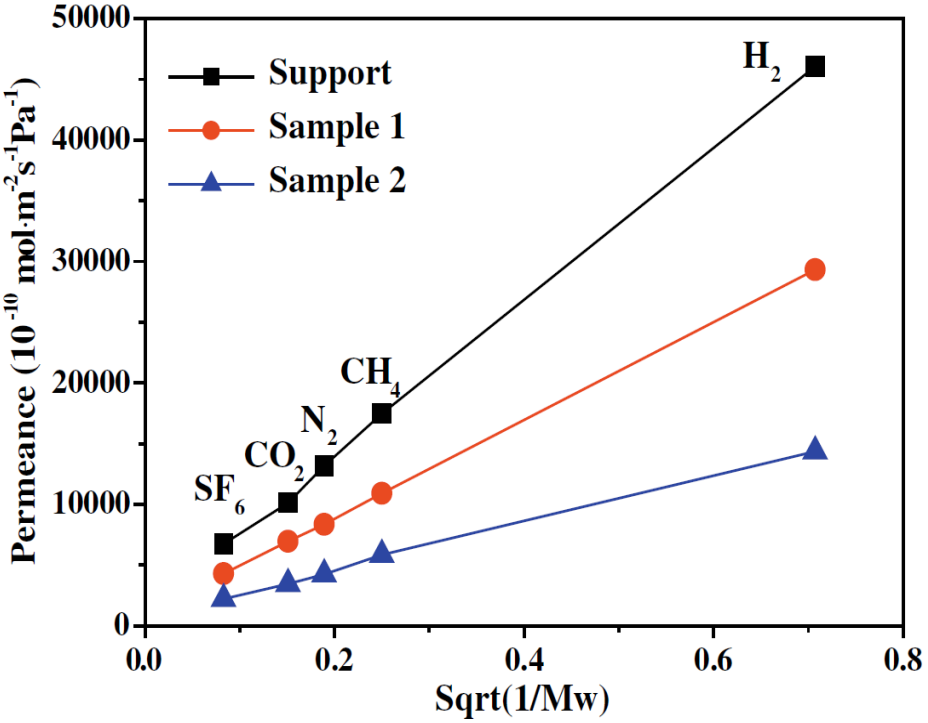

Figure 28: Single-component gas permeation results through the a-alumina support (square), MOF-5 membrane sample 1 (circle) and MOF-5 membrane sample 2 (triangle) under 800 Torr. Reproduced with permission. (Ref. 22b)

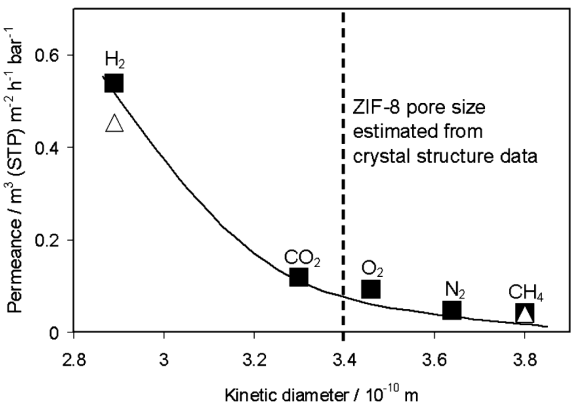

Figure 29: Single (squares) and mixed (triangles) gas permeances for a ZIF-8 membrane vs kinetic diameters. Reproduced with permission. (Ref. 6)

ZIF-8 has a reported aperture diameter of 3.4 Å.[1, 18d] This aperture diameter leads one to expect that ZIF-8 membranes would be capable of good hydrogen/methane separation. Binary mixture permeation data confirms this expectation; the membrane's H_2/CH_4 separation factor at room temperature and pressure was 11.2. As pointed out by the author, however, the membrane's hydrogen flux is about half of that obtained by zeolite membranes with similar selectivity. This was attributed to the fact that the membrane is quite thick (~ 40 μm). ZIF-8 tubular membrane reported by Venna et al.[22g] with thickness of 5 – 9 μm exhibits CO_2 permeance of ~ 2.4×10^{-5} mol/m^2·s·Pa with CO_2/CH_4 selectivities ranging from 4-7.

Recently Pan et al. [7b] reported excellent ZIF-8 membrane by secondary growth in aqueous solution at near room temperature (greener route). Single gas permeances are

shown in Figure 30. High selectivities were obtained for C2/C3 hydrocarbon separation (for mixtures, ethane/propane ~ 80, ethylene/propylene ~ 10 and ethylene/propane ~ 167). Also the membranes obtained were much thinner (2.5µm) than previously reported membranes.[6] Correspondingly, the permeances were 4 times higher. The authors reported a higher H_2/C_3H_8 separation factor than previous membranes. The superior separation performance was attributed to enhanced membrane microstructure (reduced grain boundary defects) which was possibly due to their novel aqueous recipe.

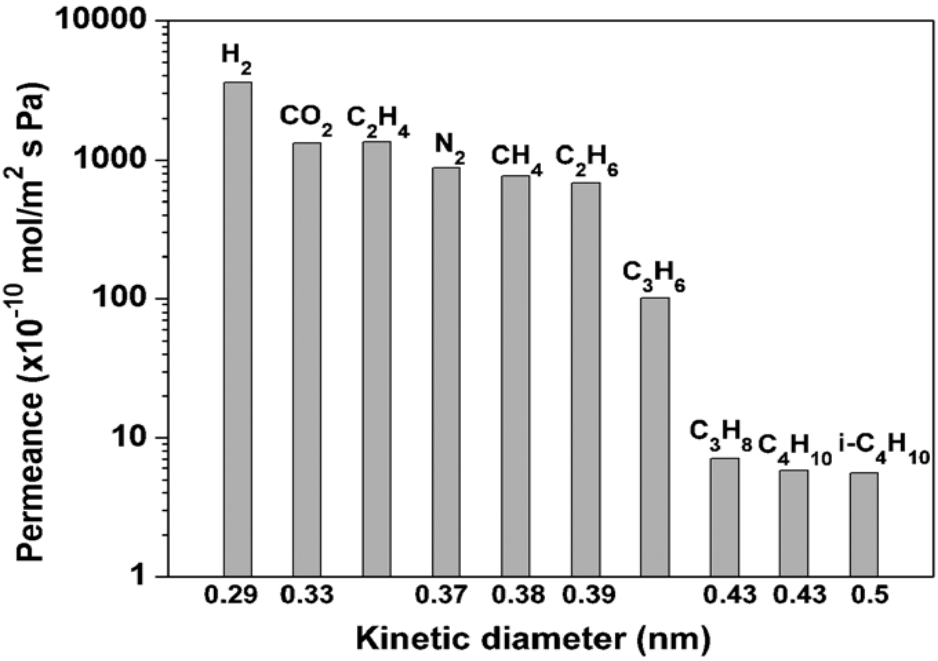

Figure 30: Single gas permeances measured on as-synthesized ZIF-8 membrane using Wicke-Kallenbach technique. Reproduced with permission. (Ref. 7b)

As stated earlier, the sharp permeance cut-offs have not been observed for ZIF membranes,[6] mainly due to the flexible nature of the framework.[39] This is in contrast to the zeolite membranes that in general exhibit substantial reduction (orders of magnitude) in permeance for molecules with kinetic diameter greater than the pore size of zeolites.[92] However, most of MOFs including ZIFs allow molecules whose kinetic diameters are greater than their pore sizes to pass through (see Figure 29) without substantial hindrance (i.e., the permeance does not decrease sharply for molecules greater than the pore size). This suggests that one has to select MOFs with much smaller pore size than the molecules of interest for membrane applications.

Post-synthetic modification of ZIF-90 reduces the pore size due to the presence of imine group and leads to significant enhancement in molecular sieving.[50] Huang et al.[50] reported a significantly selectivity enhancement for ZIF-90 without significant permeance drop. They also attribute higher selectivity to reduced pore aperture and improved grain boundary structure due to elimination of intercrystalline defects. However, Aguado et al.[31b] reported a decrease in CO_2 permeation flux for SIM-1 after post synthetic modification, which was attributed to reduced capacity of modified MOF (SIM-2). Surface modification could result in pore blocking at the surface and hinder molecular transport at the pore entrance/mouth, which could reduce the available area for gas transport, thereby decreasing the flux and permeance. Thus the extent of modification needs to be optimized to achieve selectivity enhancement without significantly affecting the permeance.

H_2/CO_2 selectivity is increased from 7.3 to 62.5. Post-synthetic modification of SIM-1 with dodecylamine to give imine groups (the new phase is called SIM-2) shows better CO_2/N_2 separation under moist conditions.[31b] For moisture sensitive MOFs like IRMOF-3, surfactant assisted drying significantly reduces fracture and crack formation.[24] This leads to enhanced gas permeation performance. Post-synthetic modification has also been demonstrated for IRMOF-3 which enables tuning the performance for CO_2/C_3H_8 separation.[24]

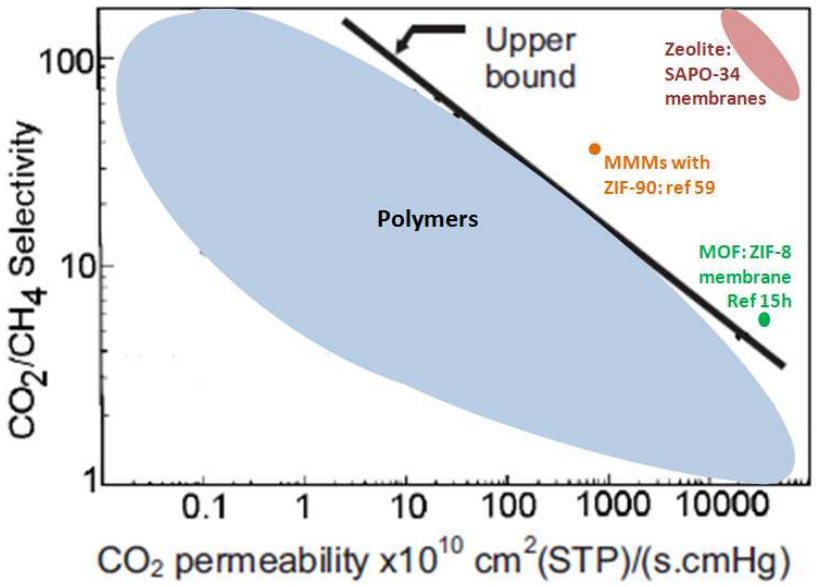

Figure 31: Comparison of different types of membranes for CO2/CH4 separation. This figure has been modified from the original figure. Reproduced with permission. (Ref. 99)

Based on single component diffusion rate measurement, Li and co-workers[2] demonstrated the probability of kinetic separation of propane/propene using ZIF materials in powder form. Gucuyener et al.[3] showed that ZIF-7 can be used for ethane/ethylene separation with selective adsorption of the paraffin due to gate-opening effect. Caro's group[93] showed, in case of ZIF-8 membrane, for an equimolar mixture, a modest selectivity of 2.8 of ethene over ethane (at 1 bar and room temperature). Using simulations they explained that faster diffusing ethene surpasses the stronger adsorption of ethane and the hence the membrane is selective for olefin and not the paraffin.

MOF membranes are still relatively new and have potentials for substantial improvement. Nevertheless, it is informative to compare MOF membranes with different types of membranes. Figure 31 presents CO_2/CH_4 separation performance of ZIF-8 membranes compared with other membranes, showing relatively high CO_2 permeability though the CO_2/CH_4 selectivity is relatively low.

2.6 Conclusions and perspectives

In conclusion, metal-organic frameworks (MOFs) offer unprecedented opportunities for membrane-based gas separations (e.g., olefin/paraffin separations) due to their facile control over pore size and functionality. Thermally and chemically stable zeolitic-imidazolate frameworks (ZIFs) are of particular interest as membrane materials.

Current MOF membrane fabrication techniques do involve several issues mainly due to the unfavorable heterogeneous nucleation on support surfaces and the coordination

chemistry of MOFs. Several strategies aimed at addressing these issues have been discussed.

A large variety of exciting MOFs have been reported in the literature which when prepared as membranes might have potential applications for commercially relevant separations. Based on diverse MOF structures reported, many new MOF membranes are still to be reported.

It is also important to note that all of the research on MOF membranes for gas separation to date has been approached with a view to application similar to that of zeolite membranes. However, it would be exciting to see the many unique properties of metal-organic frameworks be applied to gas separating membranes.

In this vein, this review will close with a few suggestions for possible research directions for MOF membranes. There are many more MOFs with exciting properties than listed here, but these examples serve at least to illustrate the potential for impact in this new and largely unexplored area of research. Future research directions should also involve carrying out detailed investigations discussing important topics such as microstructure control, grain boundaries, and defect/crack removal.

2.6.1 MOF membranes with controllable selectivity

There is also room for application of MOFs with other interesting properties for membrane separations. Ma et al.[94] have reported four different MOFs that exhibit temperature tunable molecular gates. These MOFs, termed Mesh-Adjustable Molecular Sieves (MAMS) have controllable uptake of gases, discriminating between gases based

on molecular size. This size discrimination was shown to be controlled by the temperature of the material. Controllable gas uptake has been reported before for titanosilicate zeolites, but these materials have not been reported for gas separating membranes.[95] If these materials could be applied as membranes with controllable selectivity, this could yield high resolution membrane separation of any gases with different kinetic diameters.

2.6.2 MOF membranes with enantioselective pores

Another interesting group of MOFs are those with enantioselective pores such as POST-1.[96] Different MOFs exhibiting pores with handedness have been reported, but none have been explored for membranes or thin films. Enantioselective catalysis is one application of these MOFs, but this has only been explored for powders.[97] MOF membranes with chiral channels would enable high resolution separation of racemic mixtures, providing an alternative to methods such as chiral column chromatography. In addition, enantioselective MOF membranes could also be used as membrane reactors for chiral synthesis (i.e. chemical reaction happens in the pores yielding products with both chiralities, but only one chirality can diffuse out of the pores).

2.6.3 MOF membranes with readily functionalized pores

One of the most often referred-to strengths of metal-organic frameworks is their chemical functionality. In theory, a MOF with functionalizable pores can have its pore size controllably adjusted by functionalization with different size molecules.[21m, 98] This

property would be useful for separation flexibility and control. Functionalization of a MOF membrane could also be used to change its properties such as making it hydrophobic instead of hydrophilic or increasing the solubility of CO_2 in the membrane by adding amines to the framework. This has been demonstrated by several groups.[24, 31b, 50] Also, a membrane with functionalizable pores could potentially be useful for catalytic and enantioselective membrane applications.

2.6.4 Anionic frameworks for gas separation and catalysis

The gas sorption/diffusion properties of MOFs can be tuned by incorporating cations inside the pores of MOFs. Yang et al.[99] showed that for a parent anionic framework, built using Indium (III) centers and tetracarboxylic acid ligands, the porosity and heat of adsorption for H_2 can be modified by post synthetic ion exchange using an appropriate size cation. Also, unlike post-synthetic modification demonstrated for ZIF-90[50] and SIM-1[31b] this modification seems to be reversible in nature. An et al.[100] have synthesized a zinc adenine based bio-MOF-1($Zn_8(ad)_4(BPDC)_6O \cdot 2Me_2NH_2$), which also has an anionic framework. Pore size and adsorption property of bio-MOF-1 was altered by exchanging diammonium cations (present in as-synthesized sample) with ammonium cations of different sizes, resulting in the enhanced CO_2 uptake.[101] As seen in aluminosilicate zeolites, the cations can be varied and gas adsorption/diffusion properties can be altered which gives an additional handle to finely tune the separation properties of membranes. The metal cations can also act as sites for catalysis, potentially resulting in MOF membrane reactors.

2.6.5 External surface barriers in MOFs

In a simple description of molecular diffusion in a nanoporous material, the external boundaries of the material are simple terminations of the pores enabling the adsorption and desorption of gas molecules.[102] Contrary to this simple picture, Karger and co-workers[103] have showed using sorption rate measurements on Zn(tbip) (H2tbip = 5-tertbutylisophthalic acid) crystals that surface resistances or barriers exist for sorption due to many pore entrances being blocked and very few pores being open. If this external pore blockage is general in MOFs, it is critical to open external pore mouth to minimize this barrier and to improve flux through MOF membranes. If understood and controlled, the surface barriers in MOFs may serve as a "selective filter" for gas separations.[102]

2.6.6 Grain boundaries of MOF membranes

The microstructure (size of grains and their orientation, thickness, grain boundary structure, and location of active films) of polycrystalline MOF membranes can affect their performances as well as their durabilities. The microstructure of MOF membranes may not be similar to that of zeolite membranes. It is, therefore, of critical importance to characterize microstructure (grain boundary defects in particular) of MOF membranes perhaps by applying well-known techniques used in zeolite membrane research such as He/SF_6 permeation and fluorescence confocal optical microscopy (FCOM) techniques.[104]

2.6.7 Designing ligands, MOFs and their membranes based on desired separations

Currently, membrane fabrication is pursued from MOFs that show interesting behavior in powder form. Some of these materials may not perform well, when fabricated as membranes, because kinetics (diffusion of species) plays a major role in case of membranes. However, if we could work backwards, i.e. systematically design MOF materials (even design the ligands) for membranes based on end application.[36a, 105] Also since large variety of MOFs have already been reported in the literature, potential candidates for the targeted separation could be identified using computational studies.[106] Especially, the sorption and diffusion measurements which govern the membrane selectivities could be used to selectively filter out the best MOFs. This approach would save a lot of time on investigating different MOF membranes for their gas separation performance.

CHAPTER III

EXPERIMENTAL METHODS

3.1 Introduction

Metal-organic frameworks have attracted research interest as noteworthy porous materials for over a decade.[18] MOFs are comprised of metal nodes and organic linkers connected by coordination covalent bonds

3.2 One-step *in situ* method for ZIF film fabrication

3.2.1 ZIF-8 membranes

0.55 g zinc chloride ($ZnCl_2$) and 1.43 g sodium formate were dissolved in 20 ml methanol and 2.60 g 2-methylimidazole (m-Im) was dissolved in 20 ml methanol. After stirring the two solutions separately for 10 min, the solutions were mixed together and the mixture was stirred for 20 min. The final molar ratio of the growth solution was Zn : m-Im : HCOONa : MeOH = 1 : 8.3 : 5.6 : 250. An as-prepared α-alumina support [28b] (2 mm thickness and 22 mm diameter with one side polished) was placed vertically into an autoclave using a homemade Teflon holder with the polished side slightly facing down. The growth solution was poured into the autoclave containing the support and heated in a convective oven at 120 °C for 4 h. After removal from the oven the sample was cooled down to room temperature under ambient conditions. The membrane was then rinsed with excess methanol and subjected to solvent exchange in methanol for 24 h followed by drying in an oven at 70 °C for 24 h.

3.2.2 ZIF-7 films

Synthesis recipe is based on the ZIF-7 membrane recipe from our previous work [22m] with slight modifications. One step *in situ* growth of ZIF-7 film was performed on unmodified support as compared to ligand modified support, using relatively reduced amount of sodium formate. 1.54 g of zinc nitrate hexahydrate ($Zn(NO_3)_2$.$6H_2O$) and 0.08 g of sodium formate were dissolved in 20 ml DMF (solution A) and 0.81 g of benzimidazole (b-Im) was dissolved in 20 ml DMF (solution B). After separately stirring solutions A and B for 20 min, they were mixed together and the mixture was stirred for 10 min. The final molar ratio of the growth solution was Zn : b-Im : HCOONa : DMF = 1 : 1.9 : 2.0 : 100. An unmodified α-alumina support was placed vertically in an autoclave using a homemade Teflon holder with the polished side very slightly facing down. The solution was then poured into the autoclave containing the support and then heated in a convective oven at 120 °C for 3 h. After removal from the oven it was cooled down to room temperature under ambient conditions. The ZIF-7 film was rinsed with excess methanol and dried on shelf for 6 h.

3.2.3 $Zn(Im)_2$ (ZIF-61 analogue) films

ZIF-61 with **ZNI** topology was originally reported by Yaghi et. al. [18d] ZIF-61 synthesis recipe uses a mixture of imidazole and 2-methylimidazole ligands. $Zn(Im)_2$, first reported in 1980 [107], is isostructural to ZIF-61 with **ZNI** topology and it uses only imidazole ligand. $Zn(Im)_2$ phase reported here is microporous and has **ZNI** topology, with a pore size of 3.6Å [20]. The synthesis protocol followed here is different from the

previous work [107]. 0.55 g of zinc chloride ($ZnCl_2$) and 1.43 g of sodium formate were dissolved in 20 ml methanol (solution A) and 2.15 g of imidazole (Im) was dissolved in 20 ml methanol (solution B).). After stirring the two solutions separately for 10 min, the solutions were mixed together and the mixture was stirred for 20 min. The final molar ratio of the growth solution was Zn : Im : HCOONa : MeOH = 1 : 8.3 : 5.6 : 250. An unmodified α-alumina support was placed in an autoclave in an identical way described above. The solution was poured into the autoclave containing the support and heated in a convective oven at 120 °C for 4 h. After removal from the oven it was cooled down to room temperature under ambient conditions. The ZIF-61 film was rinsed with excess methanol and dried on shelf for 6 h.

3.2.4 ZIF-90 films

ZIF-90 membranes have been reported [22n, 50] As compared to previously reported recipe [22n], one step *in situ* method uses sodium formate and methanol as solvent with reduced synthesis time. 0.21 g of zinc chloride ($ZnCl_2$) and 0.10 g of sodium formate were dissolved in 20 ml methanol (solution A) and 0.60 g of imidazole-2-carboxaldehyde (Ica) was dissolved in 20 ml methanol (solution B). Solution A was stirred for 10 min, solution B was stirred at 60 °C in a closed container until clear solution was obtained. The solutions were then mixed together and the mixture was stirred for 5 min. The final molar ratio of the growth solution was Zn : Ica : HCOONa : MeOH = 1 : 1.9 : 1.0 : 100. An unmodified α-alumina support was placed in an autoclave in an identical way described above. The solution was poured into the

autoclave containing the support and heated in a convective oven at 120 °C for 4 h. After removal from the oven it was cooled down to room temperature under ambient conditions. The ZIF-90 film was rinsed with excess methanol and dried on shelf for 6 h.

3.2.5 SIM-1 films

SIM-1 film fabrication protocol was adopted from the previously reported SIM-1 membrane [26, 108]. Sodium formate was incorporated in the growth solution for one step *in situ* method. The precursor solution for SIM-1 *in situ* synthesis was prepared by dissolving a solid mixture 0.40 g of zinc nitrate hexahydrate ($Zn(NO_3)_2$.$6H_2O$), 0.03 g of sodium formate and 0.60 g of 4-methyl-5-imidazolecarboxaldehyde (m-Ica) in 30 ml DMF. The solution was stirred for 20 min. The final molar ratio of the growth solution was Zn : m-Ica : HCOONa : DMF = 1 : 4.0 : 0.32 : 290. An unmodified α-alumina support was placed in an autoclave in an identical way described above. The solution was poured into the autoclave and then heated in a convective oven at 85 °C for 24 h. After removal from the oven it was cooled down to room temperature under ambient conditions. The SIM-1 film was rinsed with excess methanol and dried on shelf for 6 h.

3.3 Control experiments to identify role of sodium formate

In order to decouple the new role of sodium formate from its previously known role, we designed control experiments where alumina supports were modified in the presence of sodium formate. The modified supports were then subjected to *in situ* solvothermal growth in the absence of sodium formate.

3.3.1 Modification of alumina supports

To modify an alumina support with zinc and sodium formate, a modification solution was prepared by dissolving 0.55 g of zinc chloride ($ZnCl_2$) and 1.43 g of sodium formate (hereafter SF) in 40 ml methanol. The solution was stirred for 10 min. The modification solution was poured into an autoclave with an unmodified α-alumina support mounted on a homemade Teflon holder. The autoclave was heated in a convective oven at 120 °C for 4 h. It was then removed from the oven and allowed to cool down to room temperature. During this solvothermal modification, formation of white precipitate was observed in the solution. This precipitate was collected and analyzed by XRD. The zinc chloride and sodium formate modified support (hereafter Zn-SF-modified support) thus obtained, was rinsed with excess methanol and soaked in methanol overnight followed by drying on shelf for 6 h. Similarly m-Im and sodium formate modified support (hereafter mIm-SF-modified support) and only sodium formate modified support (hereafter SF-modified support) were also obtained using 40 ml methanol solutions containing 2.60 g of 2-methylimidazole and 1.43 g of sodium formate and 1.43 g of sodium formate alone, respectively.

3.3.2 *In situ* growth of modified supports in the absence of sodium formate

In situ growth was carried out on the modified supports using a growth solution free of sodium formate under similar conditions as for *in situ* synthesis of ZIF-8 membranes (see Section 2.2). In order to form ZIF-8 membranes in the absence of sodium formate during the growth, however, the aqueous solution recipe reported by Pan et al. [7b] was adopted. 1.12 g of zinc nitrate ($Zn(NO_3)_2 .6H_2O$) and 22.17 g of 2-methylimidazole were dissolved in 40 ml and 80 ml DI water, respectively. After stirring 10 min, the two solutions were mixed together and stirred for 10 min.

3.4 Synthesis of HKUST-1 membranes by RTD

2.5 g of copper nitrate hemi(pentahydrate) ($Cu(NO_3)_2. 2.5H_2O$) and 1.25 g of 1,3,5-benzene tricarboxylic acid (BTC) were dissolved in 10 ml DMF each and stirred for 10 min. The ligand solution was added to the metal solution dropwise and mixture was stirred for 10 min until a clear solution was obtained. This precursor solution with a molar ratio of Cu : BTC : DMF = 1.8 : 1 : 43.4 was used for RTD processing. Porous α-alumina disks were used as supports and obtained using a previously reported method.[28b] The supports were polished on one side. For slip coating, while the supports were held horizontally with polished side facing down, the precursor solution was brought up in contact with the supports for 30 s and then slid away and held vertically. After quickly wicking off the excess precursor solution from the sides, using a kim wipe, the slip coated support was placed in a preheated oven at 180 °C (RTD temperature) for 15 min (RTD time) with polished side facing up. After 15 min, the oven was turned off and the

HKUST-1 membranes were allowed to cool down slowly in the oven. On cooling down to room temperature, the membranes were removed from the oven, rinsed with methanol and solvent exchanged for 24 h in methanol. Membranes were dried under ambient conditions for 12 h thereafter.

HKUST-1 powder was synthesized by RTD by spreading the RTD precursor solution on a glass slide. The glass slide was placed in the preheated oven at 180 °C for 15 min and cooled down slowly to ambient conditions. The powder was scrapped off from the glass slide using a blade. The powder thus obtained was washed with methanol and solvent exchanged in methanol for 24 h followed by drying on the shelf for 12 h.

3.5 Synthesis of ZIF-8 membranes by RTD

1.32 g of zinc acetate dihydrate ($Zn(OAc)_2$. $2H_2O$) and 1.00 g of 2-methylimidazole (m-Im) were dissolved in 15 ml solvent each (total 30 ml solution). The solvent used here was a mixture of DMA and DI water in the ratio 2 : 1 (v/v ratio). The ligand solution was added dropwise to the metal salt solution and stirred for 1 min. This precursor solution with molar ratios Zn : m-Im : DMA/DI = 1 : 2 : 128 was immediately used for slip coating on α-alumina support, in a similar manner as described above. The slip-coated supports were placed in the oven at 200 °C (RTD temperature) for 15 min (RTD time). After 15 min, membranes were slowly cooled down to room temperature similar to HKUST-1 membrane. ZIF-8 membranes were rinsed with DMA, followed by ethanol rinsing and solvent exchange in ethanol for 3 days. After solvent exchange, the membranes were dried at 85 °C for 12 h.

3.6 Permeance measurement

3.6.1 Time lag method for single gas permeance

The permeance of single gas molecules were measured in a custom-made permeation cell using a time-lag method (Figure 32). The time-lag is the amount of time required for a gas to permeate through a membrane. There are two methods for obtaining the time-lag; one is a differential technique and the other is an integral method. In this study, we used the integral method to obtain the permeance of the gas molecules. The integral method monitors increasing pressure caused by accumulation of permeating gas through membrane in the evacuated chamber as a function of time. The chamber is initially degassed by vacuum and separated from the gas in feed side by a membrane. The Permeation cell is separated two parts (feed side and permeate side) by a zeolite membrane. At the permeate side, one port is connected to volume chamber which is subsequently lined to vacuum pump, and the other port is cupped. The pressure of the volume chamber is monitored by computer. Before measurement of permeance, the feed side is flushed with the gas molecules at about 1 ~ 2 bar and the permeate side is evacuated to a vacuum. The experiment is started when the inlet gas stream at the feed side is shut off. From this time, the pressure in the volume chamber at the permeate side increase and is monitored by a computer. The permeance (Π) of gas molecules through zeolite membranes can be calculated using following equations.

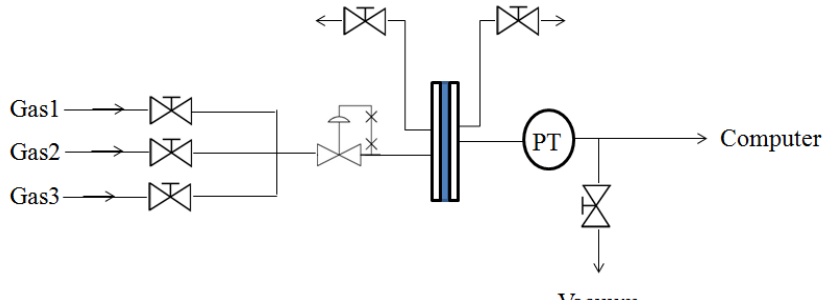

Figure 32: Single gas permeation measurement by time-lag method

$$\frac{\partial C}{\partial t} = D\frac{\partial^2 C}{\partial x^2}.$$

$$Q_t = \frac{DC_1}{l}\cdot\left(t - \frac{l^2}{6D}\right)$$

$$Q_t = \frac{P_p V}{ART} = \frac{DC_1}{1}(t - \frac{l^2}{6D}) = \frac{D\cdot S\cdot P_f}{1}(t - \frac{l^2}{6D})$$

$$P_p = \frac{A\cdot D\cdot S\cdot P_f\cdot RT}{1\cdot V}(t - \frac{l^2}{6D})$$

3.6.2 Wicke-Kallenbach (WK) method for binary gas permeance

Binary gas permeation experiments were carried out by the WK method (Figure 33). A mixture of feed stream was balanced to 101kPa by argon gas with the flow rate of around 100ml/min. At the permeate side, a pure sweep argon gas was used with the flow rate of around 100ml/min. The concentration of the component through a zeolite membrane was analyzed by Hiden Mass Spec.

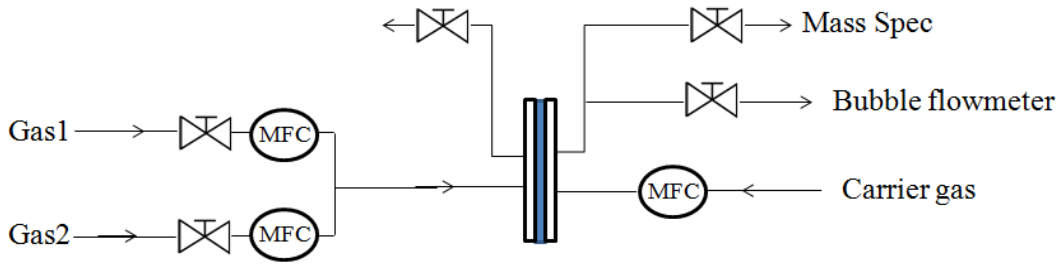

Figure 33: Binary gas permeation measurement by Wicke-Kallenbach method

$$J_A = \frac{y_A Q_t}{A}$$

$$J_A = P_A \frac{\Delta p^g{}_A}{l} = \Pi_A * \Delta p^g{}_A$$

$$\Pi_A = \frac{J_A}{\Delta p^g{}_A}$$

3.7 Analytical methods

3.7.1 Electron microscopy

Samples for SEM were coated with 16 nm Pt/Pd coating using a Cressington Sputter Coater. Scanning electron micrographs were taken with a Quanta 600 field emission scanning electron microscope operating at 30 kV acceleration voltage and 10 mm lens distance. Energy dispersive X-ray spectroscopy (EDS) was carried out using an Oxford EDS X-ray mapping and digital imaging accessory attached to the Quanta SEM.

3.7.2 X-ray diffraction

X-ray diffraction (XRD) patterns were collected with a Rigaku Miniflex II powder X-ray diffractometer with Cu-Kα radiation (λ = 1.5406 Å) with a collection time of 1 s and 2 theta resolution of 0.2°. X-ray Photoelectron spectroscopy (XPS) was performed with a Kratos Axis Ultra Imaging X-ray photoelectron spectrometer.

CHAPTER IV

ONE STEP *IN SITU* SYNTHESIS OF ZIF FILMS AND MEMBRANES: ROLE OF SODIUM FORMATE*

4.1 Introduction

Zeolitic imidazolate frameworks (ZIFs) are a sub-class of metal-organic frameworks (MOFs), comprising hybrid organic-inorganic moieties and exhibiting regular crystalline lattices with well-defined pore structures.[1, 18c, 29-30] ZIFs consist of metal nodes coordinated to imidazolate-based ligands. The metal-linker-metal bond angle (~145°) in ZIFs is comparable to the T-O-T bond angle in zeolites, thereby resulting in zeolite topologies. Their exceptional thermal and chemical stabilities coupled with microporous cavities [1] make them desirable candidates for gas sensors [21r], catalytic membrane reactors [31], and gas separation membranes [6, 22f-h, 22j, 22m, n]. As a result, synthesis of ZIF films and membranes has attracted a great deal of interest in recent years [5, 21j].

Among other ZIF systems, ZIF-8 is of particular interest due to its robust synthesis protocol as well as its potentials in small-gas separations. ZIF-8 is comprised of Zn atoms interconnected with 2-methylimidazolate ligands, forming the sodalite (SOD) zeolite-like structure with large cavities (11.6 Å) and small pore apertures (3.4 Å) [1]. Diverse synthesis protocols for ZIF films and membranes have been reported [5] and can

*Reprinted with permission from "One step *in situ* synthesis of supported zeolitic imidazolate framework ZIF-8 membranes: Role of sodium formate." by M. Shah, H.-T. Kwon, V. Tran, S. Sachdeva, H.-K. Jeong, Microporous and Mesoporous Materials 2013, 165 (0), 63-69. Copyright © 2013, Elsevier

be classified into two categories: *in situ* growth [6] and secondary (seeded) growth [4, 7]. Recently Pan et al. [4] synthesized ZIF-8 membranes using secondary growth method and showed excellent propylene/propane gas separation performance. However, secondary growth method requires seeding step in addition to solvothermal growth step. Increased number of steps adds to the complexity of the process, thereby potentially causing reproducibility issues [5]. ZIF-8 membranes have been synthesized using *in situ* method as well. To promote heterogeneous nucleation of ZIF-8 crystals, supports were often times modified [22m] or more expensive supports such porous titania than commonly-used α-alumina were used [6].

Here we report one step *in situ* synthesis of ZIF-8 membranes on unmodified porous α-alumina supports in the presence of sodium formate. This approach is different from our previously reported technique [22m] in which ligand-modified supports were used to promote heterogeneous nucleation. In this work, ZIF-8 membranes were prepared on as-prepared supports, thereby eliminating the need for support modification and simplifying the process. The focus of this work is to investigate the role of sodium formate in this one step *in situ* method. Besides the previously reported role of sodium formate as a deprotonator promoting the intergrowth of ZIF crystals [22m], we identified a previously unknown role of sodium formate of promoting heterogeneous nucleation on α-alumina supports. One step *in situ* method was used to prepare continuous films of several other ZIFs including ZIF-7 [1], $Zn(Im)_2$ (ZIF-61 analogue) [18d, 32], ZIF-90 [33], and SIM-1 [31a], suggesting the general applicability of the method.

4.2 Experimental

4.2.1 Chemicals

All the chemicals were used as received without further purification. Zinc chloride ($ZnCl_2$ > 95%, Fisher Scientific) and zinc nitrate hexahydrate ($Zn(NO_3)_2$.$6H_2O$ > 98%, Sigma-Aldrich) were used as zinc sources. 2-methylimidazole (m-Im) ($C_4H_6N_2$ > 99%), benzimidazole (b-Im) ($C_7H_6N_2$ > 98%), imidazole-2-carboxaldehyde (Ica) ($C_4H_4N_2O$ > 97%), 4-methyl-5-imidazolecarboxaldehyde (m-Ica) ($C_5H_6N_2O$ > 99%), imidazole (Im) ($C_3H_4N_2$ > 99%), sodium formate (HCOONa > 99%) were purchased from Sigma-Aldrich. Methanol (99.8%) and N,N-dimethyl formamide (DMF) (99.8%) were obtained from Alfa Aesar.

4.2.2 Synthesis of ZIF-8 membranes

0.55 g zinc chloride ($ZnCl_2$) and 1.43 g sodium formate were dissolved in 20 ml methanol and 2.60 g 2-methylimidazole (m-Im) was dissolved in 20 ml methanol. After stirring the two solutions separately for 10 min, the solutions were mixed together and the mixture was stirred for 20 min. The final molar ratio of the growth solution was Zn : m-Im : HCOONa : MeOH = 1 : 8.3 : 5.6 : 250. An as-prepared α-alumina support [28b] (2 mm thickness and 22 mm diameter with one side polished) was placed vertically into an autoclave using a homemade Teflon holder with the polished side slightly facing down. The growth solution was poured into the autoclave containing the support and heated in a convective oven at 120 °C for 4 h. After removal from the oven the sample was cooled down to room temperature under ambient conditions. The membrane was then rinsed

with excess methanol and subjected to solvent exchange in methanol for 24 h followed by drying in an oven at 70 °C for 24 h.

4.2.3 Control experiments to identify the role of sodium formate

In order to decouple the new role of sodium formate from its previously known role, we designed control experiments where alumina supports were modified in the presence of sodium formate. The modified supports were then subjected to *in situ* solvothermal growth in the absence of sodium formate.

4.2.3.1 Modification of alumina supports

To modify an alumina support with zinc and sodium formate, a modification solution was prepared by dissolving 0.55 g of zinc chloride ($ZnCl_2$) and 1.43 g of sodium formate (hereafter SF) in 40 ml methanol. The solution was stirred for 10 min. The modification solution was poured into an autoclave with an unmodified α-alumina support mounted on a homemade Teflon holder. The autoclave was heated in a convective oven at 120 °C for 4 h. It was then removed from the oven and allowed to cool down to room temperature. During this solvothermal modification, formation of white precipitate was observed in the solution. This precipitate was collected and analyzed by XRD. The zinc chloride and sodium formate modified support (hereafter Zn-SF-modified support) thus obtained, was rinsed with excess methanol and soaked in methanol overnight followed by drying on shelf for 6 h. Similarly m-Im and sodium formate modified support (hereafter mIm-SF-modified support) and only sodium formate modified support

(hereafter SF-modified support) were also obtained using 40 ml methanol solutions containing 2.60 g of 2-methylimidazole and 1.43 g of sodium formate and 1.43 g of sodium formate alone, respectively.

4.2.3.2 *In situ* growth of modified supports in the absence of sodium formate

In situ growth was carried out on the modified supports using a growth solution free of sodium formate under similar conditions as for *in situ* synthesis of ZIF-8 membranes (see Section 2.2). In order to form ZIF-8 membranes in the absence of sodium formate during the growth, however, the aqueous solution recipe reported by Pan et al. [7b] was adopted. 1.12 g of zinc nitrate ($Zn(NO_3)_2 .6H_2O$) and 22.17 g of 2-methylimidazole were dissolved in 40 ml and 80 ml DI water, respectively. After stirring 10 min, the two solutions were mixed together and stirred for 10 min.

4.2.4 Characterization

Scanning electron micrographs were taken with a Quanta 600 field emission scanning electron microscope operating at 20 keV acceleration voltage and 10 mm lens distance. Energy dispersive X-ray spectroscopy (EDS) was carried out using an Oxford EDS X-ray mapping and digital imaging accessory attached to the Quanta SEM. X-ray diffraction (XRD) patterns were collected with a Rigaku Miniflex II powder X-ray diffractometer with Cu-Kα radiation (λ = 1.5406 Å). X-ray Photoelectron spectroscopy (XPS) was performed with a Kratos Axis Ultra Imaging X-ray photoelectron spectrometer. Single gas permeation measurements were conducted for small gas

molecules (H_2, N_2, O_2, CH_4, and CO_2) through ZIF-8 membranes using a time- lag method at room temperature and a feed pressure of 1 bar.

4.3 Results and discussion

4.3.1 ZIF-8 membrane fabrication using sodium formate

ZIF-8 membranes were synthesized using one step *in situ* method in the presence of sodium formate. ZIF-8 membranes are phase-pure (Figure 34a) and well-intergrown with a thickness of about 25 µm (Figure 34b). Previously, our group reported ZIF-8 membranes synthesized *in situ* by modifying alumina supports with ligands (m-Im) and followed by growing ZIF-8 crystals in the presence of sodium formate [22m]. Though the growth conditions are similar (both in the presence of sodium formate), the grains of the one step *in situ* prepared ZIF-8 membranes are less uniform and larger than those of the previously prepared membranes[22m]. This difference in membrane microstructure can be attributed to the difference at the nucleation step. When compared to the one step *in situ* recipe, in our previously reported technique[22m], ligands anchored on supports are expected to promote formation of more nuclei with a more uniform distribution on the supports, resulting in smaller grains with a less distribution in size. Nevertheless, both ZIF-8 membranes show comparable single gas permeation properties with molecular sieving behavior (i.e., favoring smaller molecules) as shown in Figure 35.

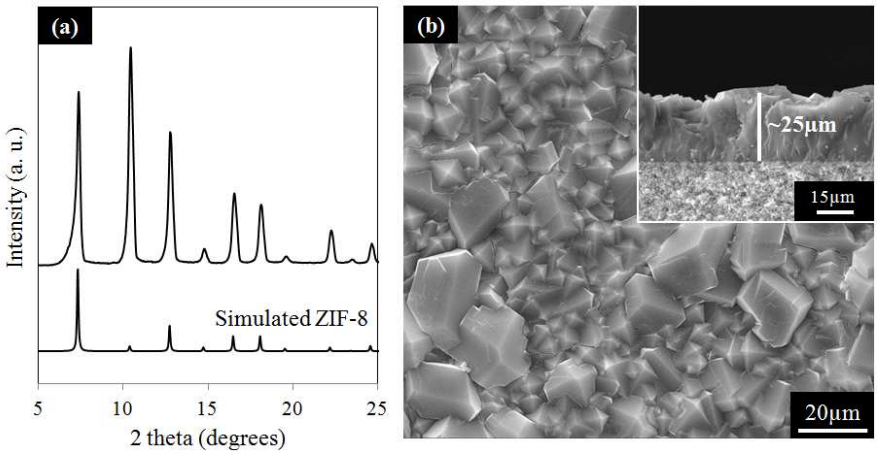

Figure 34: (a) XRD pattern of ZIF-8 membrane in comparison with simulated ZIF-8 pattern and (b) top view and cross-section (inset) of ZIF-8 membrane.

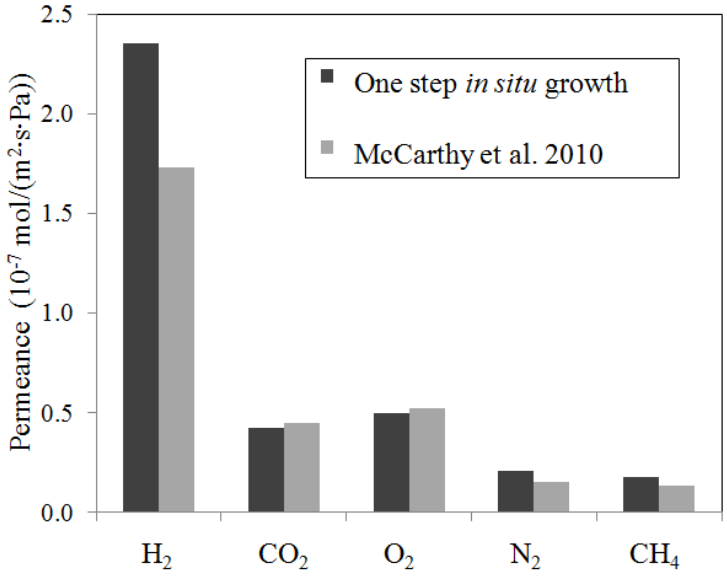

Figure 35: Single gas permeances of ZIF-8 membrane by one step in situ method in comparison with those of ZIF-8 membrane by McCarthy et al. (ref. 14)

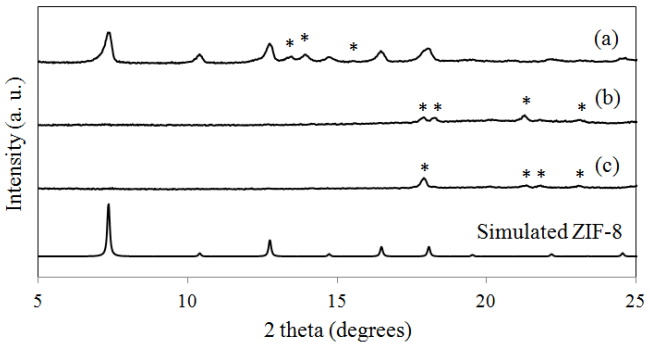

Figure 36: XRD patterns of the supports modified with (a) zinc chloride and sodium formate (Zn-SF-modified), (b) 2-methylimidazole and sodium formate (mIm-SF-modified), and (c) sodium formate (SF-modified) along with simulated ZIF-8 pattern. Note that the modified supports were subjected to in situ growth in the absence of sodium formate. * indicates unknown phase/s.

The presence of sodium formate was found critical for one step *in situ* synthesis of continuous well-intergrown ZIF-8 membranes. Under identical synthesis conditions, when no sodium formate is present in growth solution, relatively insignificant ZIF-8 nucleation was observed on the support. In order to understand how the existence of sodium formate in growth solutions promotes ZIF-8 membrane formation on α-alumina supports, we designed and carried out control experiments as discussed below.

4.3.2 The role of sodium formate in promoting heterogeneous nucleation of ZIF-8

As previously reported [22m, 109], once ZIF crystals are nucleated on support surfaces, sodium formate can act as a deprotonator and lead to uniform growth of crystals in all

directions, giving rise to continuous well-intergrown films. However, for this process to occur heterogeneous nucleation of ZIF crystals is necessary in the first place. In our previous work [22m], supports were modified with ligands to enhance heterogeneous nucleation of ZIF crystals. As stated above, since ZIF-8 films can be formed only in the presence of sodium formate on the unmodified supports, we hypothesized that sodium formate plays a role in promoting heterogeneous nucleation as well (Figure 36).

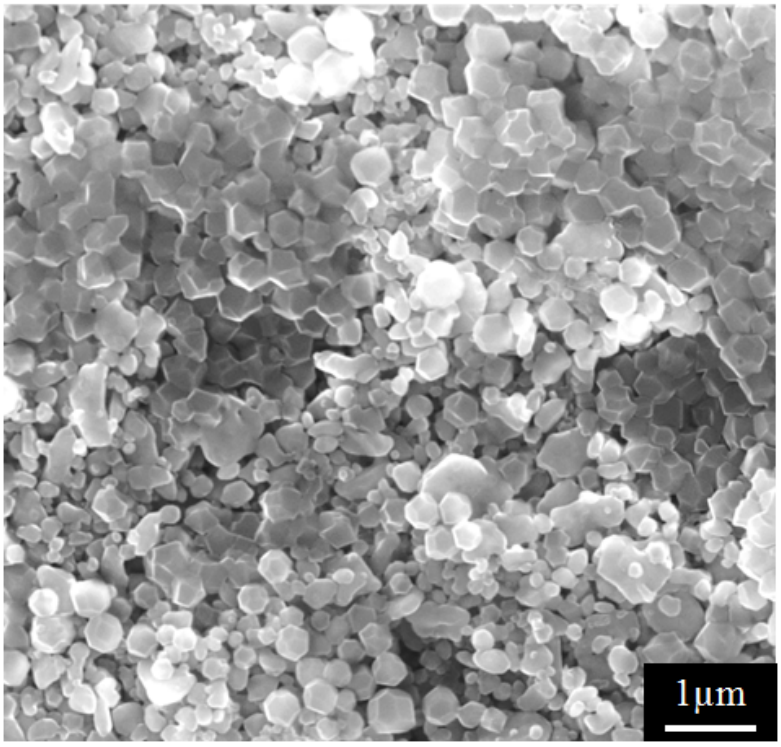

Figure 37: Scanning electron micrograph of the support modified with zinc chloride and sodium formate (Zn-SF-modified support) after in situ growth without sodium formate.

At first, it was speculated that sodium formate modified the surface charge of α-alumina supports [59], which in turn promoted heterogeneous nucleation (Figure 37 and 38). Surface charge is a function of the pH of synthesis solutions. As shown in our previous work [22m], growth solutions containing sodium formate have higher pH and are more basic in nature than formate-free solution. When *in situ* growth was carried out under identical pH conditions but using a different base (NaOH) instead of sodium formate, no significant heterogeneous nucleation was observed. Thus although surface charge modification cannot be excluded, it alone doesn't promote heterogeneous nucleation. Further, ZIF-8 films could not be obtained on silica surfaces even if growth solutions contained sodium formate. This led us to speculate a possible chemical modification specific to α-alumina supports and sodium formate such that ZIF crystal formation is stimulated on the support surface during *in situ* growth.

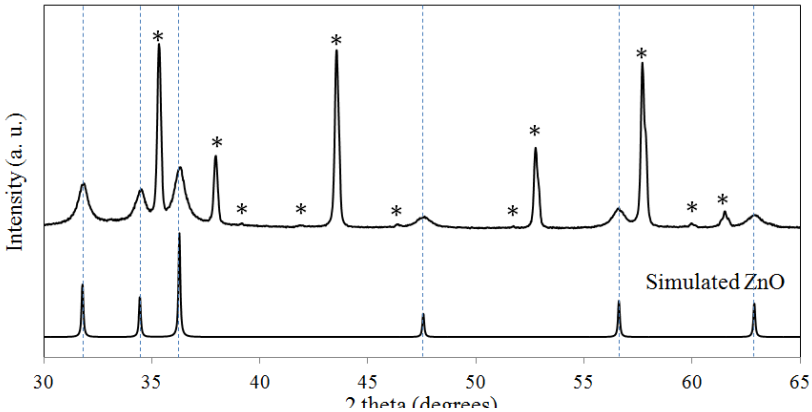

Figure 38: XRD pattern of Zn-SF-modified support along with simulated ZnO pattern. * indicates α-alumina peaks.

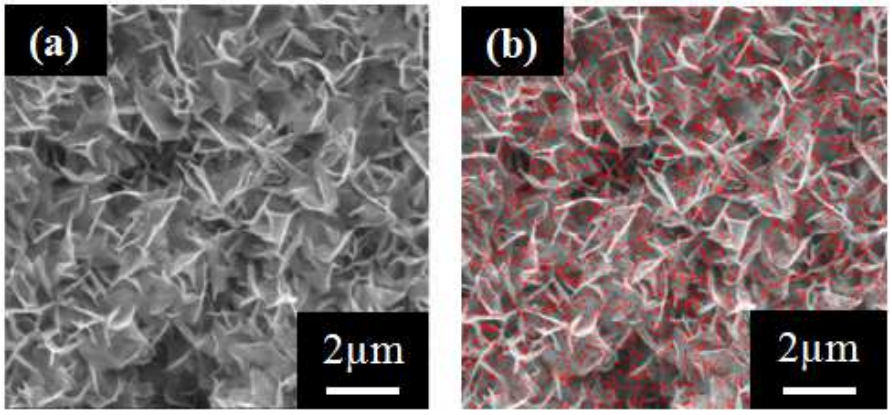

Figure 39: (a) Scanning electron micrograph and (b) energy dispersive X-ray spectroscopy (EDS) map of Zn-SF- modified support. Red color indicates the presence of zinc on the support.

As mentioned earlier, during the growth stage sodium formate enables ZIF-8 crystal intergrowth by deprotonating ligands. In order to decouple the role of sodium formate in enhancing heterogeneous nucleation from that in promoting crystal growth, control experiments were conducted where the one step *in situ* process was split into two steps. In the first step, supports were solvothermally modified (see Section 2.3 for experimental details) using methanol solutions containing only sodium formate (SF-modified), m-Im and sodium formate (mIm-SF-modified), and zinc chloride and sodium formate (Zn-SF-modified). Concentrations and solvothermal conditions were kept identical to those in the actual one step *in situ* growth. But metal and ligand were not present in the modification solution at the same time to avoid any ZIF nucleation during the support modification step. Second step consisted of *in situ* growth of ZIF-8 crystals

on Zn-SF-, mIm-SF- and SF-modified supports in the absence of sodium formate. An aqueous recipe reported by Pan et al.[7b] was adopted for this purpose. Note that in the absence of sodium formate in the growth step, films are expected to be poorly intergrown [22m].

Figure 36 presents the XRD patterns of Zn-SF-, mIm-SF- and SF-modified supports after *in situ* growth without sodium formate. In contrast to SF- and mIm-SF-modified supports (Figures 37), the support modified with sodium formate and zinc chloride exhibited significant nucleation and growth of ZIF-8 crystals (Figure 36a), along with some additional peaks (marked with asterisk). These additional peaks are not present in the actual one step *in situ* synthesis of ZIF-8 membranes (see Figure 34a). ZIF-8 film on the Zn-SF-modified support (Figure 37) has much smaller crystals and is poorly intergrown as compared to that prepared using one step *in situ* process (Figure 32a). This is attributed to the fact that the *in situ* growth was carried out in the absence of sodium formate in this control experiment [22m, 109]. Since the *in situ* growth step is identical, the difference between Zn-SF-, mIm-SF- and SF-modified supports is ascribed to the support modification. In other words, zinc and formate synergistically modify the support and promote heterogeneous nucleation. Note that modification with zinc alone does not produce ZIF crystals on the support (not shown here).

One plausible support modification is that the carboxylic group (-C=O) of formate undergoes condensation reaction with the surface hydroxyl groups of α-alumina supports as reported by Bertazzo et al. [59] Zinc source can then co-ordinate to the carboxyl group covalently linked to the surface, thereby initiating heterogeneous nucleation. If this

scenario is true, one might expect nucleation of ZIF crystals on SF-modified supports: carboxylation of the support would occur during the support modification [59] and in the subsequent *in situ* growth stage zinc cations can then co-ordinate with carboxylates, resulting in heterogeneous nucleation. Lack of ZIF-8 crystals on the SF-modified support after *in situ* growth suggests that this scenario is not likely.

It was then hypothesized that the support surface was modified with zinc-based compounds with a help of sodium formate. This zinc-based phase may enable heterogeneous nucleation of ZIF crystals. As shown in Figure 38, the XRD pattern of the Zn-SF-modified support before *in situ* growth shows that there exists a zinc oxide phase (hexagonal wurtzite structure) on the support. As compared to the alumina peaks, the peaks of the zinc oxide are much broader, suggesting the existence of nano-scale crystalline domains. Electron micrograph (Figure 39a) of the Zn-SF-modified support clearly shows the existence of a continuous layer of the ZnO phase on the support. The morphology of this phase is distinctively different from that of α-alumina support. EDS imaging (Figure 39b) as well as XPS spectrum of the support confirm the presence of zinc on the support. During the preparation step for the Zn-SF-modified support, white precipitates were formed in the solution and were analyzed to be zinc oxide. It is speculated that this zinc oxide layer formed on the support promotes heterogeneous nucleation of ZIF-8 crystals. Guo et al. [22d] showed that oxidized copper mesh can act as a heterogeneous nucleation site and as a secondary metal source for the formation of HKUST-1 membrane.

It is reasonable to surmise that the zinc oxide layer can also serve as a nucleation site and metal source in a similar manner. To further confirm that ZnO alone promotes heterogeneous nucleation, the Zn-SF-modified support was calcined at 400 °C for 4 h in air to remove any organic surface groups that might also enable nucleation. ZIF-8 crystals were formed on the calcined Zn-SF modified support after *in situ* growth without sodium formate as well as on the non-calcined sample. This further verifies that the zinc oxide layer is responsible for formation of ZIF-8 crystals on α-alumina supports.

4.3.3 Zinc oxide formation in the one step *in situ* process

To investigate formation of zinc oxide in the one step *in situ* method, we analyzed supports at different stages of film growth. A series of ZIF-8 films were synthesized by varying the synthesis time (0.5 h, 1 h, 2 h, and 4 h). After quickly removing the samples from the growth solutions, they were rinsed thoroughly with methanol, dried, and analyzed using XRD.

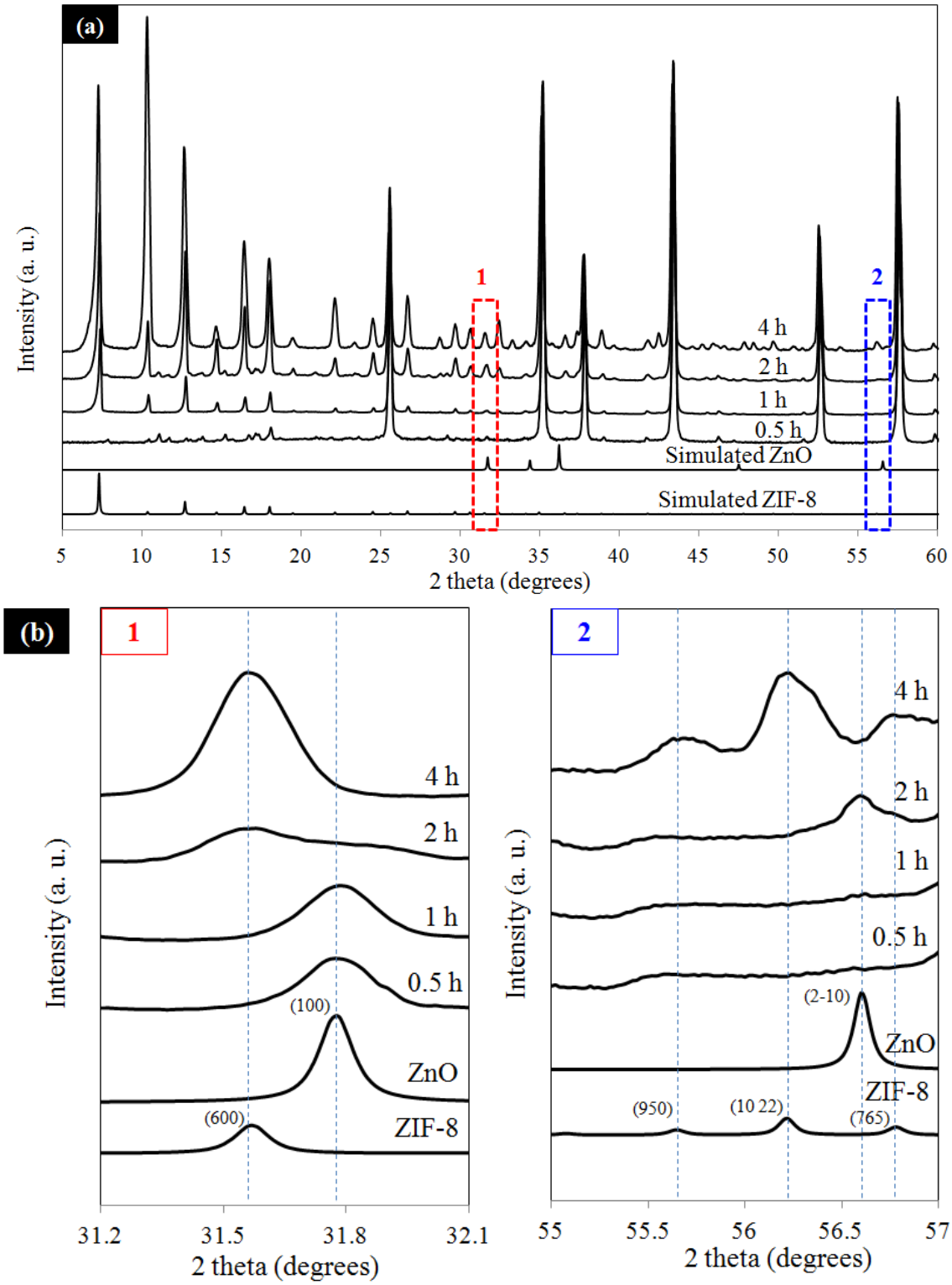

Figure 40: (a) XRD pattern of ZIF-8 films prepared at different synthesis times (0.5 h, 1 h, 2 h, and 4 h) and (b) enlarged patterns in the selected regions for clarity.

Figure 40 presents the XRD data collected for ZIF-8 films prepared for different synthesis times. As seen in the figure (see Figure 40b for clarity), ZnO was detected after 30 min. Cravillon et al. [109-110] showed that sodium formate acts as a deprotonator for the ligand at high temperature but as a competitive ligand for Zn^{+2} centers at room temperature. In the initial nucleation stage of crystallization, the temperature of the support increases from room temperature to synthesis temperature (120 °C). During this time, it is expected that the coordination modulation role of sodium formate is dominant due to low temperature. Since the solution is basic owing to excess imidazole ligands, this would provide a favorable condition for formation of zinc oxide on the support [111]. The XRD intensity of zinc oxide (Figure 40b) was fairly low as compared to that of the Zn-SF-modified support (Figure 36) for control experiment. This is because in case of one step *in situ* growth, sodium formate and ligand both compete for interacting with zinc ions. In contrast, in the preparation process of the Zn-SF-modified support, all of the zinc ions are available to interact with formate ions to form zinc oxide. As a result, formation of zinc oxide is significantly exaggerated for Zn-SF-modified support (Figure 38). Further, ZnO might have some preferred orientation, making other peaks difficult to detect. Peaks from [100] and [2-10] planes of ZnO are strong enough to be noticed. After 2 h, ZIF-8 peaks emerge (Figure 40b). It is our conjecture that the ZnO not only acts as a nucleation site but also as a secondary metal source. Hence ZnO is consumed while it promotes heterogeneous nucleation of ZIF-8. Once ZIF-8 is nucleated, then the role of sodium formate as deprotonator [22m, 109] takes over in the later growth stage (due to high temperature), promoting uniform growth of crystals in all directions leading to well-

intergrown films. By the end of 4 h, almost no ZnO is detected whereas the ZIF-8 peak increases significantly, forming pure ZIF-8 films.

Finally we applied this one step *in situ* synthesis method to synthesize continuous films of several other ZIFs including ZIF-7, $Zn(Im)_2$ (ZIF-61 analogue), ZIF-90, and SIM-1 (Figure 41) suggesting the general applicability of the technique. Detailed synthesis procedures are presented in the Supporting Information. Further optimization of synthesis conditions is required for high quality film formation for membrane applications.

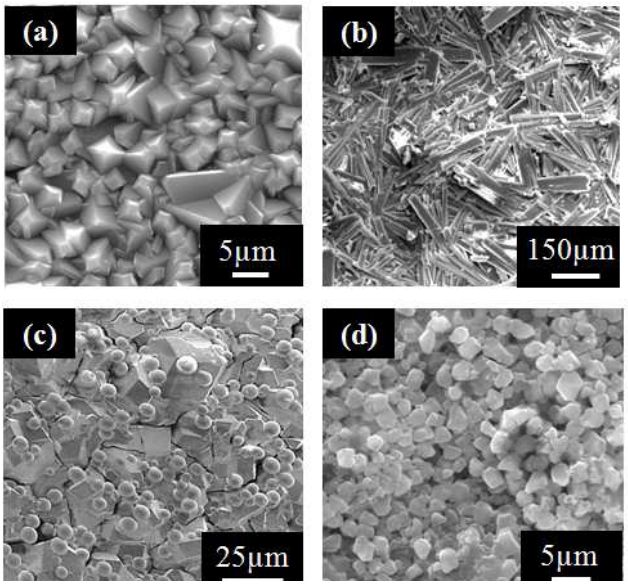

Figure 41: SEM images of (a) ZIF-7, (b) Zn(Im)2 (ZIF-61 analogue), (c) ZIF-90, and (d) SIM-1 films synthesized using one step in situ method. There are unknown phases in Zn(Im)2 and ZIF-90 films. Note that ZIF-90 and SIM-1 are isostructural to ZIF-8 (SOD structure).

4.4 Conclusions

In conclusion, we synthesized continuous well-intergrown ZIF-8 membranes by a simple one step *in situ* growth method. During *in situ* growth, sodium formate along with zinc salts leads to formation of zinc oxide on α-alumina supports. This zinc oxide acts as a heterogeneous nucleation site as well as a secondary metal source. Once ZIF crystals are nucleated, sodium formate promotes the intergrowth of ZIF crystals by acting as a deprotonator (reported previously) leading to continuous well-intergrown films. Continuous films of several other ZIFs including ZIF-7, $Zn(Im)_2$ (ZIF-61 analogue), ZIF-90, and SIM-1 were successfully synthesized using this one step *in situ* method. This simple and potentially general synthesis method may open up new opportunities for formation and applications of ZIF films and membranes.

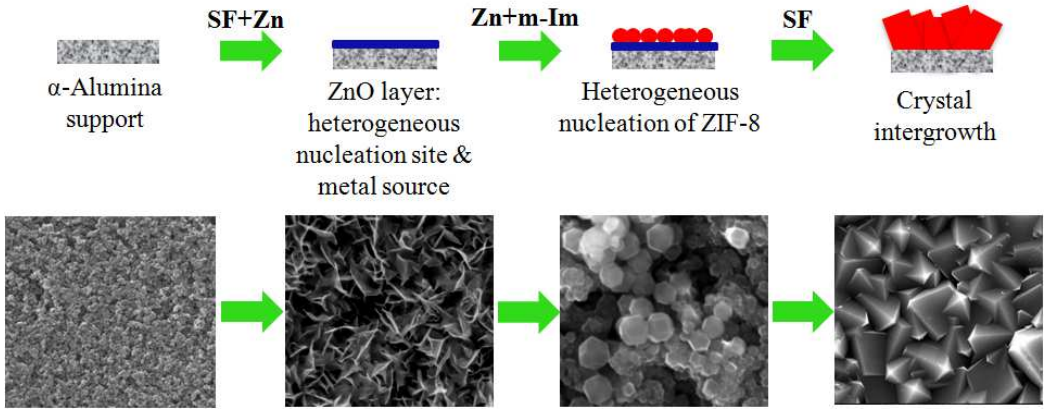

Figure 42: Schematic illustration of role of sodium formate in ZIF-8 membrane fabrication

CHAPTER V

RAPID THERMAL DEPOSITION (RTD) TECHNIQUE

5.1 Overview and motivation

As discussed earlier, there is clear need for an unconventional strategy for the fabrication of MOF membranes. The new strategy is desired to have the following advantages:

1. Rapid (membrane fabrication time in minutes not hours) and scalable(i.e. applicable to large area) more like industrially accepted techniques such as spray coating (fast and large scale manufacturing)
2. Flexible with respect to location of active films (not only outside of supports but also inside of supports) growing polycrystalline films inside the support enhances their mechanical stability during handling which is very critical for fragile films.
3. Flexible with respect to support materials (Not only to ceramic/stainless steel supports but also to polymer supports)
4. Environmentally friendly
5. General and reproducible

Here we propose to develop one such technology recognizing the unique co-ordination chemistry of MOFs, which is completely different from zeolite chemistry. Enlisted below are some of the advantages of the new Rapid Thermal Deposition (RTD) strategy over conventional techniques (Table 3).

Table 3: Comparison of RTD with conventional techniques

Conventional methods	**RTD**
Batch (hrs)	More like continuous (min)
Hardly scalable	Potentially Scalable
Thick membranes (~ 10μm)	Submicron thick
Limited choice of supports	Polymeric supports possible
Films grown outside the supports	Can grow films inside the support
No general methods	Potentially general
Reproducibility is an issue	Reproducible
Grain boundary defects	Lesser grain boundary defects

5.2 The RTD technique

Rapid Thermal Deposition (RTD) technique is a fundamentally different approach for synthesis of MOF membranes. Figure 42 illustrates the RTD technique. An unmodified α-alumina disc support is slip coated with the RTD precursor solution (for details refer to the experimental section 3.4). Then it is placed in a preheated oven at high temperature (temperature higher than boiling point of the solvent). High temperature causes rapid evaporation of solvent leading to supersaturation which in turn

promotes heterogeneous nucleation and growth of MOF crystals, yielding continous well-intergrown MOF membranes in tens of minutes. Once the solvent is evaporated the solvent present in the pores of the MOFs is also removed. Thus drying and partial activation of MOF crystals also occurs during the short time of 15 min. This technique was first demonstrated for prototypical and relatively stable MOF, HKUST-1. Thereafter it was extended to more promising MOFs, like ZIF-8.

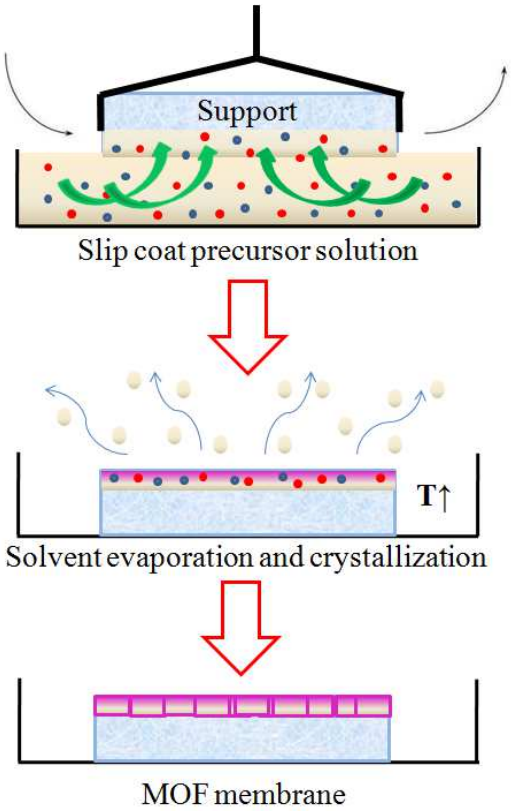

Figure 43: Schematic illustration of Rapid Thermal Deposition (RTD) technique.

5.3 Physical processes occurring during RTD and control parameters

For optimizing the growth of MOF membranes using RTD mainly two time scales need to be optimized, time scale of evaporation of solvent or rate of supersaturation and time scale of formation of MOF or reaction kinetics. These time scales can be altered by various control parameters the effect of which on both is complex. Table 4 discusses the various physicochemical processes involved in RTD.

Table 4: Major variables to control physicochemical processes in RTD

Processes	Major variables	Effects
Flow of liquid	-Temperature	- As T increases, flow of liquid increases, yielding more crystal growth on support surface
Evaporation of solvents	- Temperature -Solvent vapor pressure -Solvent partial pressure in gas phase - Deposition time	- Too high T causes fast evaporation resulting in no crystals formation - Solvent evaporation reduces as its vapor pressure reduces or partial pressure in gas phase increases - Deposition time is decided by the solvent vapor pressure, solvent partial pressure in gas phase and the RTD temperature

Table 4 continued

Formation of crystals	- Temperature -Molar composition -Presence of deprotonators - Deposition time	- Increased T leads to heterogeneous nucleation by attachment of ligands - Deprotonators enhance crystallization without increasing temperature
Drying (activation) of crystals	-Temperature - Solvent vapor pressure	- Insitu drying(activation) feasible depending on solvent vapor pressure and temperature

CHAPTER VI

HKUST-1 MEMBRANES BY RAPID THERMAL DEPOSITION

6.1 Introduction

A MOF with substantial reported literature on its material and membrane properties is desirable to demonstrate potential of the RTD technique. HKUST-1 was chosen for this purpose. Also the synthesis chemistry of HKUST-1 is robust and yields pure HKUST-1 phase over a very broad range of synthesis conditions. HKUST-1 is also relatively stable in comparison to other Zn-O co-ordination based MOFs.

6.2 Experimental

Experimental procedure has been discussed in detail in Section 3.4. HKUST-1 membranes were synthesized by RTD using slip coating followed by solvent exchange in methanol. The activation was confirmed in case of HKUST-1 powder, using TGA data. The membranes were used for gas permeation testing thereafter.

6.3 Results and discussion

6.3.1 Rapid synthesis of HKUST-1 membrane

Prototypical MOF, HKUST-1[55] was chosen to demonstrate the RTD technique. The HKUST-1 RTD precursor solution (details in the experimental section) remains clear under ambient conditions throughout the duration of the experiment, whereas it forms HKUST-1 phase when subjected to elevated temperatures in the oven (refer

experimental procedure for RTD HKUST-1 powder synthesis). This implies that temperature acts as the driving force for rapid film formation in case of membranes. To understand the evolution of HKUST-1 membranes as a function of time XRD data was collected of membranes subjected to RTD for different time durations (Figure 44a). As evidenced from Figure 44b, the peak intensities for [222] and [400] planes reach their maximum values at around 8 min and remain constant thereafter. This confirms significantly expedited film formation by RTD due to high temperature. 15 min was chosen as the optimum RTD time to ensure complete evaporation of solvent. This optimum RTD time of 15 min yields continuous, well-intergrown and reproducible membranes.

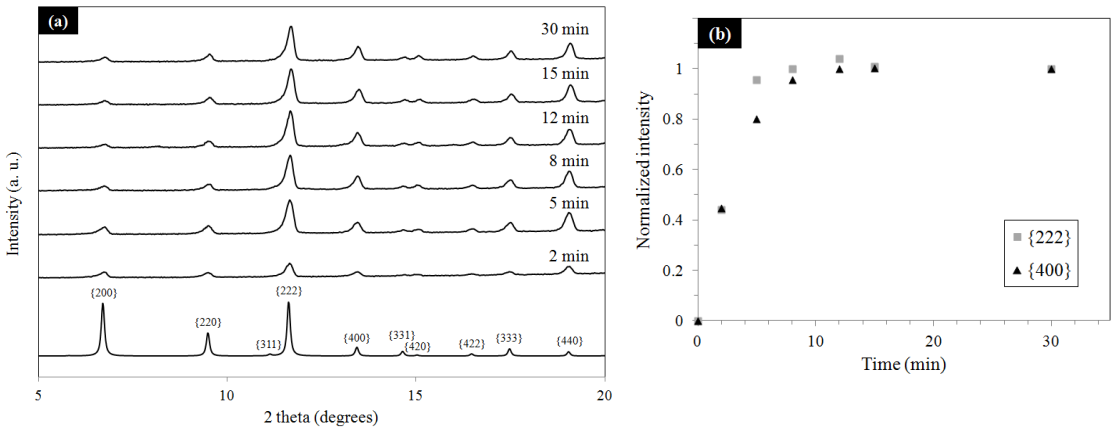

Figure 44: XRD spectra of HKUST-1 membranes synthesized for different time durations (2, 5, 8, 12, 15, 30 min) along with simulated HKUST-1 pattern. Intensities of HKUST-1 membranes are multiplied by a factor of 2 for clarity, b) Normalized XRD intensity from {222} and {400} planes for different time durations.

The membrane microstructure (grain size and orientation, grain boundary structure, thickness, location of films) greatly influences the separation performance and longevity of the membrane. Figure 45 shows the top-view and cross-sectional view (inset) of HKUST-1 RTD membrane. HKUST-1 membranes obtained by RTD vary significantly in terms of microstructure as compared to conventional polycrystalline HKUST-1 membranes.[22d, 22i, 80] Crystal sizes are much smaller and they grow around the α-alumina support particles. Grain boundaries are reduced significantly and crystals seem to be growing into each other. Crystal facets are difficult to distinguish. The smaller crystal size is attributed to the short synthesis time which inhibits growth of large crystals. Detailed mechanism of film formation and their evolution as a function of time are under investigation.

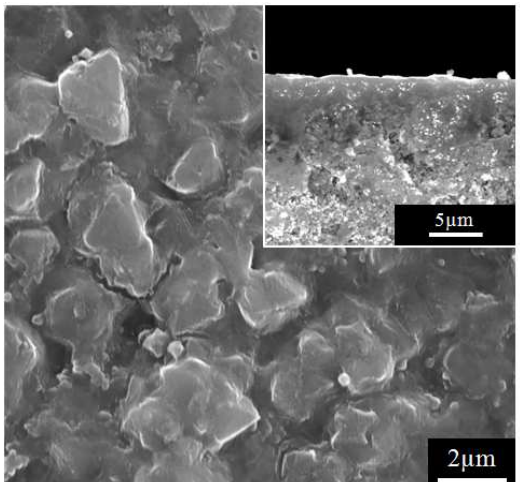

Figure 45: Scanning electron micrographs of top view and cross-section (inset) of HKUST-1 membrane synthesized by RTD.

Cross-sectional (Figure 45 inset) SEM image reveals crystals formed inside the support. Inorder to confirm the presence of HKUST-1 inside the support, EDS line mapping (Figure 46) was used. The membranes were thoroughly rinsed in methanol for 2 days to remove unreacted residual copper precursors present inside the support. Aluminum (for support) and copper (for HKUST-1 crystals) were tracked. Copper was detected upto approximately 15 μm underneath the support surface. A substantial fraction of the total copper detected, is present inside the support. Thus it is difficult to compute membrane thickness. Based on the intensity of EDS line map, the thickness can be estimated to be in the range of 10-20 μm. Growing the selective layer inside the pores of the host support (termed as pore plugging) has been reported for zeolite membrane synthesis.[112] The membrane thus obtained is strongly anchored and protected within the support (Figure 46). Thus RTD HKUST-1 membranes have enhanced mechanical

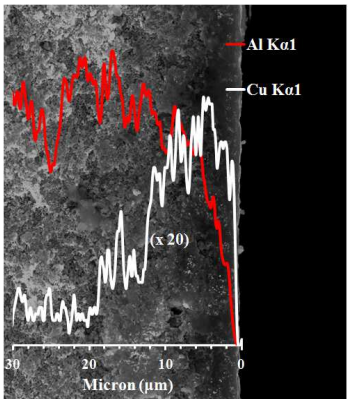

Figure 46: EDS line scan across the support cross-section for the copper and aluminum atoms. The intensity for copper is multiplied by a factor of 20 for clarity.

properties and fracture resistance. Betard et al.[81] reported $[Cu_2L_2P]_n$ membrane in which MOF crystals were present upto 30 μm deep inside the support. The authors also showed that the continuous crystal layer formed inside the support were responsible for most of the gas separation. Crystals on the support surface showed poor separation performance. Pan et al.[4] reported ZIF-8 membrane with high propylene/propane separation. Membranes were synthesized by secondary growth method, wherein ZIF-8 seeds were sucked into the pores of the support. Thus the enhanced membrane performance could possibly be due to the growth of the membrane from inside of the support. Similarly, HKUST-1 membranes obtained by RTD are also expected to show improved gas separation behavior (Figure 47 and 48).

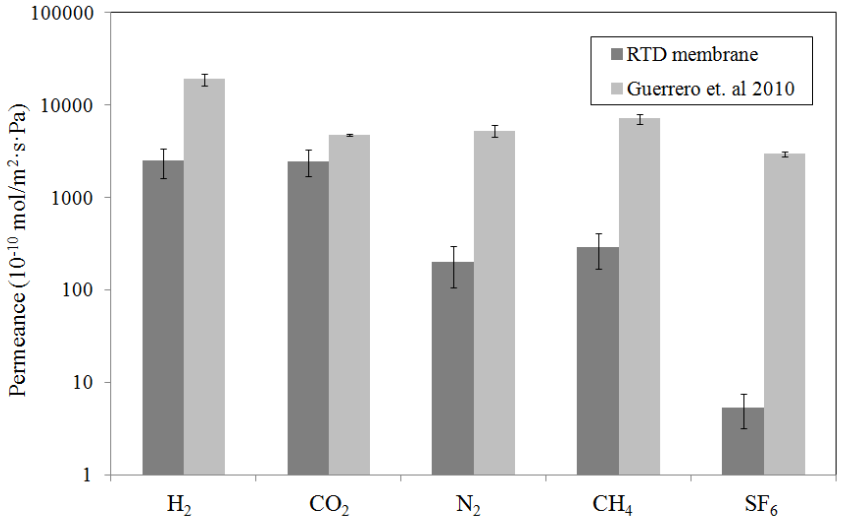

Figure 47: Single gas permeances (based on 5 membranes) of HKUST-1 membrane synthesized by RTD in comparison to conventional HKUST-1 membrane. (Ref. 29)

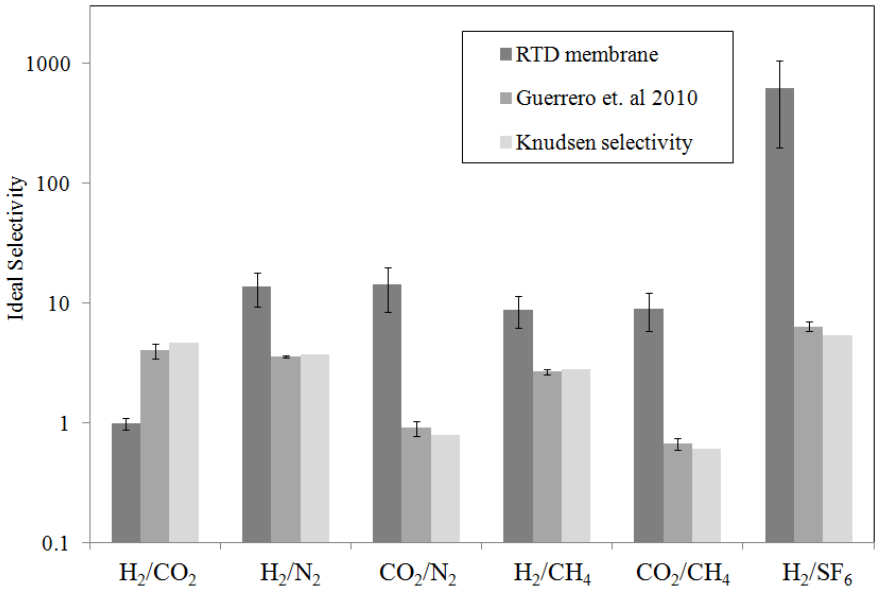

Figure 48: Ideal gas selectivities (based on 5 membranes) of HKUST-1 membrane synthesized by RTD in comparison to conventional membrane (ref. 29) and Knudsen selectivity.

Table 5: Comparison of binary CO_2/N_2 (50/50) mixture gas permeances of RTD and conventional HKUST-1 membranes (ref. 29) under dry and saturated water conditions.

HKUST-1 membrane synthesis technique	CO_2 permeance (10^{-7} mol/m^2·s·Pa)		CO_2/N_2 selectivity	
	without water	with water	without water	with water
RTD	1.62 ± 0.11	0.011 ± 0.003	1.07 ± 0.08	8.14 ± 1.92
Secondary growth	2.29 ± 0.07	1.71 ± 0.38	1.01 ± 0.21	0.79 ± 0.01

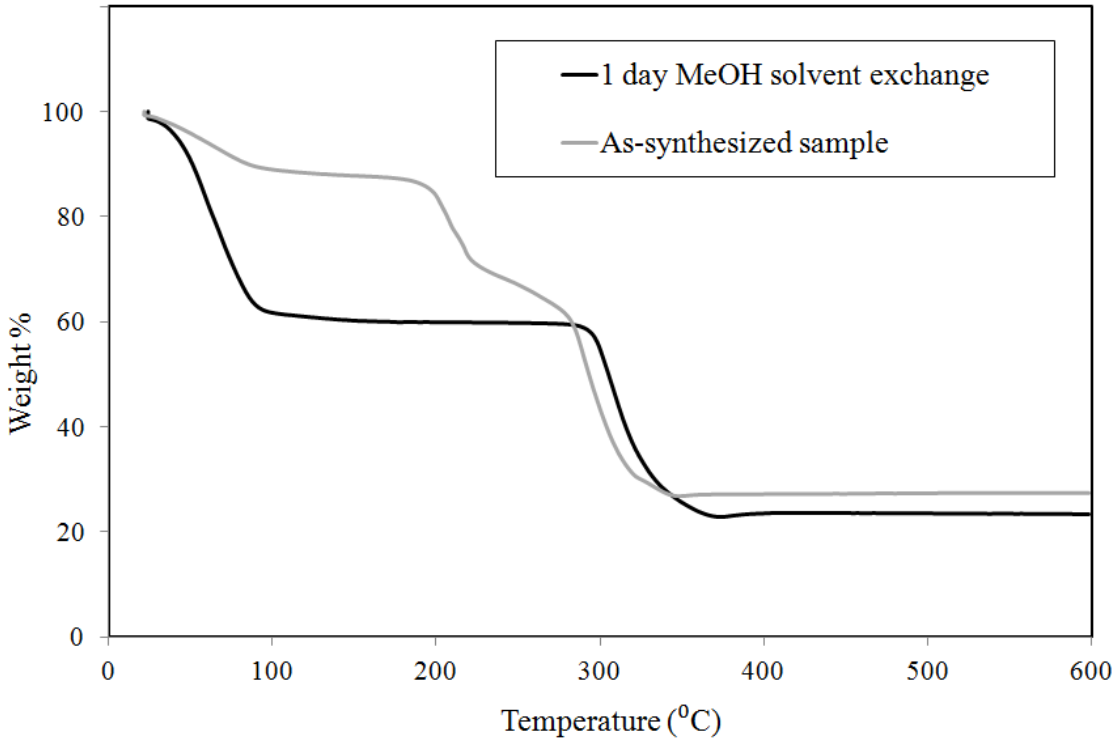

Figure 49: Thermogravimetric analysis (TGA) of (a) as-synthesized HKUST-1 powder by RTD technique (b) RTD powder after 1 day solvent exchange in methanol and (c) solvothermally synthesized HKUST-1 powder.

The thermogravimetric analysis (TGA) data collected for HKUST-1 RTD powder shows complete DMF removal after 24 h solvent exchange in methanol (Figure 49). Based on this observation, HKUST-1 membranes were also solvent exchanged in methanol for 24 h. After drying on the shelf for 12 h, membranes were placed in the gas permeation cell and flushed with helium on the feed side and vacuum on the permeate side for 24 h to remove co-ordinated water molecules. Thereafter, single gas permeances were measured for these activated samples by time lag method. Figures 47 and 48

present the single gas permeances and ideal selectivities respectively for HKUST-1 RTD membranes in comparison to conventional HKUST-1 membranes. Conventional HKUST-1 membranes were synthesized using our previously reported technique.[22i] The selectivities deviate significantly from Knudsen and previously reported values.[22d, 22i, 80] This is in agreement with the observations of Betard et al.[81] in which improved microstructure and growth of selective layer from inside the support enhances the separation performance. The CO_2 permeance is comparable to that of hydrogen. This kind of gas permeation behavior has not been reported previously for HKUST-1 membranes. Keskin et. al[113] predicted the CO_2/H_2 ideal selectivity of around 3.5 at room temperature for defect free CuBTC membrane. Further, the extremely slow diffusion of SF_6 through the RTD HKUST-1 membrane indicates reduced grain boundary defects and improved microstructure. Gas permeation measurements conducted for binary CO_2/N_2 (50/50) mixture under dry and saturated water conditions also support this observation. Under dry conditions, CO_2 permeance through both the membranes is fairly similar (see table 5). However, when binary CO_2/N_2 mixture saturated with water (CO_2 : N_2 : H_2O = 48.7 : 48.7 : 2.6) is used, permeance of CO_2 drops 2 orders of magnitude for RTD membrane, whereas its only slightly lowered for conventional HKUST-1 membrane. Water strongly co-ordinates with the unsaturated copper metal site and as a result the diffusion of CO_2 and N_2 through the MOF pores is slowed down dramatically. Thus water will effectively block the micropores. As a result, permeance should drop significantly if no gas transport occurs through grain boundary defects. The high CO_2 permeance seen for the conventional membrane in presence of water essentially

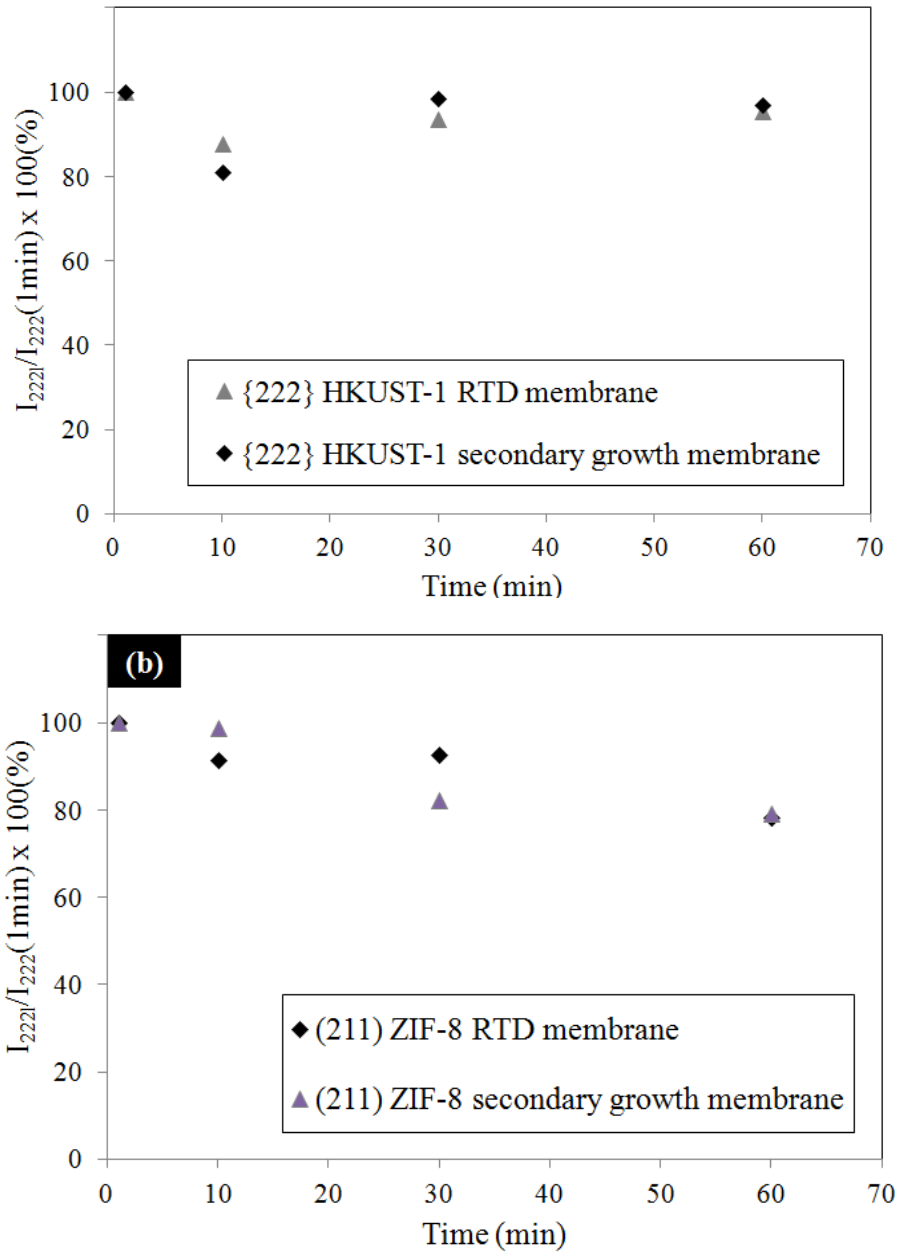

Figure 50: Comparison of binding strength of (a) HKUST-1 RTD membrane and HKUST-1 membrane synthesized secondary growth (ref. 29); (b) ZIF-8 RTD membrane and ZIF-8 membrane synthesized secondary growth (ref. 12) on α-alumina support.

corresponds to the diffusion of CO_2 through non-selective pathways indicating poor membrane microstructure. Also the CO_2/N_2 selectivity (0.77) is close to Knudsen selectivity (0.78). In case of RTD membrane, diffusion occurs mainly through the pores of the MOF and as a result, the permeance also decreases significantly in presence of water. Thus non-selective grain boundary transport pathways are significantly reduced for RTD synthesized membrane in comparison to conventional membrane.

Membrane microstructure control (grain size and orientation, grain boundary, thickness and location of films) is extremely important in order to optimize the separation performance (Figure 50). RTD membrane thickness can be controlled by changing the concentration of the RTD precursor solution. When four times dilute solution was used, a thinner film (6 μm) was obtained. This is expected, since the amount of precursors available for growth is reduced. Also the crystal size is smaller when dilute solution is used. Thus RTD allows for a certain degree of control over the membrane thickness and crystal size.

The RTD technique offers other potential advantages. Since RTD is carried out at elevated temperatures, there is a possibility of covalent bond formation between the ligands and the substrate as evidenced in our earlier work.[22i, 22m] This will enhance the attachment of the film to the support even further. The amount of precursor solution used per support is approximately 0.36 g. Atleast 20 HKUST-1 membranes from 20 ml solution without losing the membrane performance. This is very difficult to achieve using conventional batch methods wherein one membrane typically requires around 40 ml growth solution. At an industrial scale of production, these numbers are expected to

become even more significant. Also in conventional systems, homogeneous nucleation is unavoidable and causes significant loss of precursors that could be utilized for synthesis of membrane. In RTD, not only the metal sources and expensive exotic ligands but also the solvent consumption is immensely reduced, which gives RTD a very strong economic and greener edge towards its commercialization. A wide variety of synthesis conditions can be explored which enable membrane fabrication using greener solvents like alcohol and water and thereby eliminate the activation step. Unlike the conventional batch solvothermal methods that use autoclaves, in which pressures often exceed atmospheric pressure. RTD is carried out at atmospheric pressure and this would simplify the equipment design in a commercial setting. Instead of slip coating or dip the support, it can be spray coated as well followed by rapid heating. Thus this technique has potential to be scaled up in the form of spray coating that is, using existing infrastructure.

6.4 Conclusions

In conclusion, we reported a novel strategy, RTD, for synthesis of MOF membranes. RTD allows rapid synthesis of HKUST-1 membranes in 15 min. The crystal morphology and membrane microstructure of RTD membranes is quite different from their conventional counterparts. Membranes show significantly reduced grain boundary defects and improved gas separation performance. Crystal growth occurs inside the support which offers them enhanced mechanical strength and fracture resistance. Superior attachment of films to substrates, minimum consumption of precursors, mild

pressure conditions for synthesis (atmospheric pressure) in combination with a scalable technique using existing commercial infrastructure, make RTD a greener and economical technique for commercial scale synthesis of MOF membranes.

Cost of membrane fabrication and expensive modules/supports required are two major deterrents for their commercialization of inorganic zeolite membranes. RTD technique significantly reduces the fabrication cost. The next step is to fabricate MOF membranes on polymer hollow fibers using RTD. By doing this, the need for expensive ceramic supports can be eliminated.

CHAPTER VII

ZIF-8 MEMBRANES BY RAPID THERMAL DEPOSITION

7.1 Introduction

As stated earlier, ZIF-8 membranes have demonstrated potential for propylene/propane separation. Further, the permeabilities and selectivities lie in the more favorable and attractive region for commercialization of these membranes. Hence ZIF-8 was chosen to extend the RTD technique to more promising materials. Note that, unlike HKUST-1, forming pure ZIF-8 phase is challenging, especially over a broad range of synthesis conditions.

7.2 Experimental

Experimental procedure is detailed in Section 3.5. ZIF-8 membranes were synthesized by RTD using slip coating followed by solvent exchange in methanol. The activation was confirmed in case of ZIF-8 powder, using TGA data. The membranes were used for gas permeation testing thereafter.

7.3 Results and discussion

Like HKUST-1 membrane, ZIF-8 membranes were also rapidly synthesized in 15 min. As expected, the membrane microstructure (Figure 51) was different from previously reported membranes.[6, 22m] Figure 52 show EDS line map for ZIF-8 membrane. Based on the intensity of Zn $K_{\alpha 1}$, the membrane thickness can be estimated

to be ranging from 5-20 μm. Assuming the permeability and grain boundary structure comparable to the ZIF-8 membrane reported previously using secondary growth,[4] the effective thickness of RTD membrane can be estimated to be 8.3 μm, which falls in the 5-20 μm range.

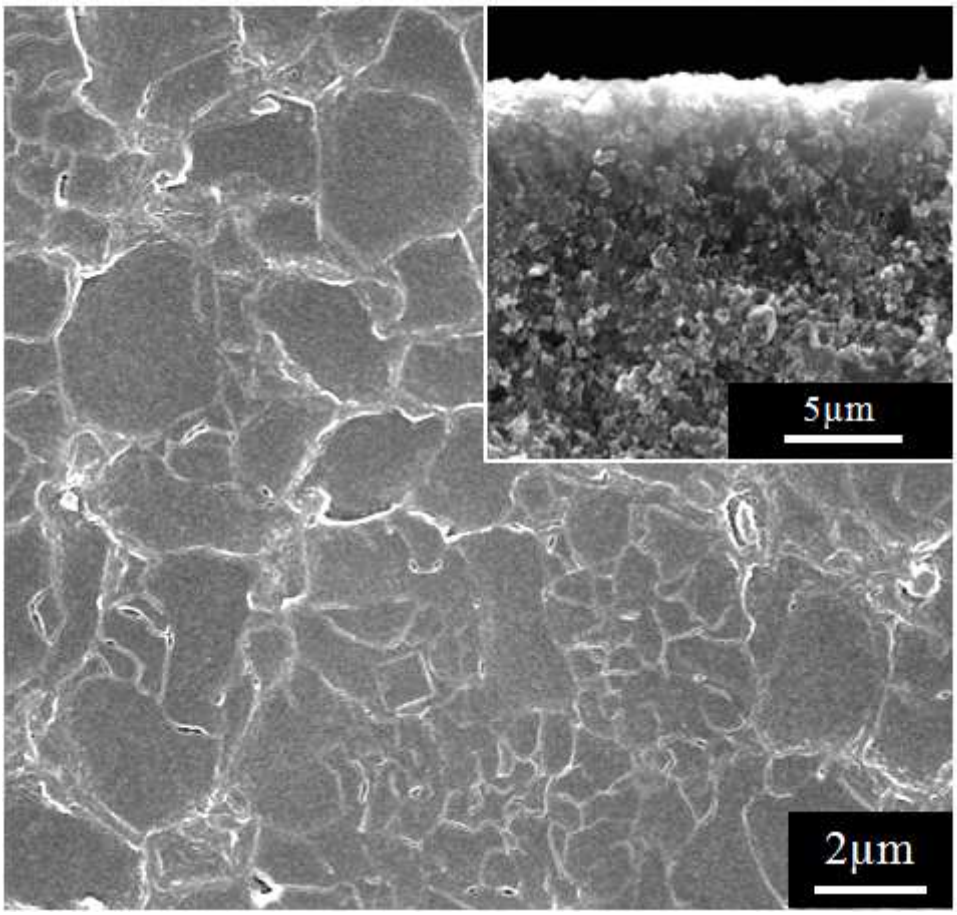

Figure 51: Scanning electron micrographs of top view and cross-section (inset) of ZIF-8 membrane synthesized by RTD.

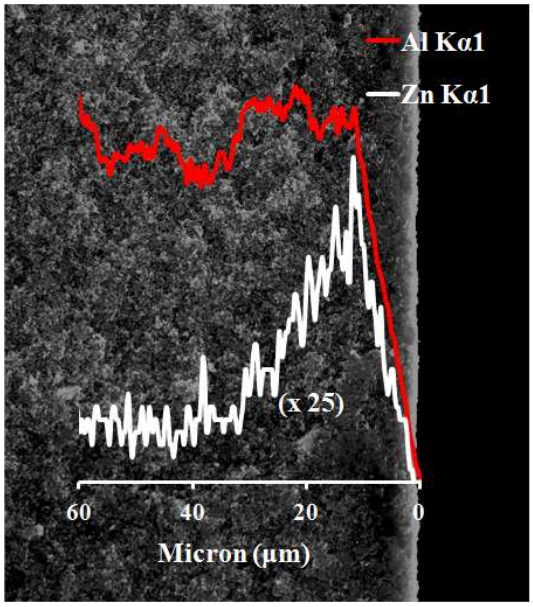

Figure 52: EDS line scan across the support cross-section for the copper and aluminum atoms. The intensity for zinc is multiplied by a factor of 25 for clarity.

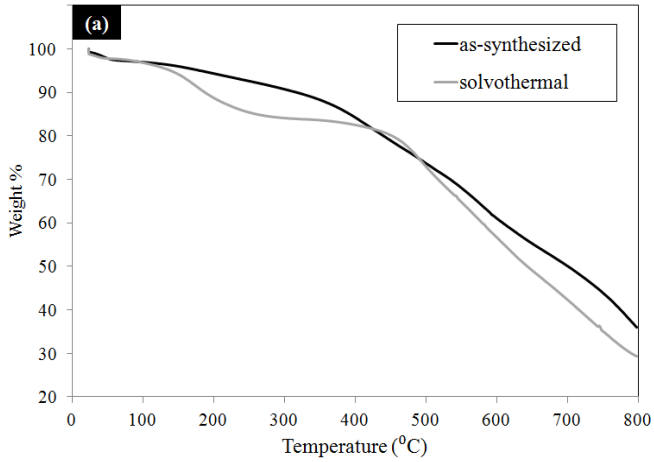

Figure 53: Thermogravimetric analysis (TGA) of ZIF-8 powder synthesized solvothermally and as-synthesized by RTD technique.

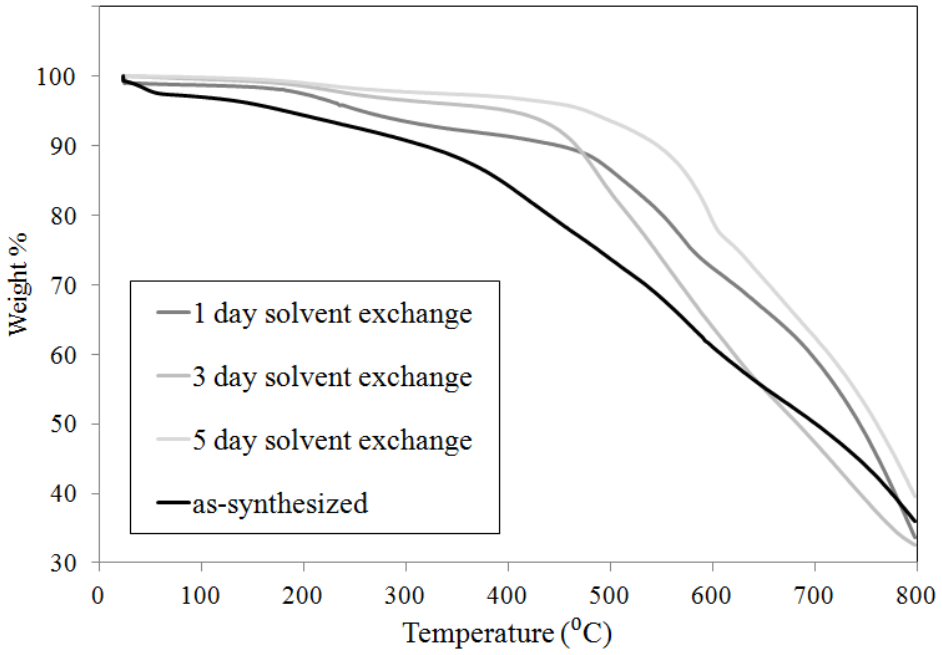

Figure 54: Thermogravimetric analysis (TGA) of ZIF-8 powder by RTD technique; as-synthesized, after 1 day, 3 days and 5 days solvent exchange in ethanol.

TGA data was collected for ZIF-8 powder synthesized solvothermally using RTD precursor solution (Figure 53 and 54). ZIF-8 powder synthesized by RTD showed partial activation. It was further activated by solvent exchange in ethanol for 1, 3 and 5 days. For ZIF-8 membrane, no significant change in permeance was observed after 3 day ethanol exchange. Figure 55 shows single gas permeation data of ZIF-8 RTD membrane. The H_2/C_3H_8 ideal selectivity was approximately 800. This is greater than previously reported values[7] which suggests superior membrane microstructure. ZIF-8 RTD membrane shows high selectivity for binary propylene/propane (50/50) separation

(Table 6). Enhanced propylene/propane separation emanates from improved microstructure.[7b] Figure 56 depicts C_3H_6/C_3H_8 permeation and separation performance of ZIF-8 RTD membrane in comparison to polymer membranes,[12] carbon membranes,[114] ZIF-8 6FDA-DAM mixed matrix membrane[115] and ZIF-8 polycrystalline membrane synthesized by conventional secondary growth technique.[4] Membrane based technique for separation of C_3H_6/C_3H_8 can economically replace current fractional distillation process with a mere permeability of 1 barrer and selectivity of 35.[116] Permeability of ZIF-8 RTD membranes ranges from 250-600 barrer with an average selectivity of 26, making them exciting for commercial applications.

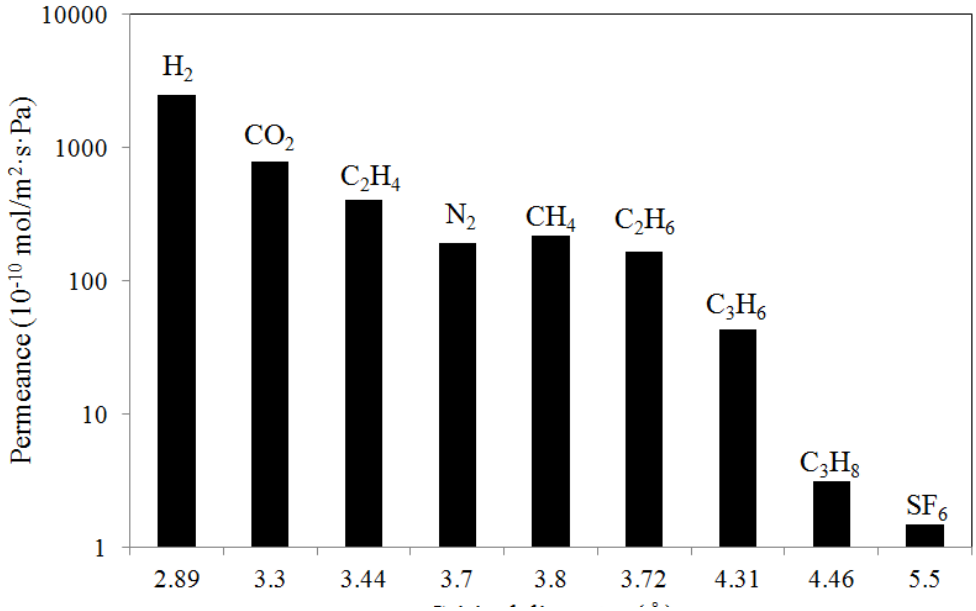

Figure 55: Single gas permeances of ZIF-8 RTD membrane by time-lag method at room temperature and 1 bar feed pressure.

Table 6: Binary propylene/propane separation performance of ZIF-8 membranes synthesized by RTD measured using Wicke-Kallenbach technique.

ZIF-8 membrane	C_3H_6 binary permeance (10^{-10} mol/m^2·s·Pa)	C_3H_6 /C_3H_8 selectivity
M1	80.9	41
M2	70.3	30
M3	70.4	16

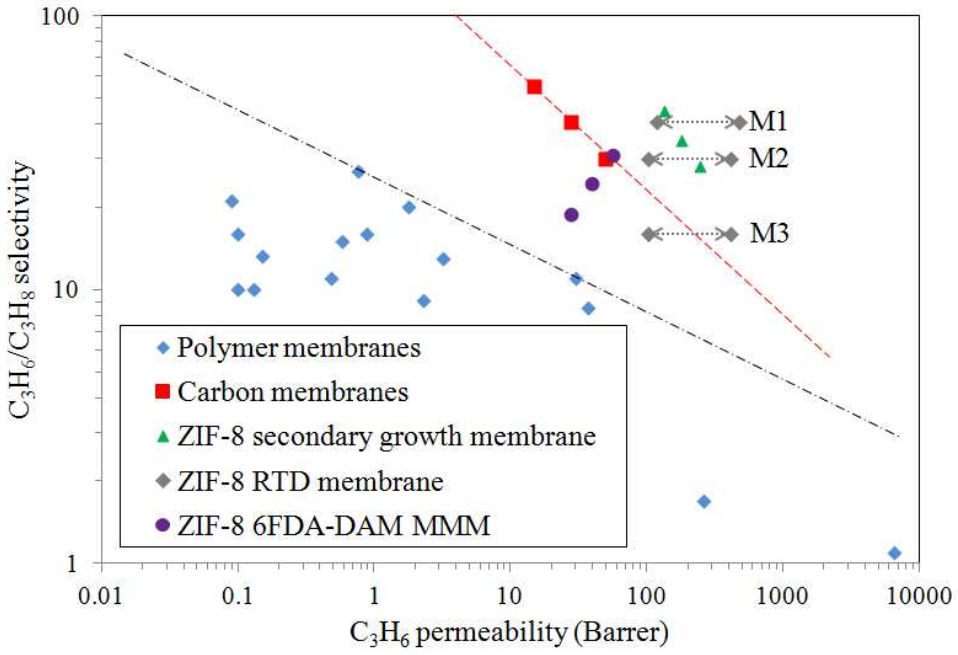

Figure 56: Permeation and separation properties of ZIF-8 membranes for C_3H_6/C_3H_8 separation in comparison to polymer membranes (ref. 37), carbon membranes (ref. 38), ZIF-8 6FDA-DAM mixed matrix membrane (ref. 36), ZIF-8 membrane by secondary growth (ref. 12). Permeability for RTD membrane lies between the endpoints of the line segment, due to uncertainty in thickness (5-20 μm).

7.4 Conclusions

Thus, ZIF-8 membranes were synthesize rapidly in 15 min. Membrane microstructure of RTD membranes is substantially different from previously reported membranes synthesized by conventional techniques. Grain boundary defects are reduced and improved gas separation performance is obtained. Further, crystals grow from inside of the support which improves the mechanical properties of the membrane and protects it. Reduced precursor consumption, atmospheric pressure conditions for synthesis and a potentially scalable technique using available infrastructure, make RTD a greener and economical technique for commercial scale synthesis of MOF membranes.

Membrane fabrication cost (poor reproducibility and scalability) and cost of supports are two major deterrents for the commercialization of inorganic zeolite membranes. RTD technique is very robust, easily reproducible and potentially scalable. These factors significantly reduce the fabrication cost. RTD can be potentially applied for fabrication of MOF membranes on polymer hollow fibers. By doing this, the cost due to expensive ceramic supports can be minimized.

CHAPTER VIII

b-ORIENTED MFI FILM FABRICATION BY MICROCONTACT PRINTING PASSIVATION

8.1 Introduction

Zeolite films have been studied for many years and in particular MFI membranes are attractive for hydrocarbon separation such as xylene isomers.[117] b-oriented MFI membranes have demonstrated superior separation performance.[13c] Lai et al.[66] have synthesized b-oriented MFI silicalite-1 membranes by secondary growth. They showed remarkable separation capability but its scalability is limited mainly due to time-consuming preparation steps, need for organic solvents and template synthesis.

Here we report an effective passivation method that does not require metal deposition for the synthesis of highly b-oriented MFI films.[28c] Use Sigmacote, surface functional groups were passivated, preventing nucleation and growth from the flat surface of MFI seed crystals. Nucleation and growth occurs in the plane leading to highly b-oriented MFI films and membranes.

8.2 Experimental

Tetraethyl orthosilicate (TEOS, 98%, Sigma-Aldrich), tetrapropylammonium hydroxide (TPAOH, 1.0M in water, Sigma-Aldrich), Sigmacote (Sigma-Aldrich), triethoxysilylpropyl-modified-polyethyleneimine (TMS-PEI, Gelest) and ethanol

(99.5%, Acros) were used. Poly (dimethylsiloxane) elastomer (Sylgard 184) was bought from Dow corning. Deionized water (DI water) was used all experiments.

8.2.1 Seed preparation

MFI seed crystals of 2.3 μm size were synthesized by hydrothermal synthesis using a gel mixture of 6.84TMOS : 1TPAOH : 500H_2O.[68] 6 g TEOS was mixed with TPAOH aqueous solution (4.9g in 1 M TPAOH in 24.6 g H_2O) under vigorous stirring. After stirring the mixture for 12 h at room temperature, it was filtered into an autoclave and placed in an oven at 150 °C for 5 h under rotation.

8.2.2 Seed monolayer deposition via manual self-assembly

3 wt% PEI was spin coated at 3000 rpm for 1min, on reactive ion etched silicon substrate. The PEI coated substrate was heated to 110 °C for 45 min. Monolayer of 2.3 μm crystals was prepared by rubbing[68] to give seed monolayer. Packing density was increased by rubbing multiple times.

8.2.3 Silane passivation using microcontact printing

Silane passivation was carried out using microcontact printing technique[118] as illustrated in Figure 57. Sigmacote is spin coated on PDMS stamp at 3000 rpm for 1min. It is then flipped, pressed on the seed monolayer and placed in an oven at 110 °C for 5 min.

8.2.4 Secondary growth

The silane passivated seed monolayer was then used for secondary growth. Secondary growth was carried out in 5TEOS : 1TPAOH : 100H_2O solution. 2g of TEOS was mixed with TPAOH aqueous solution (2 g of 1 M TPAOH in 36g H_2O) under vigorous stirring for 4 h at room temperature. The clear solution was filtered into an autoclave. The seeded substrate was placed vertically in the autoclave with the aid of custom-made Teflon holder. The autoclave was placed in a convective oven at 150 °C for 3 h.

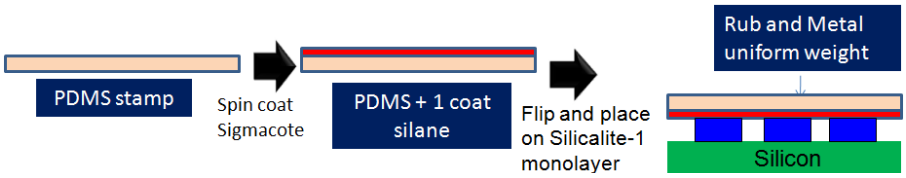

Figure 57: Schematic illustration of silane passivation using micro-contact printing

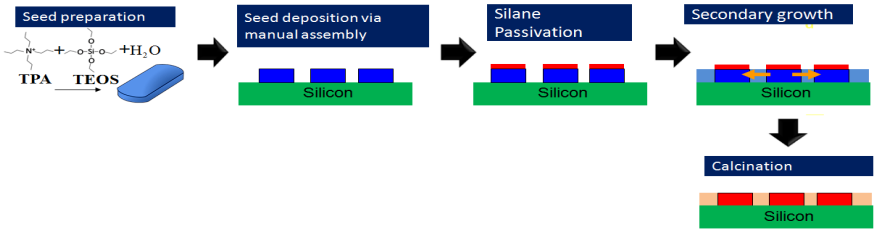

Figure 58: Schematic illustration of b-oriented MFI film fabrication by microcontact printing passivation

8.3 Results and discussion

Here we use secondary growth approach for fabrication of b-oriented MFI films on silicon substrates. The seed monolayer was assembled on PEI coated silicon substrate by a manual deposition technique.[68] Due to hydrogen bonding interactions between the PEI layer and the surface hydroxyl groups of zeolite crystals, seed monolayer formation is feasible. By adding crystals again and rubbing multiple times, the packing density can be improved. As a result the time required for the crystals to intergrow and fill the gaps is substantially lowered i.e. secondary growth time is reduced.

The flat faces of the b-oriented MFI seed crystals were then passivated using microcontact printing. As shown in Figure 57 and 58, Sigmacote was spin coated on a PDMS stamp. The organosilane molecules were then transferred from PDMS stamp to the flat faces of MFI seed layer by pressing and heating to ensure complete reaction and passivation of surface hydroxyl groups. Silane passivation was confirmed by contact angle measurements with water (Figure 59). A fixed volume of DI water was dropped on the seed monolayer (Figure 60) on silicon before and after silane passivation.

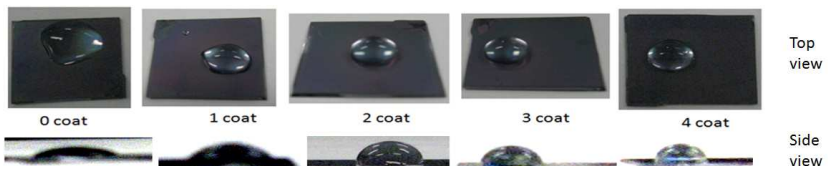

Figure 59: Images of changing contact angle of DI water on seed monolayer as a function of number of coats

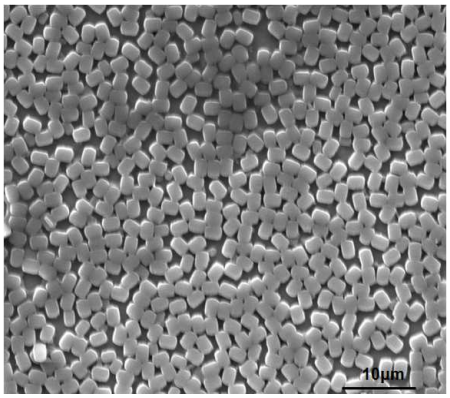

Figure 60: SEM image of b-oriented MFI seed layer on silicon substrate

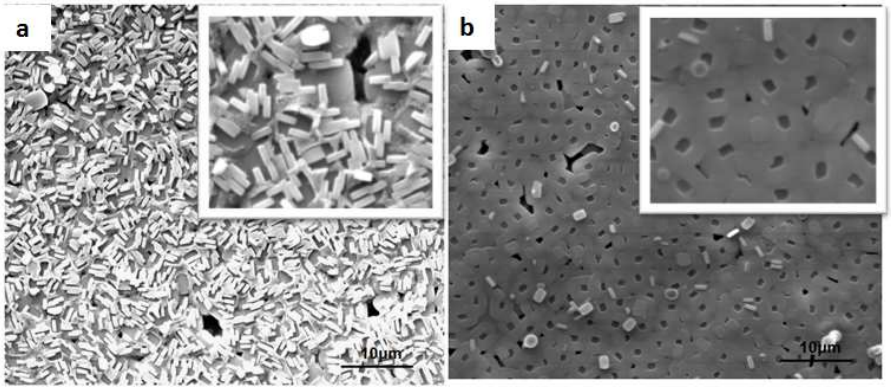

Figure 61: Secondary growth of b-oriented MFI seedlayer (a) without passivation (b) with passivation

These passivated seed crystals were then subjected to hydrothermal growth. To understand the effect of silane passivation layer, a non passivated b-oriented seed layer

was also subjected to secondary growth under identical conditions (control sample). As shown in Figure 61, the non-passivated seed layer shows substantial twinning. Nucleation and growth occur both in the plane and out of plane direction. As a result substantial orientation along a-axis is observed. Whereas for the silane passivated seed layer nucleation and growth is significantly suppressed in the out of plane direction. This can be further confirmed from XRD pattern (Figure 62) of passivated and non-passivated sample after secondary growth. The XRD data for non-passivated sample shows significant peaks for [8 0 0] and [10 0 0] directions i.e. a-axis whereas these peaks are not detectable for the silane passivated sample.

Thus micro contact printing passivation allows fabrication of b-oriented MFI films. It prevents twinning, nucleation and growth in the out of plane direction. Thus high performance gas separation can be achieved when fabricated as membranes and thickness can be effectively controlled.

8.4 Conclusion

We have demonstrated a new method for growth of b-oriented MFI films. By successfully combining our tile-and-mortar approach with microcontact printing passivation we were able to reduce nucleation and growth in out of plane direction i.e. reduce twin growth. This is confirmed by comparsion of SEM images and XRD pattern of an unpassivated sample with a passivated one. This technique has a potential to be superior than our previously demonstrated Au passivation technique that uses metal deposition and expensive etchants to remove the passivation layer. Also the metal

deposition on the edges of the crystals leads to grain boundary defects which provide non-zeolitic pathways for gas diffusion and reduced selectivity. These challenges can possibly be overcome by using silane passivation technique.

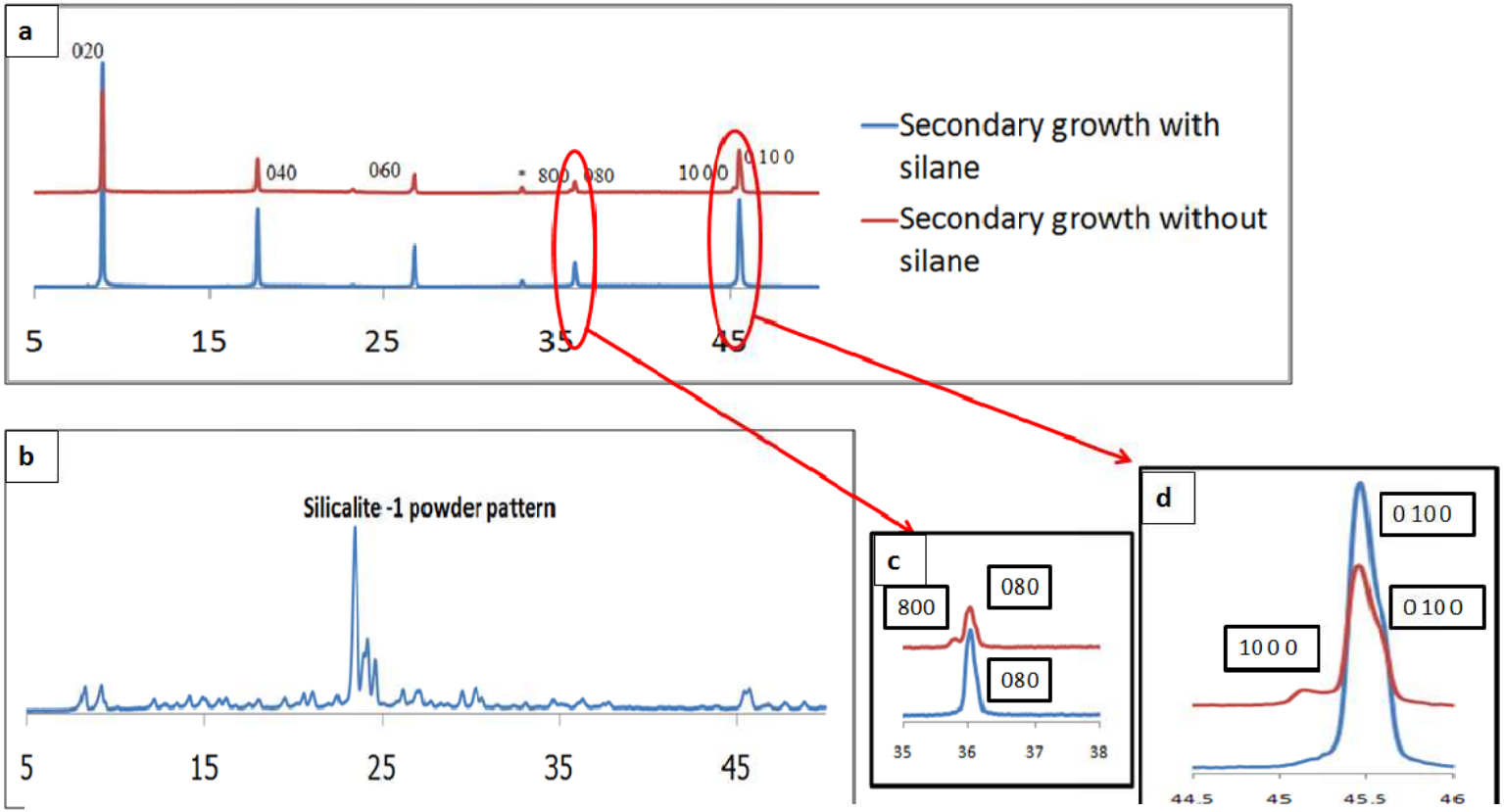

Figure 62: X-ray diffraction patterns for a) Secondary growth samples with and without silane passivation; b) Powder pattern of Silicalite-1; c) Magnified image of 080 and 800 peaks; d) Magnified image of 0 10 0 and 10 0 0 peaks

CHAPTER IX

SUMMARY AND FUTURE RESEARCH DIRECTIONS

The RTD technique still needs to overcome one more challenge for its commercialization., namely fabrication on relatively cheaper supports.

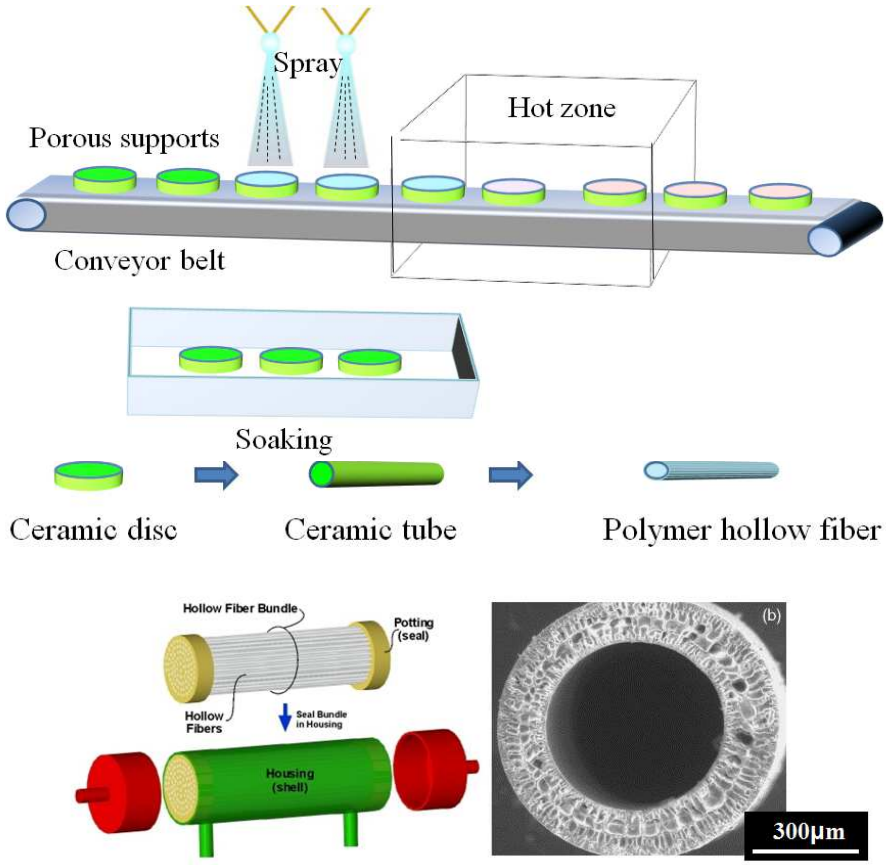

Figure 63: RTD technique on a commercial scale.

Inorder to apply membranes for gas separation on a commercial scale they should be fabricated on hollow fiber polymer membranes. Currently we prepare membranes on ceramic disc supports. The next step is to synthesize membranes on hollow ceramic fibers. If the membrane quality is maintained on ceramic tubular support then we can extend it further to hollow fiber polymer supports.

The polymer supports can then be easily assembled into a membrane module to give high membrane separation areas for commercial scales of production (Figure 63).

REFERENCES

1. Park, K. S.; Ni, Z.; Cote, A. P.; Choi, J. Y.; Huang, R. D.; Uribe-Romo, F. J.; Chae, H. K.; O'Keeffe, M.; Yaghi, O. M., Exceptional chemical and thermal stability of zeolitic imidazolate frameworks. *Proceedings of the National Academy of Sciences of the United States of America* **2006,** *103* (27), 10186-10191.

2. Li, K. H.; Olson, D. H.; Seidel, J.; Emge, T. J.; Gong, H. W.; Zeng, H. P.; Li, J., Zeolitic Imidazolate Frameworks for Kinetic Separation of Propane and Propene. *Journal of the American Chemical Society* **2009,** *131* (30), 10368-10369.

3. Gücüyener, C.; van den Bergh, J.; Gascon, J.; Kapteijn, F., Ethane/Ethene Separation Turned on Its Head: Selective Ethane Adsorption on the Metal−Organic Framework ZIF-7 through a Gate-Opening Mechanism. *Journal of the American Chemical Society* **2010,** *132* (50), 17704-17706.

4. Pan, Y.; Li, T.; Lestari, G.; Lai, Z., Effective separation of propylene/propane binary mixtures by ZIF-8 membranes. *Journal of Membrane Science* **2012,** *390–391* (0), 93-98.

5. Shah, M.; McCarthy, M. C.; Sachdeva, S.; Lee, A. K.; Jeong, H.-K., Current Status of Metal–Organic Framework Membranes for Gas Separations: Promises and Challenges. *Industrial & Engineering Chemistry Research* **2012,** *51* (5), 2179-2199.

6. Bux, H.; Liang, F. Y.; Li, Y. S.; Cravillon, J.; Wiebcke, M.; Caro, J., Zeolitic Imidazolate Framework Membrane with Molecular Sieving Properties by Microwave-

Assisted Solvothermal Synthesis. *Journal of the American Chemical Society* **2009,** *131* (44), 16000-16001.

7. (a) Bux, H.; Feldhoff, A.; Cravillon, J.; Wiebcke, M.; Li, Y.-S.; Caro, J., Oriented Zeolitic Imidazolate Framework-8 Membrane with Sharp H2/C3H8 Molecular Sieve Separation. *Chemistry of Materials* **2011,** *23* (8), 2262-2269; (b) Pan, Y.; Lai, Z., Sharp separation of C2/C3 hydrocarbon mixtures by zeolitic imidazolate framework-8 (ZIF-8) membranes synthesized in aqueous solutions. *Chemical Communications* **2011,** *47* (37), 10275-10277.

8. Council, N. R., *Separation Technologies for the Industries of the Future*. National Academy Press: Washington, D.C., 1998.

9. Baker, R. W., Future directions of membrane gas separation technology. *Industrial & Engineering Chemistry Research* **2002,** *41* (6), 1393-1411.

10. Robeson, L. M., Co-relation of separation factor versus permeability for polymeric membranes. *Journal of Membrane Science* **1991,** *62* (2), 165-185.

11. Robeson, L. M., The upper bound revisited. *Journal of Membrane Science* **2008,** *320* (1-2), 390-400.

12. Burns, R. L.; Koros, W. J., Defining the challenges for C3H6/C3H8 separation using polymeric membranes. *Journal of Membrane Science* **2003,** *211* (2), 299-309.

13. (a) Matsukata, M.; Kikuchi, E., Zeolitic membranes: Synthesis, properties, and prospects. *Bulletin of the Chemical Society of Japan* **1997,** *70* (10), 2341-2356; (b) Lin, Y. S.; Kumakiri, I.; Nair, B. N.; Alsyouri, H., Microporous inorganic membranes. *Separation and Purification Methods* **2002,** *31* (2), 229-379; (c) Caro, J.; Noack, M.,

Zeolite membranes - Recent developments and progress. *Microporous and Mesoporous Materials* **2008,** *115* (3), 215-233; (d) Caro, J.; Noack, M.; Kolsch, P.; Schafer, R., Zeolite membranes - state of their development and perspective. *Microporous and Mesoporous Materials* **2000,** *38* (1), 3-24; (e) Gavalas, G. R., Zeolite Membranes for Gas and Liquid Separations. In *Materials Science of Membranes for Gas and Vapor Separation*, Yampolskii, Y.; Pinnau, I.; Freeman, B. D., Eds. John Wiley & Sons, Ltd.: New York, 2006; pp 307-336; (f) Zacher, D.; Shekhah, O.; Woll, C.; Fischer, R. A., Thin films of metal-organic frameworks. *Chemical Society Reviews* **2009,** *38* (5), 1418-1429.

14. (a) Choi, J.; Jeong, H.; Snyder, M.; Stoeger, J.; Masel, R.; Tsapatsis, M., Grain Boundary Defect Elimination in a Zeolite Membrane by Rapid Thermal Processing. *Science* **2009,** *325* (5940), 590; (b) Lai, Z.; Bonilla, G.; Diaz, I.; Nery, J. G.; Sujaoti, K.; Amat, M. A.; Kokkoli, E.; Terasaki, O.; Thompson, R. W.; Tsapatsis, M.; Vlachos, D. G., Microstructural Optimization of a Zeolite Membrane for Organic Vapor Separation. *Science* **2003,** *300* (5618), 456-460; (c) Poshusta, J. C.; Tuan, V. A.; Pape, E. A.; Noble, R. D.; Falconer, J. L., Separation of light gas mixtures using SAPO-34 membranes. *Aiche Journal* **2000,** *46* (4), 779-789.

15. Caro, J.; Noack, M., Zeolite Membranes - Status and Prospective. In *Advances in Nanoporous Materials*, Stefan, E., Ed. Elsevier: 2010; Vol. Volume 1, pp 1-96.

16. Mahajan, R.; Vu, D. Q.; Koros, W. J., Mixed matrix membrane materials: An answer to the challenges faced by membrane based gas separations today? *Journal of the Chinese Institute of Chemical Engineers* **2002,** *33* (1), 77-86.

17. Moore, T. T.; Koros, W. J., Non-ideal effects in organic-inorganic materials for gas separation membranes. *Journal of Molecular Structure* **2005,** *739* (1-3), 87-98.

18. (a) Eddaoudi, M.; Kim, J.; Rosi, N.; Vodak, D.; Wachter, J.; O'Keefe, M.; Yaghi, O. M., Systematic design of pore size and functionality in isoreticular MOFs and their application in methane storage. *Science* **2002,** *295* (5554), 469-472; (b) Rosi, N. L.; Eckert, J.; Eddaoudi, M.; Vodak, D. T.; Kim, J.; O'Keeffe, M.; Yaghi, O. M., Hydrogen storage in microporous metal-organic frameworks. *Science* **2003,** *300* (5622), 1127-1129; (c) Ferey, G., Hybrid porous solids: past, present, future. *Chemical Society Reviews* **2008,** *37* (1), 191-214; (d) Banerjee, R.; Phan, A.; Wang, B.; Knobler, C.; Furukawa, H.; O'Keeffe, M.; Yaghi, O. M., High-throughput synthesis of zeolitic imidazolate frameworks and application to CO2 capture. *Science* **2008,** *319* (5865), 939-943; (e) Zhuang, J. L.; Ceglarek, D.; Pethuraj, S.; Terfort, A., Rapid Room-Temperature Synthesis of Metal-Organic Framework HKUST-1 Crystals in Bulk and as Oriented and Patterned Thin Films. *Advanced functional materials* **2011,** *21* (8), 1442-1447.

19. (a) Sholl, D. S.; Watanabe, T.; Keskin, S.; Nair, S., Computational identification of a metal organic framework for high selectivity membrane-based CO(2)/CH(4) separations: Cu(hfipbb)(H(2)hfipbb)(0.5). *Physical Chemistry Chemical Physics* **2009,** *11* (48), 11389-11394; (b) Sholl, D. S.; Haldoupis, E.; Nair, S., Efficient Calculation of Diffusion Limitations in Metal Organic Framework Materials: A Tool for Identifying Materials for Kinetic Separations. *Journal of the American Chemical Society* **2010,** *132* (21), 7528-7539; (c) Keskin, S.; van Heest, T. M.; Sholl, D. S., Can Metal–Organic

Framework Materials Play a Useful Role in Large-Scale Carbon Dioxide Separations? *ChemSusChem* **2010,** *3* (8), 879-891.

20. Phan, A.; Doonan, C. J.; Uribe-Romo, F. J.; Knobler, C. B.; O'Keeffe, M.; Yaghi, O. M., Synthesis, Structure, and Carbon Dioxide Capture Properties of Zeolitic Imidazolate Frameworks. *Accounts of Chemical Research* **2009,** *43* (1), 58-67.

21. (a) Arnold, M.; Kortunov, P.; Jones, D. J.; Nedellec, Y.; Karger, J.; Caro, J., Oriented crystallisation on supports and anisotropic mass transport of the metal-organic framework manganese formate. *European Journal of Inorganic Chemistry* **2007,** (1), 60-64; (b) Hermes, S.; Schroder, F.; Chelmowski, R.; Woll, C.; Fischer, R. A., Selective nucleation and growth of metal-organic open framework thin films on patterned COOH/CF3-terminated self-assembled monolayers on Au(111). *Journal of the American Chemical Society* **2005,** *127* (40), 13744-13745; (c) Hermes, S.; Zacher, D.; Baunemann, A.; Woll, C.; Fischer, R. A., Selective growth and MOCVD loading of small single crystals of MOF-5 at alumina and silica surfaces modified with organic self-assembled monolayers. *Chemistry of Materials* **2007,** *19* (9), 2168-2173; (d) Biemmi, E.; Scherb, C.; Bein, T., Oriented growth of the metal organic framework Cu-3(BTC)(2)(H2O)(3)center dot xH(2)O tunable with functionalized self-assembled monolayers. *Journal of the American Chemical Society* **2007,** *129* (26), 8054-8055; (e) Zou, X. Q.; Zhu, G. S.; Hewitt, I. J.; Sun, F. X.; Qiu, S. L., Synthesis of a metal-organic framework film by direct conversion technique for VOCs sensing. *Dalton Transactions* **2009,** (16), 3009-3013; (f) Zacher, D.; Baunemann, A.; Hermes, S.; Fischer, R. A., Deposition of microcrystalline [Cu-3(btc)(2)] and [Zn-2(bdc)(2)(dabco)] at alumina and

silica surfaces modified with patterned self assembled organic monolayers: evidence of surface selective and oriented growth. *Journal of Materials Chemistry* **2007,** *17* (27), 2785-2792; (g) Allendorf, M. D.; Houk, R. J. T.; Andruszkiewicz, L.; Talin, A. A.; Pikarsky, J.; Choudhury, A.; Gall, K. A.; Hesketh, P. J., Stress-induced Chemical Detection Using Flexible Metal-Organic Frameworks. *Journal of the American Chemical Society* **2008,** *130* (44), 14404-+; (h) Biemmi, E.; Darga, A.; Stock, N.; Bein, T., Direct growth of Cu-3(BTC)(2)(H2O)(3)center dot xH(2)O thin films on modified QCM-gold electrodes - Water sorption isotherms. *Microporous and Mesoporous Materials* **2008,** *114* (1-3), 380-386; (i) Yoo, Y.; Jeong, H. K., Rapid fabrication of metal organic framework thin films using microwave-induced thermal deposition. *Chemical Communications* **2008,** (21), 2441-2443; (j) Shekhah, C.; Wang, H.; Kowarik, S.; Schreiber, F.; Paulus, M.; Tolan, M.; Sternemann, C.; Evers, F.; Zacher, D.; Fischer, R. A.; Woll, C., Step-by-step route for the synthesis of metal-organic frameworks. *Journal of the American Chemical Society* **2007,** *129* (49), 15118-15119; (k) Gascon, J.; Aguado, S.; Kapteijn, F., Manufacture of dense coatings of Cu-3(BTC)(2) (HKUST-1) on alpha-alumina. *Microporous and Mesoporous Materials* **2008,** *113* (1-3), 132-138; (l) Ameloot, R.; Pandey, L.; Van der Auweraer, M.; Alaerts, L.; Sels, B. F.; De Vos, D. E., Patterned film growth of metal-organic frameworks based on galvanic displacement. *Chemical Communications* **2010,** *46* (21), 3735-3737; (m) Yoo, Y.; Jeong, H. K., Heteroepitaxial Growth of Isoreticular Metal-Organic Frameworks and Their Hybrid Films. *Crystal Growth & Design* **2010,** *10* (3), 1283-1288; (n) Scherb, C.; Schodel, A.; Bein, T., Directing the structure of metal-organic frameworks by oriented surface growth

on an organic monolayer. *Angew. Chem.-Int. Edit.* **2008,** *47* (31), 5777-5779; (o) Zou, X. Q.; Zhu, G. S.; Zhang, F.; Guo, M. Y.; Qiu, S. L., Facile fabrication of metal-organic framework films promoted by colloidal seeds on various substrates. *Crystengcomm* **2010,** *12* (2), 352-354; (p) Horcajada, P.; Serre, C.; Grosso, D.; Boissiere, C.; Perruchas, S.; Sanchez, C.; Ferey, G., Colloidal Route for Preparing Optical Thin Films of Nanoporous Metal-Organic Frameworks. *Advanced Materials* **2009,** *21* (19), 1931-1935; (q) Patricia, H.; Christian, S.; David, G.; Cedric, B. e.; Sandrine, P.; Clement, S.; Ferey, G., Colloidal Route for Preparing Optical Thin Films of Nanoporous Metal-Organic Frameworks. *Advanced Materials* **2009,** *21* (19), 1931-1935; (r) Lu, G.; Hupp, J. T., Metal-Organic Frameworks as Sensors: A ZIF-8 Fabry-Perot Device as a Selective Sensor for Chemical Vapors and Gases. *J. Am. Chem. Soc.* **2010,** *132* (23), 7832-7833.

22. (a) Li, Y.-S.; Bux, H. G.; Feldhoff, A.; Li, G.-L.; Yang, W. S.; Caro, J., Controllable Synthesis of Metal-Organic Frameworks: From MOF Nanorods to Oriented MOF Membranes. *Advanced Materials* **2010,** *Advance Online Publication*, DOI: 10.1002/adma.201000857; (b) Yoo, Y.; Lai, Z. P.; Jeong, H. K., Fabrication of MOF-5 membranes using microwave-induced rapid seeding and solvothermal secondary growth. *Microporous and Mesoporous Materials* **2009,** *123* (1-3), 100-106; (c) Liu, Y. Y.; Ng, Z. F.; Khan, E. A.; Jeong, H. K.; Ching, C. B.; Lai, Z. P., Synthesis of continuous MOF-5 membranes on porous alpha-alumina substrates. *Microporous and Mesoporous Materials* **2009,** *118* (1-3), 296-301; (d) Guo, H.; Zhu, G.; Hewitt, I. J.; Qiu, S., "Twin Copper Source" Growth of Metal-organic Framework Membrane: Cu3(BTC)2 with High Permeability and Selectivity for Recycling H2. *Journal of the American Chemical*

Society **2009,** *131* (5), 1646-1647; (e) Li, Y. S.; Liang, F. Y.; Bux, H.; Feldhoff, A.; Yang, W. S.; Caro, J., Molecular Sieve Membrane: Supported Metal-Organic Framework with High Hydrogen Selectivity. *Angew. Chem.-Int. Edit.* **2010,** *49* (3), 548-551; (f) Li, Y. S.; Liang, F. Y.; Bux, H. G.; Yang, W. S.; Caro, J., Zeolitic imidazolate framework ZIF-7 based molecular sieve membrane for hydrogen separation. *J. Membr. Sci.* **2010,** *354* (1-2), 48-54; (g) Venna, S. R.; Carreon, M. A., Highly Permeable Zeolite Imidazolate Framework-8 Membranes for CO2/CH4 Separation. *Journal of the American Chemical Society* **2010,** *132* (1), 76-78; (h) Liu, Y.; Hu, E.; Khan, E. A.; Lai, Z., Synthesis and characterization of ZIF-69 membranes and separation for CO2/CO mixture. *Journal of Membrane Science* **2010,** *353* (1-2), 36-40; (i) Guerrero, V. V.; Yoo, Y.; McCarthy, M. C.; Jeong, H. K., HKUST-1 Membranes on Porous Supports using Secondary Growth. *Journal of Materials Chemistry* **2010,** *20*, 3938-3943; (j) Huang, A.; Bux, H.; Steinbach, F.; Caro, J., Molecular-Sieve Membrane with Hydrogen Permselectivity: ZIF-22 in LTA Topology Prepared with 3-Aminopropyltriethoxysilane as Covalent Linker. *Angewandte Chemie International Edition* **2010,** *49* (29), 4958-4961; (k) Takamizawa, S.; Takasaki, Y.; Miyake, R., Single-Crystal Membrane for Anisotropic and Efficient Gas Permeation. *Journal of the American Chemical Society* **2010,** *132* (9), 2862-2863; (l) Ranjan, R.; Tsapatsis, M., Microporous Metal Organic Framework Membrane on Porous Support Using the Seeded Growth Method. *Chemistry of Materials* **2009,** *21* (20), 4920-4924; (m) McCarthy, M. C.; Guerrero, V. V.; Barnett, G.; Jeong, H. K., Synthesis of Zeolitic Imidazolate Framework Films and Membranes with Controlled Microstructure. *Langmuir* **2010,** *26* (18), 14636-14641; (n) Huang, A.;

Dou, W.; Caro, J., Steam-stable zeolitic imidazolate framework ZIF-90 membrane with hydrogen selectivity through covalent functionalization. *Journal of the American Chemical Society* **2010,** *132* (44), 15562-15564; (o) Hu, Y.; Dong, X.; Nan, J.; Jin, W.; Ren, X.; Xu, N.; Lee, Y. M., Metal-organic framework membranes fabricated *via* reactive seeding. *Chemical Communications* **2011,** *47*, 737-739.

23. Mitzi, D. B., Thin-film deposition of organic-inorganic hybrid materials. *Chemistry of Materials* **2001,** *13* (10), 3283-3298.

24. Yoo, Y.; Varela-Guerrero, V.; Jeong, H.-K., Isoreticular Metal−Organic Frameworks and Their Membranes with Enhanced Crack Resistance and Moisture Stability by Surfactant-Assisted Drying. *Langmuir* **2011,** *27* (6), 2652-2657.

25. Hu, Y.; Dong, X.; Nan, J.; Jin, W.; Ren, X.; Xu, N.; Lee, Y. M., Metal-organic framework membranes fabricated via reactive seeding. *Chemical Communications* **2011,** *47* (2), 737-739.

26. Aguado, S.; Nicolas, C.-H.; Moizan-Basle, V.; Nieto, C.; Amrouche, H.; Bats, N.; Audebrand, N.; Farrusseng, D., Facile synthesis of an ultramicroporous MOF tubular membrane with selectivity towards CO2. *New Journal of Chemistry* **2011,** *35* (1), 41-44.

27. Centrone, A.; Yang, Y.; Speakman, S.; Bromberg, L.; Rutledge, G. C.; Hatton, T. A., Growth of Metal−Organic Frameworks on Polymer Surfaces. *Journal of the American Chemical Society* **2010,** *132* (44), 15687-15691.

28. (a) Lovallo, M. C.; Gouzinis, A.; Tsapatsis, M., Synthesis and characterization of oriented MFI membranes prepared by secondary growth. *Aiche J.* **1998,** *44* (8), 1903-1913; (b) Lai, Z. P.; Tsapatsis, M.; Nicolich, J. R., Siliceous ZSM-5 membranes by

secondary growth of b-oriented seed layers. *Advanced Functional Materials* **2004,** *14* (7), 716-729; (c) Lee, I.; Buday, J. L.; Jeong, H. K., mu-Tiles and mortar approach: A simple technique for the facile fabrication of continuous b-oriented MFI silicalite-1 thin films. *Microporous and Mesoporous Materials* **2009,** *122* (1-3), 288-293.

29. Shekhah, O.; Liu, J.; Fischer, R. A.; Woll, C., MOF thin films: existing and future applicationsPart of the themed issue on hybrid materials. *Chemical Society reviews* **2011,** *40* (2), 1081-1106.

30. (a) Carne, A.; Carbonell, C.; Imaz, I.; Maspoch, D., Nanoscale metal-organic materials. *Chemical Society reviews* **2011,** *40* (1), 291-305; (b) Jian Rong, L.; Yuguang, M.; M, C. M.; Julian, S.; Jiamei, Y.; Hae Kwon, J.; Perla, B. B.; Hong Cai, Z., Carbon dioxide capture-related gas adsorption and separation in metal-organic frameworks. *Coordination chemistry reviews* **2011,** *255* (15-16), 1791-1823; (c) Li, J. R.; Kuppler, R. J.; Zhou, H. C., Selective gas adsorption and separation in metal-organic frameworks. *Chemical Society Reviews* **2009,** *38* (5), 1477-1504; (d) Czaja, A. U.; Trukhan, N.; Muller, U., Industrial applications of metal-organic frameworks. *Chemical Society reviews* **2009,** *38* (5), 1284-1293; (e) Long, J. R.; Yaghi, O. M., The pervasive chemistry of metal-organic frameworks. *Chemical Society reviews* **2009,** *38* (5), 1213-1214; (f) Kitagawa, S.; Kitaura, R.; Noro, S.-i., Functional Porous Coordination Polymers. *Angewandte Chemie International Edition* **2004,** *43* (18), 2334-2375.

31. (a) Aguado, S.; Canivet, J.; Farrusseng, D., Facile shaping of an imidazolate-based MOF on ceramic beads for adsorption and catalytic applications. *Chemical Communications* **2010,** *46* (42), 7999-8001; (b) Aguado, S.; Canivet, J.; Farrusseng, D.,

Engineering structured MOF at nano and macroscales for catalysis and separation. *Journal of Materials Chemistry* **2011,** *21* (21), 7582-7588.

32. Lehnert, R.; Seel, F., Preparation and crystal-structure of the manganese(II) and zinc(II) derivative of imidazole *Zeitschrift für anorganische und allgemeine Chemie* **1980,** *464* (1), 187-194.

33. Morris, W.; Doonan, C. J.; Furukawa, H.; Banerjee, R.; Yaghi, O. M., Crystals as Molecules: Postsynthesis Covalent Functionalization of Zeolitic Imidazolate Frameworks. *Journal of the American Chemical Society* **2008,** *130* (38), 12626-12627.

34. Stoeger, J. A.; Choi, J.; Tsapatsis, M., Rapid thermal processing and separation performance of columnar MFI membranes on porous stainless steel tubes. *Energy & Environmental Science* **2011,** *4* (9), 3479-3486.

35. Bernardo, P.; Drioli, E.; Golemme, G., Membrane Gas Separation: A Review/State of the Art. *Industrial & Engineering Chemistry Research* **2009,** *48* (10), 4638-4663.

36. (a) Haldoupis, E.; Nair, S.; Sholl, D. S., Efficient Calculation of Diffusion Limitations in Metal Organic Framework Materials: A Tool for Identifying Materials for Kinetic Separations. *Journal of the American Chemical Society* **2010,** *132* (21), 7528-7539; (b) Zacher, D.; Liu, J. N.; Huber, K.; Fischer, R. A., Nanocrystals of [Cu-3(btc)(2)] (HKUST-1): a combined time-resolved light scattering and scanning electron microscopy study. *Chemical Communications* **2009,** (9), 1031-1033.

37. Murray, L. J.; Dinca, M.; Long, J. R., Hydrogen storage in metal-organic frameworks. *Chemical Society Reviews* **2009,** *38* (5), 1294-1314.

38. Hayashi, H.; Cote, A. P.; Furukawa, H.; O'Keeffe, M.; Yaghi, O. M., Zeolite a imidazolate frameworks. *Nature Materials* **2007,** *6* (7), 501-506.

39. Fairen-Jimenez, D.; Moggach, S. A.; Wharmby, M. T.; Wright, P. A.; Parsons, S.; Düren, T., Opening the Gate: Framework Flexibility in ZIF-8 Explored by Experiments and Simulations. *Journal of the American Chemical Society* **2011,** *133* (23), 8900-8902.

40. (a) Yaghi, O.; O'Keeffe, M.; Ockwig, N.; Chae, H.; Eddaoudi, M.; Kim, J., Reticular synthesis and the design of new materials. *Nature* **2003,** *423* (6941), 705-714; (b) Eddaoudi, M.; Moler, D. B.; Li, H. L.; Chen, B. L.; Reineke, T. M.; O'Keeffe, M.; Yaghi, O. M., Modular chemistry: Secondary building units as a basis for the design of highly porous and robust metal-organic carboxylate frameworks. *Accounts of Chemical Research* **2001,** *34* (4), 319-330; (c) Yaghi, O. M.; Li, H. L., HYDROTHERMAL SYNTHESIS OF A METAL-ORGANIC FRAMEWORK CONTAINING LARGE RECTANGULAR CHANNELS. *Journal of the American Chemical Society* **1995,** *117* (41), 10401-10402; (d) Rowsell, J. L. C.; Yaghi, O. M., Metal-organic frameworks: a new class of porous materials. *Microporous and Mesoporous Materials* **2004,** *73* (1-2), 3-14; (e) Perry, J. J.; Perman, J. A.; Zaworotko, M. J., Design and Synthesis of Metal-Organic Frameworks Using Metal-Organic Polyhedra as Supermolecular Building Blocks. *Chemical Society Reviews* **2009,** *38*, 1400-1417.

41. Surble, S.; Millange, F.; Serre, C.; Ferey, G.; Walton, R. I., *Chemical Communications* **2006**, 1518-1520.

42. (a) Ramanan, A.; Whittingham, M. S., How Molecules Turn into Solids: the Case of Self-Assembled Metal-Organic Frameworks. *Crystal Growth & Design* **2006,** *6* (11), 2419-2421; (b) Michaelides, A.; Skoulika, S., Crystallographic Evidence for Ionic Molecular Building Blocks in the Assembly of a Two Dimensional Metal-Organic Framework. *Crystal Growth & Design* **2009,** *9* (12), 4998-5002.

43. Gispert, J. R., *Coordination Chemistry*. Wiley-VCH: 2008.

44. Irving, H. M. N. H.; Williams, R. J. P., The stability of transition-metal complexes. *Journal of the Chemical Society* **1953**, 3192-3210.

45. Housecroft, C. E.; Sharpe, A. G., *Inorganic chemistry*. Pearson Prentice Hall: 2008.

46. (a) Kaye, S. S.; Dailly, A.; Yaghi, O. M.; Long, J. R., Impact of Preparation and Handling on the Hydrogen Storage Properties of Zn4O(1,4-benzenedicarboxylate)3 (MOF-5). *Journal of the American Chemical Society* **2007,** *129*, 14176-14177; (b) Wu, T.; Shen, L.; Luebbers, M.; Hu, C.; Chen, Q.; Ni, Z.; Masel, R. I., Enhancing the stability of metal-organic frameworks in humid air by incorporating water repellent functional groups. *Chemical Communications* **2010,** *46*, 6120-6122.

47. Pearson, R. J., Hard and Soft Acids and Bases. *Journal of the American Chemical Society* **1963,** *85* (22), 3533-3539.

48. Thomas, G., *Medicinal Chemistry: An Introduction, Second Edition*. Wiley: 2007.

49. Zhang, J.-P.; Zhu, A.-X.; Lin, R.-B.; Qi, X.-L.; Chen, X.-M., Pore Surface Tailored SOD-Type Metal-Organic Zeolites. *Advanced Materials* **2011,** *23* (10), 1268-1271.

50. Huang, A.; Caro, J., Covalent Post-Functionalization of Zeolitic Imidazolate Framework ZIF-90 Membrane for Enhanced Hydrogen Selectivity. *Angewandte Chemie International Edition* **2011,** *50* (21), 4979-4982.

51. Yaghi, O. M., Metal-organic Frameworks: A tale of two entanglements. *Nat Mater* **2007,** *6* (2), 92-93.

52. Moggach, S. A.; Bennett, T. D.; Cheetham, A. K., The Effect of Pressure on ZIF-8: Increasing Pore Size with Pressure and the Formation of a High-Pressure Phase at 1.47 GPa. *Angew. Chem.-Int. Edit.* **2009,** *48* (38), 7087-7089.

53. Nijem, N.; Thissen, P.; Yao, Y.; Longo, R. C.; Roodenko, K.; Wu, H.; Zhao, Y.; Cho, K.; Li, J.; Langreth, D. C.; Chabal, Y. J., Understanding the Preferential Adsorption of CO2 over N2 in a Flexible Metal–Organic Framework. *Journal of the American Chemical Society* **2011**, null-null.

54. (a) Tranchemontagne, D. J.; Hunt, J. R.; Yaghi, O. M., Room temperature synthesis of metal-organic frameworks: MOF-5, MOF-74, MOF-177, MOF-199, and IRMOF-0. *Tetrahedron* **2008,** *64* (36), 8553-8557; (b) Pan, Y.; Liu, Y.; Zeng, G.; Zhao, L.; Lai, Z., Rapid synthesis of zeolitic imidazolate framework-8 (ZIF-8) nanocrystals in an aqueous system. *Chemical Communications* **2011,** *47* (7), 2071-2073.

55. Chui, S. S. Y.; Lo, S. M. F.; Charmant, J. P. H.; Orpen, A. G.; Williams, I. D., A chemically functionalizable nanoporous material [Cu-3(TMA)(2)(H2O)(3)](n). *Science* **1999,** *283* (5405), 1148-1150.

56. Zhao, Y.; Padmanabhan, M.; Gong, Q.; Tsumori, N.; Xu, Q.; Li, J., CO catalytic oxidation by a metal organic framework containing high density of reactive copper sites. *Chemical Communications* **2011,** *47* (22), 6377-6379.

57. Aguado, S.; Bergeret, G.; Titus, M. P.; Moizan, V.; Nieto-Draghi, C.; Bats, N.; Farrusseng, D., Guest-induced gate-opening of a zeolite imidazolate framework. *New Journal of Chemistry* **2011,** *35* (3), 546-550.

58. *Fundamentals of Inorganic Membrane Science and Technology*. Elsevier: 1996; Vol. 4.

59. Bertazzo, S.; Rezwan, K., Control of α-Alumina Surface Charge with Carboxylic Acids. *Langmuir* **2009,** *26* (5), 3364-3371.

60. Nguyen, J. G.; Cohen, S. M., Moisture-Resistant and Superhydrophobic Metal-Organic Frameworks Obtained via Postsynthetic Modification. *Journal of the American Chemical Society* **2010,** *132*, 4560-4561.

61. Millward, A. R.; Yaghi, O. M., Metal-Organic Frameworks with Exceptionally High Capacity for Storage of Carbon Dioxide at Room Temperature. *Journal of the American Chemical Society* **2005,** *127* (51), 17998-17999.

62. Wang, Z.; Cohen, S. M., Postsynthetic Covalent Modification of a Neutral Metal-Organic Framework. *Journal of the American Chemical Society* **2007,** *129* (41), 12368-12369.

63. Ma, D.; Li, Y.; Li, Z., Tuning the moisture stability of metal-organic frameworks by incorporating hydrophobic functional groups at different positions of ligands. *Chemical Communications* **2011,** *47* (26), 7377-7379.

64. Brinker, C. J.; Scherer, G. W., *Sol-gel science: the physics and chemistry of sol-gel processing*. Academci Press, Inc.: New York, 1990.

65. Cravillon, J.; Munzer, S.; Lohmeier, S. J.; Feldhoff, A.; Huber, K.; Wiebcke, M., Rapid Room-Temperature Synthesis and Characterization of Nanocrystals of a Prototypical Zeolitic Imidazolate Framework. *Chem. Mat.* **2009,** *21* (8), 1410-1412.

66. Lai, Z. P.; Bonilla, G.; Diaz, I.; Nery, J. G.; Sujaoti, K.; Amat, M. A.; Kokkoli, E.; Terasaki, O.; Thompson, R. W.; Tsapatsis, M.; Vlachos, D. G., Microstructural optimization of a zeolite membrane for organic vapor separation. *Science* **2003,** *300* (5618), 456-460.

67. Snyder, M. A.; Tsapatsis, M., Hierarchical nanomanufacturing: From shaped zeolite nanoparticles to high-performance separation membranes. *Angew. Chem.-Int. Edit.* **2007,** *46* (40), 7560-7573.

68. Lee, J. S.; Kim, J. H.; Lee, Y. J.; Jeong, N. C.; Yoon, K. B., Manual assembly of microcrystal monolayers on substrates. *Angewandte Chemie-International Edition* **2007,** *46* (17), 3087-3090.

69. Ni, Z.; Masel, R. I., Rapid Production of Metal−Organic Frameworks via Microwave-Assisted Solvothermal Synthesis. *Journal of the American Chemical Society* **2006,** *128* (38), 12394-12395.

70. Carson, C. G.; Brown, A. J.; Sholl, D. S.; Nair, S., Sonochemical Synthesis and Characterization of Submicrometer Crystals of the Metal–Organic Framework Cu[(hfipbb)(H2hfipbb)0.5]. *Crystal Growth & Design* **2011,** *11* (10), 4505-4510.

71. Bae, T.-H.; Lee, J. S.; Qiu, W.; Koros, W. J.; Jones, C. W.; Nair, S., A High-Performance Gas-Separation Membrane Containing Submicrometer-Sized Metal–Organic Framework Crystals. *Angewandte Chemie International Edition* **2010,** *49* (51), 9863-9866.

72. Nune, S. K.; Thallapally, P. K.; Dohnalkova, A.; Wang, C.; Liu, J.; Exarhos, G. J., Synthesis and properties of nano zeolitic imidazolate frameworks. *Chemical Communications* **2010,** *46* (27), 4878-4880.

73. (a) Li, Z.-Q.; Qiu, L.-G.; Xu, T.; Wu, Y.; Wang, W.; Wu, Z.-Y.; Jiang, X., Ultrasonic synthesis of the microporous metal–organic framework Cu3(BTC)2 at ambient temperature and pressure: An efficient and environmentally friendly method. *Materials Letters* **2009,** *63* (1), 78-80; (b) Biemmi, E.; Scherb, C.; Bein, T., Oriented Growth of the Metal Organic Framework Cu3(BTC)2(H2O)3·xH2O Tunable with Functionalized Self-Assembled Monolayers. *Journal of the American Chemical Society* **2007,** *129* (26), 8054-8055.

74. (a) Ma, M.; Zacher, D.; Zhang, X.; Fischer, R. A.; Metzler-Nolte, N., A Method for the Preparation of Highly Porous, Nanosized Crystals of Isoreticular Metal−Organic Frameworks. *Crystal Growth & Design* **2010,** *11* (1), 185-189; (b) Perez, E. V.; Balkus Jr, K. J.; Ferraris, J. P.; Musselman, I. H., Mixed-matrix membranes containing MOF-5 for gas separations. *J. Membr. Sci.* **2009,** *328* (1-2), 165-173.

75. Huang, L.; Wang, H.; Chen, J.; Wang, Z.; Sun, J.; Zhao, D.; Yan, Y., Synthesis, morphology control, and properties of porous metal–organic coordination polymers. *Microporous and Mesoporous Materials* **2003,** *58* (2), 105-114.

76. Zhang, Y.; Musselman, I. H.; Ferraris, J. P.; Balkus Jr, K. J., Gas permeability properties of Matrimid® membranes containing the metal-organic framework Cu–BPY–HFS. *J. Membr. Sci.* **2008,** *313* (1-2), 170-181.

77. (a) Pan, L.; Sander, M. B.; Huang, X. Y.; Li, J.; Smith, M.; Bittner, E.; Bockrath, B.; Johnson, J. K., Microporous metal organic materials: Promising candidates as sorbents for hydrogen storage. *Journal of the American Chemical Society* **2004,** *126* (5), 1308-1309; (b) Pan, L.; Olson, D. H.; Ciemnolonski, L. R.; Heddy, R.; Li, J., Separation of hydrocarbons with a microporous metal-organic framework. *Angew. Chem.-Int. Edit.* **2006,** *45* (4), 616-619.

78. Van der Drift, A., Evolutionary Selection, A Principle Governing Growth Orientation in Vapour-Deposited Layers. *Philips Research Reports* **1967,** *22*, 267-288.

79. Shekhah, O.; Hirai, K.; Wang, H.; Uehara, H.; Kondo, M.; Diring, S.; Zacher, D.; Fischer, R. A.; Sakata, O.; Kitagawa, S.; Furukawa, S.; Woll, C., MOF-on-MOF heteroepitaxy: perfectly oriented [Zn2(ndc)2(dabco)]n grown on [Cu2(ndc)2(dabco)]n thin films. *Dalton Transactions* **2011,** *40* (18), 4954-4958.

80. Nan, J.; Dong, X.; Wang, W.; Jin, W.; Xu, N., Step-by-Step Seeding Procedure for Preparing HKUST-1 Membrane on Porous α-Alumina Support. *Langmuir* **2011,** *27* (8), 4309-4312.

81. Bétard, A.; Bux, H.; Henke, S.; Zacher, D.; Caro, J.; Fischer, R. A., Fabrication of a CO2-selective membrane by stepwise liquid-phase deposition of an alkylether functionalized pillared-layered metal-organic framework [Cu2L2P]n on a macroporous support. *Microporous and Mesoporous Materials* **2012,** *150* (0), 76-82.

82. Arslan, H. K.; Shekhah, O.; Wohlgemuth, J.; Franzreb, M.; Fischer, R. A.; Wöll, C., High-Throughput Fabrication of Uniform and Homogenous MOF Coatings. *Advanced functional materials* **2011**, n/a-n/a.

83. Yao, J.; Dong, D.; Li, D.; He, L.; Xu, G.; Wang, H., Contra-diffusion synthesis of ZIF-8 films on a polymer substrate. *Chemical Communications* **2011,** *47* (9), 2559-2561.

84. Wang, Z.; Cohen, S. M., Postsynthetic modification of metal-organic frameworks. *Chemical Society reviews* **2009,** *38* (5), 1315-1329.

85. Yang, T.; Xiao, Y.; Chung, T.-S., Poly-/metal-benzimidazole nano-composite membranes for hydrogen purification. *Energy & Environmental Science* **2011,** *4* (10), 4171-4180.

86. Car, A.; Stropnik, C.; Peinemann, K.-V., Hybrid membrane materials with different metal–organic frameworks (MOFs) for gas separation. *Desalination* **2006,** *200* (1-3), 424-426.

87. Basu, S.; Cano-Odena, A.; Vankelecom, I. F. J., MOF-containing mixed-matrix membranes for CO2/CH4 and CO2/N2 binary gas mixture separations. *Separation and Purification Technology* **2011,** *81* (1), 31-40.

88. Ordoñez, M. J. C.; Balkus Jr, K. J.; Ferraris, J. P.; Musselman, I. H., Molecular sieving realized with ZIF-8/Matrimid® mixed-matrix membranes. *J. Membr. Sci.* **2010,** *361* (1-2), 28-37.

89. Hu, J.; Cai, H.; Ren, H.; Wei, Y.; Xu, Z.; Liu, H.; Hu, Y., Mixed-Matrix Membrane Hollow Fibers of Cu3(BTC)2 MOF and Polyimide for Gas Separation and Adsorption. *Ind. Eng. Chem. Res.* **2010,** *49* (24), 12605-12612.

90. Basu, S.; Cano-Odena, A.; Vankelecom, I. F. J., Asymmetric Matrimid®/[Cu3(BTC)2] mixed-matrix membranes for gas separations. *J. Membr. Sci.* **2010,** *362* (1-2), 478-487.

91. Basu, S.; Maes, M.; Cano-Odena, A.; Alaerts, L.; De Vos, D. E.; Vankelecom, I. F. J., Solvent resistant nanofiltration (SRNF) membranes based on metal-organic frameworks. *J. Membr. Sci.* **2009,** *344* (1-2), 190-198.

92. Caro, J.; Noack, M., Chapter 1 - Zeolite Membranes – Status and Prospective. In *Advances in Nanoporous Materials*, Stefan, E., Ed. Elsevier: 2010; Vol. Volume 1, pp 1-96.

93. Bux, H.; Chmelik, C.; Krishna, R.; Caro, J., Ethene/ethane separation by the MOF membrane ZIF-8: Molecular correlation of permeation, adsorption, diffusion. *Journal of Membrane Science* **2011,** *369* (1-2), 284-289.

94. (a) Ma, S. Q.; Sun, D. F.; Wang, X. S.; Zhou, H. C., A mesh-adjustable molecular sieve for general use in gas separation. *Angew. Chem.-Int. Edit.* **2007,** *46* (14), 2458-2462; (b) Ma, S. Q.; Sun, D. F.; Yuan, D. Q.; Wang, X. S.; Zhou, H. C., Preparation and Gas Adsorption Studies of Three Mesh-Adjustable Molecular Sieves

with a Common Structure. *Journal of the American Chemical Society* **2009,** *131* (18), 6445-6451.

95. Kuznicki, S. M.; Bell, V. A.; Nair, S.; Hillhouse, H. W.; Jacubinas, R. M.; Braunbarth, C. M.; Toby, B. H.; Tsapatsis, M., A titanosilicate molecular sieve with adjustable pores for size-selective adsorption of molecules. *Nature* **2001,** *412* (6848), 720-724.

96. Ma, L. Q.; Abney, C.; Lin, W. B., Enantioselective catalysis with homochiral metal-organic frameworks. *Chemical Society Reviews* **2009,** *38* (5), 1248-1256.

97. (a) Li, J. R.; Tao, Y.; Yu, Q.; Bu, X. H.; Sakamoto, H.; Kitagawa, S., Selective gas adsorption and unique structural topology of a highly stable guest-free zeolite-type MOF material with N-rich chiral open channels. *Chemistry-a European Journal* **2008,** *14* (9), 2771-2776; (b) Wu, C. D.; Hu, A.; Zhang, L.; Lin, W. B., Homochiral porous metal-organic framework for highly enantioselective heterogeneous asymmetric catalysis. *Journal of the American Chemical Society* **2005,** *127* (25), 8940-8941.

98. Tanabe, K. K.; Wang, Z. Q.; Cohen, S. M., Systematic functionalization of a metal-organic framework via a postsynthetic modification approach. *Journal of the American Chemical Society* **2008,** *130* (26), 8508-8517.

99. Yang, S.; Lin, X.; Blake, A. J.; Walker, G. S.; Hubberstey, P.; Champness, N. R.; Schröder, M., Cation-induced kinetic trapping and enhanced hydrogen adsorption in a modulated anionic metal–organic framework. *Nat Chem* **2009,** *1* (6), 487-493.

100. An, J.; Geib, S. J.; Rosi, N. L., Cation-Triggered Drug Release from a Porous Zinc−Adeninate Metal−Organic Framework. *Journal of the American Chemical Society* **2009,** *131* (24), 8376-8377.

101. An, J.; Rosi, N. L., Tuning MOF CO2 Adsorption Properties via Cation Exchange. *Journal of the American Chemical Society* **2010,** *132* (16), 5578-5579.

102. Sholl, D. S., Metal-organic frameworks: A porous maze. *Nat Chem* **2011,** *3* (6), 429-430.

103. Hibbe, F.; Chmelik, C.; Heinke, L.; Pramanik, S.; Li, J.; Ruthven, D. M.; Tzoulaki, D.; Kärger, J. r., The Nature of Surface Barriers on Nanoporous Solids Explored by Microimaging of Transient Guest Distributions. *Journal of the American Chemical Society* **2011,** *133* (9), 2804-2807.

104. (a) Bonilla, G.; Tsapatsis, M.; Vlachos, D. G.; Xomeritakis, G., Fluorescence confocal optical microscopy imaging of the grain boundary structure of zeolite MFI membranes made by secondary (seeded) growth. *Journal of Membrane Science* **2001,** *182* (1-2), 103-109; (b) Snyder, M. A.; Lai, Z.; Tsapatsis, M.; Vlachos, D. G., Combining simultaneous reflectance and fluorescence imaging with SEM for conclusive identification of polycrystalline features of MFI membranes. *Microporous and Mesoporous Materials* **2004,** *76* (1-3), 29-33; (c) Snyder, M. A.; Vlachos, D. G., Nano-patterned standards for improving the quantitative capability of laser scanning confocal microscopy for materials characterization. *Microporous and Mesoporous Materials* **2007,** *102* (1-3), 101-110.

105. Keskin, S.; Sholl, D. S., Assessment of a Metal−Organic Framework Membrane for Gas Separations Using Atomically Detailed Calculations: CO2, CH4, N2, H2 Mixtures in MOF-5. *Industrial & Engineering Chemistry Research* **2008,** *48* (2), 914-922.

106. Watanabe, T.; Keskin, S.; Nair, S.; Sholl, D. S., Computational identification of a metal organic framework for high selectivity membrane-based CO2/CH4 separations: Cu(hfipbb)(H2hfipbb)0.5. *Phys Chem Chem Phys* **2009,** *11* (48), 11389-11394.

107. Lehnert, R.; Seel, F., Darstellung und Kristallstruktur des Mangan(II)- und Zink(II)-Derivates des Imidazols. *Z. anorg. allg. Chem.* **1980,** *464* (1), 187-194.

108. Aguado, S.; Canivet, J.; Farrusseng, D., Facile shaping of an imidazolate-based MOF on ceramic beads for adsorption and catalytic applications. *Chem. Commun.* **2010,** *46* (42), 7999-8001.

109. Cravillon, J.; Schroder, C. A.; Bux, H.; Rothkirch, A.; Caro, J.; Wiebcke, M., Formate modulated solvothermal synthesis of ZIF-8 investigated using time-resolved in situ X-ray diffraction and scanning electron microscopy. *Crystengcomm* **2011**.

110. Cravillon, J.; Nayuk, R.; Springer, S.; Feldhoff, A.; Huber, K.; Wiebcke, M., Controlling Zeolitic Imidazolate Framework Nano- and Microcrystal Formation: Insight into Crystal Growth by Time-Resolved In Situ Static Light Scattering. *Chemistry of Materials* **2011,** *23* (8), 2130-2141.

111. Pacholski, C.; Kornowski, A.; Weller, H., Self-Assembly of ZnO: From Nanodots to Nanorods. *Angewandte Chemie International Edition* **2002,** *41* (7), 1188-1191.

112. (a) Li, Y.; Pera-Titus, M.; Xiong, G.; Yang, W.; Landrivon, E.; Miachon, S.; Dalmon, J. A., Nanocomposite MFI-alumina membranes via pore-plugging synthesis: Genesis of the zeolite material. *Journal of Membrane Science* **2008,** *325* (2), 973-981; (b) Miachon, S.; Landrivon, E.; Aouine, M.; Sun, Y.; Kumakiri, I.; Li, Y.; Prokopová, O. P.; Guilhaume, N.; Giroir-Fendler, A.; Mozzanega, H.; Dalmon, J. A., Nanocomposite MFI-alumina membranes via pore-plugging synthesis: Preparation and morphological characterisation. *Journal of Membrane Science* **2006,** *281* (1–2), 228-238.

113. Keskin, S.; Liu, J.; Johnson, J. K.; Sholl, D. S., Atomically detailed models of gas mixture diffusion through CuBTC membranes. *Microporous and Mesoporous Materials* **2009,** *125* (1–2), 101-106.

114. Hayashi, J.-i.; Mizuta, H.; Yamamoto, M.; Kusakabe, K.; Morooka, S.; Suh, S.-H., Separation of Ethane/Ethylene and Propane/Propylene Systems with a Carbonized BPDA−pp‘ODA Polyimide Membrane. *Industrial & Engineering Chemistry Research* **1996,** *35* (11), 4176-4181.

115. Zhang, C.; Dai, Y.; Johnson, J. R.; Karvan, O.; Koros, W. J., High performance ZIF-8/6FDA-DAM mixed matrix membrane for propylene/propane separations. *Journal of Membrane Science* **2012,** *389* (0), 34-42.

116. Colling, C. W. H., Jr.; Georgia, A.; Bartels, J.V.; Processes using solid perm-selective membranes in multiple groups for simultaneous recovery of specified products from a fluid mixture. 2004.

117. Arruebo, M.; Coronas, J.; Menéndez, M.; Santamaría, J., Separation of hydrocarbons from natural gas using silicalite membranes. *Separation and Purification Technology* **2001,** *25* (1–3), 275-286.

118. Xia, Y.; Qin, D.; Whitesides, G. M., Microcontact printing with a cylindrical rolling stamp: A practical step toward automatic manufacturing of patterns with submicrometer-sized features. *Advanced Materials* **1996,** *8* (12), 1015-1017.